THESIS
Z

This is to certify that the

dissertation entitled

Electrospray Mass Spectrometry of Metal Ion Complexes with Chelating and Macrocyclic Ligands

presented by

CALIN GEORGE ZNAMIROVSCHI

has been accepted towards fulfillment of the requirements for

Ph.D. degree in Chemistry

Christie G Enke
Major professor

Date April 30, 1996

MSU is an Affirmative Action/Equal Opportunity Institution

O-12771

PLACE IN RETURN BOX to remove this checkout from your record.
TO AVOID FINES return on or before date due.

DATE DUE	DATE DUE	DATE DUE

MSU Is An Affirmative Action/Equal Opportunity Institution
c:\circ\datedue.pm3-p.1

ELECTROSPRAY MASS SPECTROMETRY OF METAL ION COMPLEXES WITH CHELATING AND MACROCYCLIC LIGANDS

By

Calin George Znamirovschi

A DISSERTATION

Submitted to
Michigan State University
in partial fulfillment of the requirements
for the degree of

DOCTOR OF PHILOSOPHY

Department of Chemistry

1996

ABSTRACT

ELECTROSPRAY MASS SPECTROMETRY OF METAL ION COMPLEXES WITH CHELATING AND MACROCYCLIC LIGANDS

By

Calin George Znamirovschi

The earlier methods of mass spectrometry, especially electron impact ionization, were limited in their application to inorganic systems, due to the low volatility of most ionic species. More recent methods of "soft" ionization, included but not limited to electrospray, have had a major impact on inorganic mass spectrometric analysis.

A preliminary part of this work focuses on the behavior of simple models, like metal ions in solution, mainly to assess the extent to which the mass spectrometric analytical response is consistent with their speciation in solution. The appearance of metal - solvent adducts of various structures in the mass spectra allowed us to assess their stability, as a function of the solution matrix composition and the operational parameters of electrospray.

The inherent processes that accompany the transfer of ionic and molecular associations from solution into the gas phase are double-edge swords and they determine how closely a mass spectrum resembles the

solution chemistry of the analyte. The effect of several instrumental parameters is presented, with respect to their consequences on ion adduct formation and their rate of "survival" during the transfer through the electrospray interface.

We also applied electrospray as a means of sample introduction in mass spectrometry, taking advantage of its ability to generate gaseous ions from ionic, non-volatile solution species. We have obtained important results regarding the gas phase stability of several metal complexes with macrocyclic ligands, by using collisionally activated dissociation with tandem mass spectrometry.

The application of electrospray mass spectrometry as a means of analysis which is complementary to solid state and solution studies in synthetic coordination chemistry is also a part of our study. Our results on the complexation of transition metals by a novel calixarene macrocyclic ligand contribute to a more complete image of their solution chemistry as well as their structural stability.

Copyright© by
CALIN GEORGE ZNAMIROVSCHI
1996

ACKNOWLEDGEMENTS

The research leading to this dissertation was only possible with the help, inspiration, guidance, and friendship of many people. People who have had a tremendous impact on all aspects of my life and career, both in and outside a classroom or a laboratory. A comprehensive list of friends, teachers and coworkers who have helped me throughout twenty-two years of formal education and who deserve recognition cannot be compiled, simply because it is continuously growing.

First and foremost I would like to convey my deepest gratitude to my research advisor, Dr. Christie Enke. I have been very fortunate, honored, and privileged to have such a prestigious scientist, a genuinely talented educator, and a great friend as my mentor. Words are not enough to describe how thankful I am to him, for his guidance, support and patience during my tenure as a graduate student. Far from my family and home, I have often turned to Dr. Enke seeking a word of advice, at happy or difficult times. Needless to say, it has always been readily and graciously offered.

Special thanks and words of recognition are immensely deserved by my first chemistry teacher, Ms. Monica Stanca, who supported and encouraged me while I was a student at "Nicolae Balcescu" High School in

Cluj-Napoca, Romania. I would also like to thank Dr. Sorin Mager, my research advisor during my undergraduate studies at the University of Cluj-Napoca.

The financial support I have received during my graduate studies, from Michigan State University and the University of New Mexico was crucially important and it is gratefully acknowledged. I also consider myself privileged to have been part of a wonderful research group, a true and supportive family. Eric Hemenway was always willing to help, to share his knowledge and experience, and I am very thankful to him. Paul Miyares, Douglas Beussman, Paul Vlasak, Qinching Ji, Fei Liu, Michael Davenport, Tina Erickson, Terri Constantopoulos, Gregor Overney, Kristi Hughes and Gail Bradley, all have been, at one point or another, part of our team, and I enjoyed their friendship and support very much throughout these years.

Lastly but most importantly, I would like to acknowledge my family. I thank my parents and grandparents for everything they have done for me, for their priceless contribution to my formation as a citizen and as a scientist. I have permanently felt their love, thoughts and support, across the ocean and across the miles. To my wife Karin and our son Patrick, just a few words, my thanks and my love, along with the pledge that I will always make them proud.

TABLE OF CONTENTS

LIST OF TABLES

LIST OF FIGURES

Chapter 1

Introduction

Introduction

In recent decades the advances in high-resolution mass analyzers and the discovery of new methods of sample introduction and ionization have made mass spectrometry a widespread and absolutely necessary tool in chemical research. Although organic and biochemical areas previously accounted for the vast majority of its uses and applications, mass spectrometry has lately emerged as a very powerful means of investigation in inorganic, coordination, and organometallic chemistry [1-3].

For many years the main obstacle to the study of mass spectra of inorganic and organometallic compounds was the process of generating ions in the gas phase. The mass spectrometry of inorganic compounds and metal complexes usually required the volatilization of species prior to ion formation. Even though many desorption techniques were gradually

developed [4,5], most of the studies were limited to non-ionic, volatile compounds, and were mainly based on electron impact (EI) ionization [6,7]. Although used as reagents in various mass spectrometric techniques since the early 1970s [8], metal ions, along with other related chemical species, such as metal adducts and complexes, were not suitable for EI ionization mass spectrometric studies because of their low volatility, high thermal lability, and tendency to undergo irreversible secondary reactions during the ionization process. Although derivatization techniques were generally available, the methodology was time consuming and required large amounts of sample.

The development of soft ionization techniques, such as fast atom bombardment (FAB) [9,10], matrix-assisted LASER desorption ionization (MALDI) [11], and chemical ionization (CI) [12,13] lifted many of the earlier limitations. This trend was later continued by the development of desorption chemical ionization (DCI) [14], ^{252}Cf plasma desorption (PD) [15], and the whole family of field-assisted desorption methods, which includes electrospray (ES), thermospray (TS), and ionspray (IS) ionization [16].

In a field-assisted desorption process, a strong electrostatic field is used to extract ions from a liquid substrate. Two generic methods have emerged, one in which ions desorb directly into the vacuum, named electrohydrodynamic (EH) ionization [17,18], and one in which the analyte is dispersed as a mist of droplets, from which the solvent gradually evaporates and the ions desorb into a bath gas, under atmospheric pressure. The latter

is generically called atmospheric pressure (AP) ionization. The ionization either occurs in the gas phase, as in the case of atmospheric pressure chemical ionization (APCI), or ions are preformed in the analyte solution and subsequently nebulized into a chamber, also held at atmospheric pressure, in the process of electrospray (ES). Electrospray has lately become one of the most attractive and widely employed variant of the atmospheric pressure ionization methods. Also, electrospray enjoys today the reputation of being the most versatile interfacing technique for coupling liquid chromatography with mass spectrometry (Figure 1.1) [19] due to its principal features, namely the capability to produce multiply charged ions, even from thermally labile and extremely fragile molecules, and its gentleness, which allows such species to be transferred to the gas phase while undergoing little or no fragmentation. The possibility of generating intact gaseous ionic species has triggered a great deal of research aimed at obtaining new and improved structure information in the gas phase.

Electrospray Mass Spectrometry of Metal-Ligand Systems

Even though the study of electrospray phenomena extends back early this century, to the work of Bose [20] and Zeleny [21], and later to the studies of Dole *et al.* [22,23], electrospray ionization combined with mass spectrometry was reported, essentially simultaneously, much later, in 1984, by both

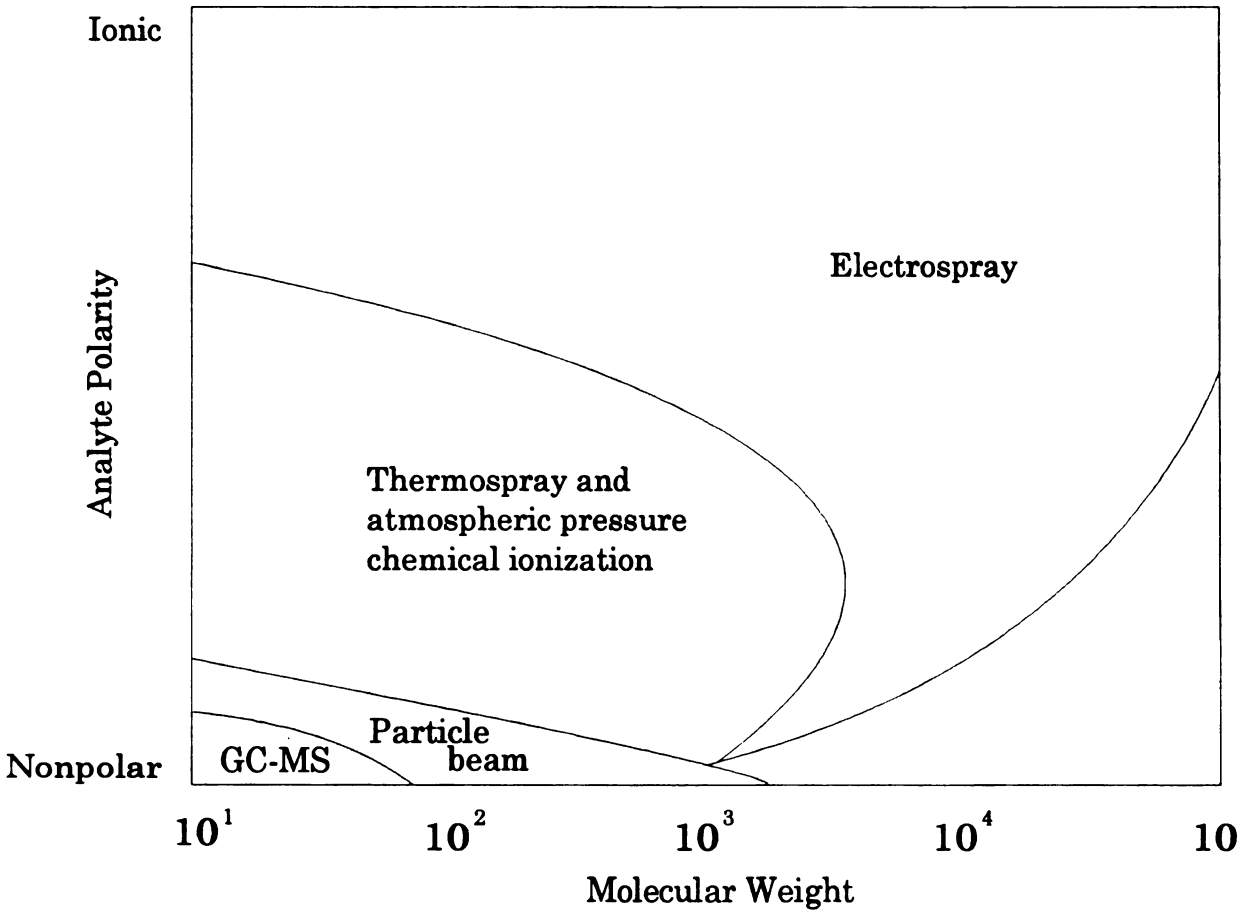

Figure 1.1 *Application ranges of modern interfacing techniques in mass spectrometry [19]*

Yamashita and Fenn [24] and Aleksandrov *et al.* [25,26]. Since its inception, in 1988, first as a tool for the analysis of large biomolecules [27], the practice of ES-MS has grown impressively [28-31]. Recently, electrospray has shown itself capable of producing intact ions, either positive or negative, multiply charged, from remarkably large, complex, and fragile analyte molecules [32,33].

Electrospray mass spectrometry (ES-MS) provides an unrivaled method for the transfer of preexisting ions and ionic associations from solution into the gas phase. Although the goal of most researchers has been on the utilization of electrospray as a sample introduction device for the mass analysis of organic and biochemical species [34,35], Kebarle and co-workers [36-39] have focused most of their efforts on the gas phase chemistry of metal ions and their reactions. The potential of electrospray to evolve into a generic ion source for elemental mass spectrometry has been reported by different groups [40,41] who consider it may become competitive with inductively coupled plasma (ICP) mass spectrometry.

During the development of ES-MS, mass spectra of alkali metals were generally observed [24], while spectra of alkaline earth and transition metals have been reported only in the last few years [37-39]. The reasons may be that other sensitive and selective analytical techniques existed for metal ions, or that it had been believed for a long time that desorption of multiply charged metal ions from solution would be difficult or impossible [42].

The determination of gas phase equilibria involving singly charged ions and solvent molecules was initiated more than two decades ago [43] and results providing extensive data on ion-solvent and ion-ligand interactions [44] were reported. However, the transfer of singly and multiply [37-39] charged ions from the solution to the gas phase involves processes that often alter their form (charge, degree of solvation, coordination pattern).

As frequently occurs with a rapidly advancing technique, the understanding of the physico-chemical processes behind electrospray ionization has not kept pace with the tremendously rapid expansion in applications. The mechanism of electrospray, that is, the mechanism of formation and desolvation of ions during their transfer from solution to gas phase, does not have yet an unanimously accepted scenario [22,45-48].

Electrospray mass spectrometric studies of aqueous solutions of metal salts [41] revealed that an unambiguous correlation between the peak intensities in the ES-MS spectra and the ionic concentrations in solution may not be readily observable. Although the solution chemistry dictates the types of ions that are present in the electrospray spectrum, other processes, mainly desorption-related, may modify the relative abundances of these ions [49-51]. Most of these processes occur in the electrospray source, being therefore affected by various instrumental and operational parameters. In specifically designed experiments, the solvation and desorption-related contributions could be minimized or even canceled, which would allow quantitative

correlations between the equilibrium concentrations of the ionic species in solution and the electrospray mass spectrometric response.

One of the major problems faced in the analytical application of ES-MS to metal analysis is the formation of metal-solvent adduct ions. These adducts complicate the spectra and spread the analyte signal over several different ionic species, thereby raising the detection limits. This problem is less severe for singly charged ions, but it becomes quite complicated for multiply charged species [38,39]. Another problem encountered in the analysis of metal ions and their adducts is the loss of charge state information, that is, the original charge state of the ionic species in solution is not always preserved in the gas phase.

The first of the problems, and possibly the second, can be largely overcome by the use of particular macrocyclic compounds, such as crown ethers, as complexation agents for metal ions [52]. The ability to form host-guest type complexes with metal ions is one of the most important properties of crown ethers and related compounds [53]. Macrocyclic ligands were found to prevent the formation of various metal-solvent adducts and to help preserve the charge state of the metal ions [54].

The involvement of mass spectrometry in this area of coordination chemistry started with the need to characterize these complex systems with progressively higher masses and lower volatility. Mass spectrometric studies of various aspects of the gas phase chemistry of metal coordination compounds had been performed even before ES ionization proved its

suitability for such applications. Hence, investigations to elucidate the mechanisms of ion formation and transport and the stability of the gas phase complexes were carried out by means of fast atom bombardment [55] and plasma desorption mass spectrometry [15]. Significant results on ion-molecule reactions involving particularly transition metals and polyethers were obtained by Huang and Allison [56] by using ion cyclotron resonance (ICR) spectrometry.

The application of ES-MS in studying the interaction of metals with chelating and macrocyclic ligands has lately been found to be very useful in understanding the behavior of metal ions in complex organic matrices [57]. Metal chelates play an important role in environmental chemistry [58] especially by regulating the bioavailability of certain metals in natural waters. The study of such complexes as they exist in solution requires *in situ* methods of analysis. ES-MS of solvated metal chelates provides the structural information which complements data obtained by other techniques.

Electrospray mass spectrometry, due to its ability to transfer intact ionic species from solution to the gas phase is expected to enable more insightful investigations on a wider array of metal ions and their interactions with various chelating and macrocyclic ligands. The use of an electrospray ion source in conjunction with tandem mass spectrometry (MS/MS) [59] can generate new and more complex information about fundamental ion

formation processes, structure and reactivity, as well as the gas phase chemical equilibria between metal ions and the species with which they associate.

Our study has a high degree of complexity, being structured in five distinct parts. The general behavior of solvated metal ions under electrospray conditions is the subject of Chapter 2. Its emphasis is on qualitative correlations that exist between the solution concentrations and the distribution of ions in the gas phase. The appearance of ES-MS spectra help rationalize the relative affinity of various solvent molecules for certain metal ions. The ligand-metal binding strength within the clusters translates into the ease with which the ionic associations preformed in solution "survive" desolvation and the transport processes within the electrospray source and through the interface.

Although the degree of structural degradation of solvated ionic associations is greatly minimized in electrospray when compared to other "soft" ionization techniques, dissociation occurs to a certain extent, mainly as a function of experimental conditions. Hence, the so-called "source CAD" or "up-front CAD" is exploited in order to achieve an "orchestrated survival" of the species of interest, subsequently used as precursor ions in tandem mass spectrometry. Chapter 3 deals with the study of the processes involved in "source CAD", and the optimization of instrumental parameters according to our experimental goals.

A comparative study of the coordination chemistry of two metal ions known for their opposite behavior both in solution and in the gas phase, potassium and silver, is the main objective of Chapter 4. The character and strength of the metal-ligand interactions are the key factors that determine the stability of the complexes. Our goal is to establish a relationship, beyond qualitative considerations, between the appearance of the electrospray mass spectra and the composition of the analyte solution.

Chapter 5 consists of a more systematic study of collisionally activated dissociation in conjunction with tandem mass spectrometry. The effect of particular experimental factors, such as the collision gas pressure and the collision energy is rigorously studied on specific, well-defined examples. The study of CAD processes provides a great deal of information about mechanistic aspects of reactions, as well as the stability of various ions in the gas phase.

The last chapter of the dissertation concentrates on the applicability of electrospray mass spectrometry as a method of analysis complementary to the "classic" methods widely employed in analytical and synthetic coordination chemistry. A novel macrocyclic ligand and its complexes with three transition metal ions gave us the opportunity to perform experiments leading to results unattainable through most other techniques, regarding the structure and reactivity of the complexes and related structures in solution and in the gas phase.

References

1. Gregor, I. K.; Guilhaus, M. *Mass Spectrom. Rev.* **1984**, *3*, 39.

2. Allison, J. *Prog. Inorg. Chem.* **1986**, *34*, 627.

3. Bruce, M. I.; Liddell, M. J. *Appl. Organometallic Chem.* **1987**, *1*, 191.

4. van Breemen, R. B.; Martin, L. B.; Schreiner, A. F. *Anal. Chem.* **1988**, *60*, 1314.

5. Detter, L. D.; Conner, K. A.; Rothwell, A. P.; Walton, R. A. *Inorg. Chimica Acta* **1988**, *143*, 109.

6. Distefano, G.; Innorta, G.; Pignataro, S.; Foffani, A. *J. Organomet. Chem.* **1968**, *14*, 165.

7. Distefano, G.; Innorta, G.; Pignataro, S.; Foffani, A. *J. Organomet. Chem.* **1974**, *65*, 209.

8. Teesch, L. M.; Adams, J. *Org. Mass Spectrom.* **1992**, *27*, 931.

9. Cochran, R. L. *Appl. Spectrosc. Rev.* **1986**, *22*, 137.

10. Miller, J. M. *Mass Spectrom. Rev.* **1989**, *9*, 319.

11. Karas, M.; Killenkamp, F. *Anal. Chem.* **1988**, *60*, 2299.

12. Allison, J.; Ridge, P. D. *J. Am. Chem. Soc.* **1979**, *101*, 4998.

13. Bombick, D.; Pinkston, J. D.; Allison, J. *Anal. Chem.* **1984**, *56*, 396.

14. Bryant, J. A.; Blanda, M. T.; Vincenti, M.; Cram, D. J. *J. Am. Chem. Soc.* **1991**, *113*, 2167.

15. Malhotra, N.; Roepstorff, P.; Hansen, T. K.; Becher, J. *J. Am. Chem. Soc.* **1990**, *112*, 3709.

16. Li, Y.-T.; Hsieh, Y.-T.; Henion, J. D.; Ocain, T. D.; Schiehser, G. A.; Ganem, B. *J. Am. Chem. Soc.* **1994**, *116*, 7487.

17. Man, V. F.; Dale Lin, J.; Cook, K. D. *J. Am. Chem. Soc.* **1985**, *107*, 4635.

18. Cook, K. S. *Mass Spectrom. Rev.* **1986**, *5*, 467.

19. Volmer, D. A.; Vollmer, D. L. *LC-GC* **1996**, *14*, 236.

20. Bose, G. M. In *Recherches sur la cause et sur la véritable théorie de l'électricité*, Wittenberg, 1745.

21. Zeleny, J. *J. Phys. Rev.* **1917**, *10*, 1.

22. Dole, M.; Mach, L. L.; Hines, R. L.; Mobley, R. C.; Ferguson, L. D.; Alice, M. B. *J. Chem. Phys.* **1968**, *49*, 2240.

23. Mach, L. L.; Kralik, P.; Rheude, A.; Dole, M. *J. Chem. Phys.* **1970**, *52*, 4977.

24. Yamashita, M.; Fenn, J. B. *J. Phys. Chem.* **1984**, *88*, 4451.

25. Aleksandrov, M. L.; Gall, L. N.; Krasnov, V. N.; Nikolaev, V. I.; Pavlenko, V. A.; Skurov, V. A. *Dokl. Akad. Nauk. SSSR* **1984**, *277*, 379.

26. Aleksandrov, M. L.; Gall, L. N.; Krasnov, V. N.; Nikolaev, V. I.; Pavlenko, V. A.; Skurov, V. A.; Baram, G. I.; Gracher, M. A.; Knorre, V. D.; Kusner, Y. S. *Bioorg. Kim.* **1984**, *10*, 712.

27. Fenn, J. B.; Mann, M.; Meng, C. K.; Wong, S. F.; Whitehouse, C. M. *Science*, **1989**, *246*, 64.

28. Katta, V.; Chowdhury, S. K.; Chait, B. T. *J. Am. Chem. Soc.* **1990**, *112*, 5348.

29. Colton, R.; Traeger, J. C. *Inorg. Chimica Acta* **1992**, *201*, 153.

30. Maleknia, S.; Brodbelt, J. S. *Rapid Commun. Mass Spectrom.* **1992**, *6*, 376.

31. Colton R.; Kläui, W. *Inorg. Chimica Acta* **1993**, *211*, 235.

32. Cody, R. B.; Tamura, J.; Musselman, B. *Anal. Chem.* **1992**, *64*, 1561.

33. Nohmi, T.; Fenn, J. B. *J. Am. Chem. Soc.* **1992**, *114*, 3421.

34. Smith, R. D.; Loo, J. A.; Edmonds, C. G.; Barinaga, C. J.; Udseth, H. R.; *Anal. Chem.* **1990**, *62*, 882.

35. Smith, R. D.; Loo, J. A.; Ogorzalek Loo, R. R.; Busman, M.; Udseth, H. R. *Mass Spectrom. Rev.* **1991**, *10*, 359.

36. Blades, A. T.; Jayaweera, P.; Ikonomou, M. G.; Kebarle, P. *J. Chem. Phys.* **1990**, *92*, 5900.

37. Blades, A. T.; Jayaweera, P.; Ikonomou, M. G.; Kebarle, P. *Int. J. Mass Spectrom. Ion Processes* **1990**, *101*, 325.

38. Blades, A. T.; Jayaweera, P.; Ikonomou, M. G.; Kebarle, P. *Int. J. Mass Spectrom. Ion Processes* **1990**, *102*, 251.

39. Jayaweera, P.; Blades, A. T.; Ikonomou, M. G.; Kebarle, P. *J. Am. Chem. Soc.* **1990**, *112*, 2452.

40. Agnes, G. R.; Horlick, G. *Appl. Spectrosc.* **1992**, *46*, 401.

41. Cheng, Z. L.; Siu, K. W. M.; Guevremont, R.; Berman, S. S. *J. Am. Soc. Mass Spectrom.* **1992**, *3*, 281.

42. Iribarne, J. V.; Dziedzic, P. J.; Thomson, B. A. *Int. J. Mass Spectrom. Ion Processes* **1983**, *50*, 331.

43. Dzidic, I.; Kebarle, P. *J. Phys. Chem.* **1970**, *74*, 1466.

44. Keesee, R. G.; Castleman, A. W. *J. Phys. Chem. Ref. Data* **1986**, *15*, 1011.

45. Iribarne, J. V.; Thomson, B. A. *J. Chem. Phys.* **1976**, *64*, 2287.

46. Schmelzeisen-Redeker, G.; Butfering, L.; Rollgen, F. W. *Int. J. Mass Spectrom. Ion Processes* **1989**, *90*, 139.

47. Luttgens, U.; Rollgen, F. W. In *Proceedings of the 39th ASMS Conference on Mass Spectrometry and Allied Topics*, Nashville, TN, May 19-24, 1991.

48. Fenn, J. B.; Rosell, J. In *Proceedings of the 43rd ASMS Conference on Mass Spectrometry and Allied Topics*, Atlanta, GA, May 21-26, 1995.

49. Tang, L.; Kebarle, P. *Anal. Chem.* **1991**, *63*, 2709.

50. Fenn, J. B. *J. Am. Soc. Mass Spectrom.* **1993**, *4*, 524.

51. Dupont, A.; Leize, E.; Marquis-Rigault, A.; Funeriu, D.; Lehn, J.-M.; Van Doesselaer, A. In *Proceedings of the 43rd ASMS Conference on Mass Spectrometry and Allied Topics*, Atlanta, GA, May 21-26, 1995.

52. Zagorevskii, D. V.; Nekrasov, Y. S. *Org. Mass Spectrom.* **1993**, *28*, 1562.

53. Weber, E.; Toner, J. L.; Goldberg, I.; Vögtle, F.; Laidler, D. A.; Stoddart, J. F.; Bartsch, R. A.; Liotta, C. L. In *Crown Ethers and Analogs*, S. Patai and Z. Rappoport, Eds.; John Wiley & Sons: Chichester-New York-Brisbane-Toronto-Singapore, 1989, Chapter 4.

54. Van Berkel, G. J.; McLuckey, S. A.; Glish, G. L. In *Proceedings of the 39th ASMS Conference on Mass Spectrometry and Allied Topics*, Nashville, TN, May 19-24, 1991.

55. Bonas, G.; Bosso, C.; Vignon, M. R. *Rapid Commun. Mass Spectrom.* **1988**, *2*, 88.

56. Huang, S. K.; Allison, J. *Organometallics* **1983**, *2*, 883.

57. Wahl, K. L.; Stromatt, R. W.; Blanchard, D. L. In *Proceedings of the 43rd ASMS Conference on Mass Spectrometry and Allied Topics*, Atlanta, GA, May 21-26, 1995.

58. Ross, A. R. S.; Ikonomou, M. G.; Orians, K. J. In *Proceedings of the 43rd ASMS Conference on Mass Spectrometry and Allied Topics*, Atlanta, GA, May 21-26, 1995.

59. Gatlin, C. L.; Turecek, F.; Vaisar, T. In *Proceedings of the 43rd ASMS Conference on Mass Spectrometry and Allied Topics*, Atlanta, GA, May 21-26, 1995.

Chapter 2

Metal Ions in the Electrospray Process

Introduction

The increased involvement of metal ions in analytical mass spectrometry has lately been the immediate result of a continuously emerging need for new and improved information for structure analysis. Adducts and complexes of metal ions can be used to determine relative molecular masses of unknown species, to assist in mixture analysis, and to elucidate structures. Metal ions used to be primarily used as analytical reagents mainly in conjunction with desorption ionization techniques such as field desorption (FD) [1,2], secondary ion mass spectrometry (SIMS) [3,4], plasma desorption (PD) [5], matrix-assisted LASER desorption ionization (MALDI) [6], and fast atom bombardment (FAB) [7,8]. Both Hodges and Beauchamp [9] and Allison and

co-workers [10,11] proposed and demonstrated the use of alkali-metal ions as chemical ionization (CI) reagents for relative molecular mass determinations.

The main drawback of the above methods consisted of the very limited amount of structural information that could be obtained. The most direct information concerning the nature and strength of the interaction of an ion with a given solvent is obtained when the interaction takes place in a dilute gaseous phase. The interaction of the ion with one or more solvent molecules to form so called "solvation clusters" can be studied under such conditions by applying appropriate experimental conditions [12]. It has been only during the last two decades that the gas phase chemistry of such compounds has been investigated to a greater extent for comprehensive structural information [13,14].

The development of electrospray mass spectrometry (ES-MS), which exploits the formation of molecular associations involving metal ions in solution, has recently emerged as the method of choice for the investigation of metal adducts and complexes, due to its versatility and relative simplicity. To date it has been shown that ES-MS, operated under specific experimental conditions, can be used to quantitatively determine trace levels of both elemental and molecular inorganic cations and anions with ppb and sub-ppb detection limits [15]. Also, ES-MS can provide, in some cases, valence state information [16] and can be employed to establish the presence of ligands and study complexation [17,18]. The sharp increase in the volume of recent research concerning electrospray in connection with the chemistry of metal

complexes [19-21] has been triggered by its potential to generate abundant information.

Interaction of Metal Ions in Solution

An ideal analysis technique for solution samples would provide both qualitative and quantitative information on all solution components. Solution components include, in addition to the solvent matrix, anions, cations, and all the forms they may be found in, that is, elemental, molecular, and complexed. Because solvated ions are sampled directly from the liquid phase, ES-MS can yield two types of complementary information regarding ion solvation: the distribution of adduct ions reflects the patterns and degrees of association in solution, whereas their stability in the gas phase is a measure of ion-ligand binding in the absence of the liquid phase.

Metal Ion - Solvent Adduct Formation

The potential of ES-MS to evolve into a generic method for elemental analysis was reported by Agnes and Horlick [15]. One of the limitations most widely encountered was that a large variety of peaks due to metal-solvent clusters may be present in the mass spectrum, clusters that further complicate the spectra and spread the analytical signal of metal-containing

ions over a large range of masses. The distribution of these peaks can however be altered as a function of the experimental conditions [15,22].

Studying simple inorganic metal ions as analytes in the electrospray process has the advantage that such species have no solvophobic moieties and they provide good models for ion solvation-desolvation phenomena. Solutions of metal salts are suitable analytes for our study because first, metal ions produce readily interpretable electrospray mass spectra, and second, the solution chemistry of metal salts is generally well characterized, reliable stability constants of a large number of metal salt species being available [23].

Experimental. Solutions of 0.1 M NaCl and KCl respectively were made by dissolving the appropriate amount of salt (ACS-grade) in minimum required amount of water, followed by dilution with HPLC-grade methanol (Merck) to the desired concentration. The water content of the solutions was kept around 0.3%. Electrospray mass spectra (positive ion mode) were obtained using a Finnigan MAT–TSQ® 7000 triple-stage quadrupole mass spectrometer system equipped with an electrospray source (Finnigan MAT, San Jose, CA). The solutions were introduced into the electrospray source using a syringe pump (Harvard Apparatus, South Natick, MA) at a flow rate of 5 μL/min. Electrospray voltage was 5 kV and the temperature of the

transfer capillary was maintained at 110 C. For the study of the composition and distribution of metal-solvent clusters, "mild" conditions (i.e., low voltage settings and temperature on the interface components) were employed.

In the ES-MS spectrum of the NaCl solution (Figure 2.1) it is evident that the quantitation of sodium is practically impossible. Sodium is contained in at least nine ionic species whose peaks have outstanding intensities and vary significantly with any change in solution matrix or experimental conditions. Besides, the solvation energies and the instrumental response factors for various species in the spectrum are unknown, a reliable relationship between peak intensities and the concentrations in solution being unfeasible at this point.

Even though the ES mass spectrum does not reflect the relative concentrations of various ions in solution, it qualitatively consists of species that either preexist in solution or are formed during the solvent evaporation and interface processes. Metal ion adducts containing methanol in their solvation shell are generally present in higher abundances than the ones containing water molecules. Although the very low water concentration in the analyte solution warrants a partial reason for this situation, the enhancement in the stability of adduct cations can be attributed to a more favorable structure of the primary solvation shell toward coordination of the metal ion, due to the presence of methanol molecules. Clusters with

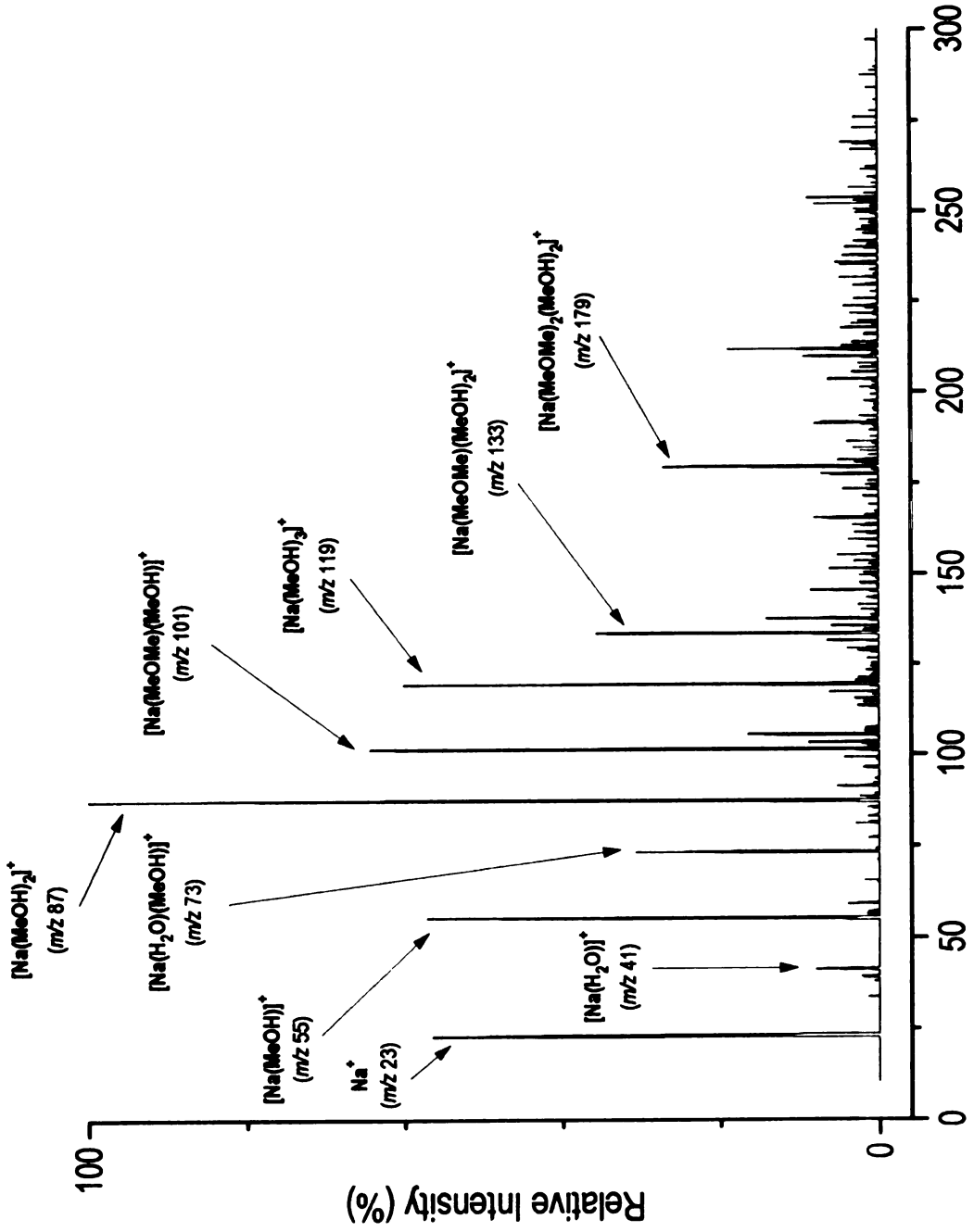

Figure 2.1 *ES-MS spectrum of NaCl in methanol. Capillary temperature = 110 C*

coordination numbers of 1 (*m/z* 55), 2 (*m/z* 87), and 3 (*m/z* 119), corresponding to three of the predominant ions in the spectrum illustrate not only that they or at least their precursors originate in solution, but also their ability to "survive", as intact structures, the desolvation and ion transfer processes. Species containing water, such as the (1:1) sodium-water adduct (*m/z* 41) and the (1:1:1) sodium-water-methanol ion (*m/z* 73) are present in the spectrum, but their peaks have relatively low intensity.

Furthermore, another solvent-derived ligand takes part in the metal adduct formation. We assume that *in situ* intermolecular dehydration of methanol (Reaction 2.1) is responsible for the existence of dimethylether as a ligand in some varieties of partially desolvated clusters. Joint coordination of sodium by methanol and dimethylether is characteristic of the ions at *m/z* 101, *m/z* 133, and *m/z* 179. It can be noticed that coordination with dimethylether allows for a coordination number of 4 (i.e., *m/z* 179), compared to a maximum of 3, encountered in sodium clusters that contain methanol only, or methanol and water.

$$CH_3OH + CH_3OH \longrightarrow CH_3OCH_3 + H_2O \qquad (2.1)$$

The ES-MS spectrum of a potassium chloride solution (Figure 2.2) is similar to that of sodium chloride, in terms of the generic structures present. However, the relative ionic abundances of clusters with higher coordination numbers (3 and 4) are greater than those of analogous sodium clusters. Due

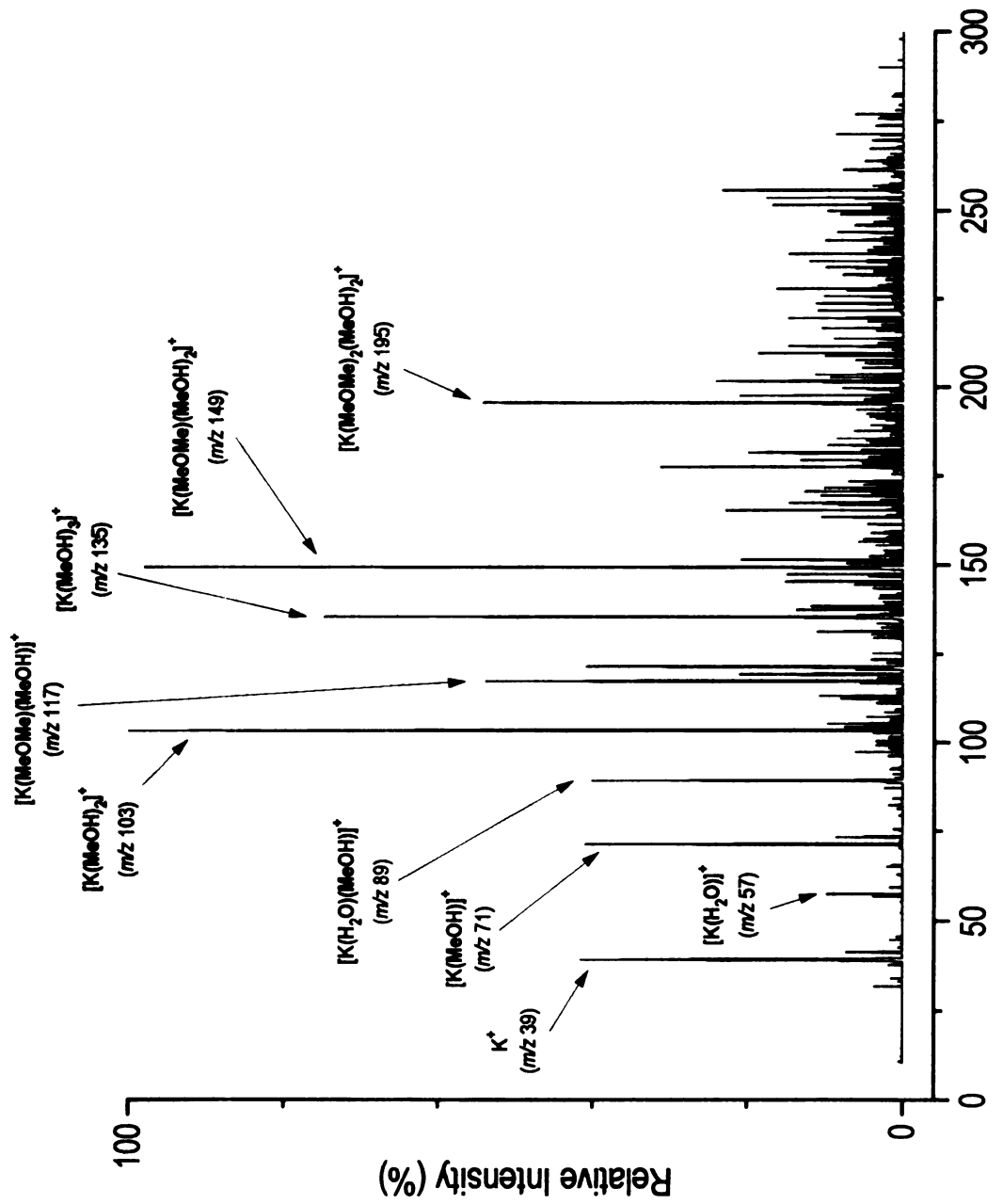

Figure 2.2 *ES-MS spectrum of KCl in methanol. Capillary temperature = 110 C*

to its larger ionic radius and electron affinity [24], potassium can more easily accomodate more solvent and solvent-derived ligands in its primary coordination sphere.

Solvation Effects

The term "selective solvation" is applied to the case where the composition of the solvent components in the neighborhood of the ions, that is, their solvation shell, is different from the composition of the bulk solution. The selective solvation of ions in binary mixtures depends on the free energy of solvation of these ions in the two pure solvents. In mixed solvents it must be recognized that different types of solvent molecules may interact individually and to different extents with the metal ions present in solution.

It was commonly assumed [25] that ions in binary solvents are predominantly surrounded by molecules of the more polar constituent, namely, water in partially aqueous organic media, such as the methanol-water solutions employed in our study. Grunwald and co-workers [26] reported that simple inorganic ions are, on the contrary, appreciably solvated by the organic solvent molecules in mixed aqueous organic solutions.

The ion cluster formation and binding in solution is part of the reason for their behavior during the electrospray and transport processes. The complexity of ion-solvent interactions is well illustrated by the evidence concerning the relative "basicity" of, for instance, methanol and water. The

coordination of methanol molecules around an alkali-metal ion is enhanced compared to the coordination of water (Figure 2.3.a and 2.3.b), due to the electron-releasing (+I) effect of the methyl functional groups involved. This electronic effect increases the electron density on the oxygen atom, therefore increasing its donor character, that is, the coordination affinity for the metal ion. In the case of dimethylether, the effect is even more significant, two methyl groups being now responsible for the increased binding ability of the oxygen atom in the ligand (Figure 2.3.c).

A similar experiment, conducted with a solution of 0.1 M potassium chloride in 1-propanol, is useful for the partial assessment of the solvation trend within a homologous series of alcohols. The temperature of the transfer capillary was in this case 120 C. Unlike the methanol solutions, according to the appearance of the ES-MS spectrum (Figure 2.4), there is no indication of intermolecular condensation of the solvent molecules involved in coordination. Propanol and propanol-water adducts are present with variable coordination numbers between 1 and 4. The peak intensity of the uncomplexed metal ion (K^+) is significantly lower compared to its intensity in methanol solution. This is due to a more favored complexation of K^+ by the alcohol molecules, facilitated by an increased donor character of 1-propanol.

By increasing the temperature of the transfer capillary to 160 C, the appearance of the ES-MS spectrum changes (Figure 2.5). Smaller relative peak intensities for the adducts containing water, such as m/z 177 and m/z

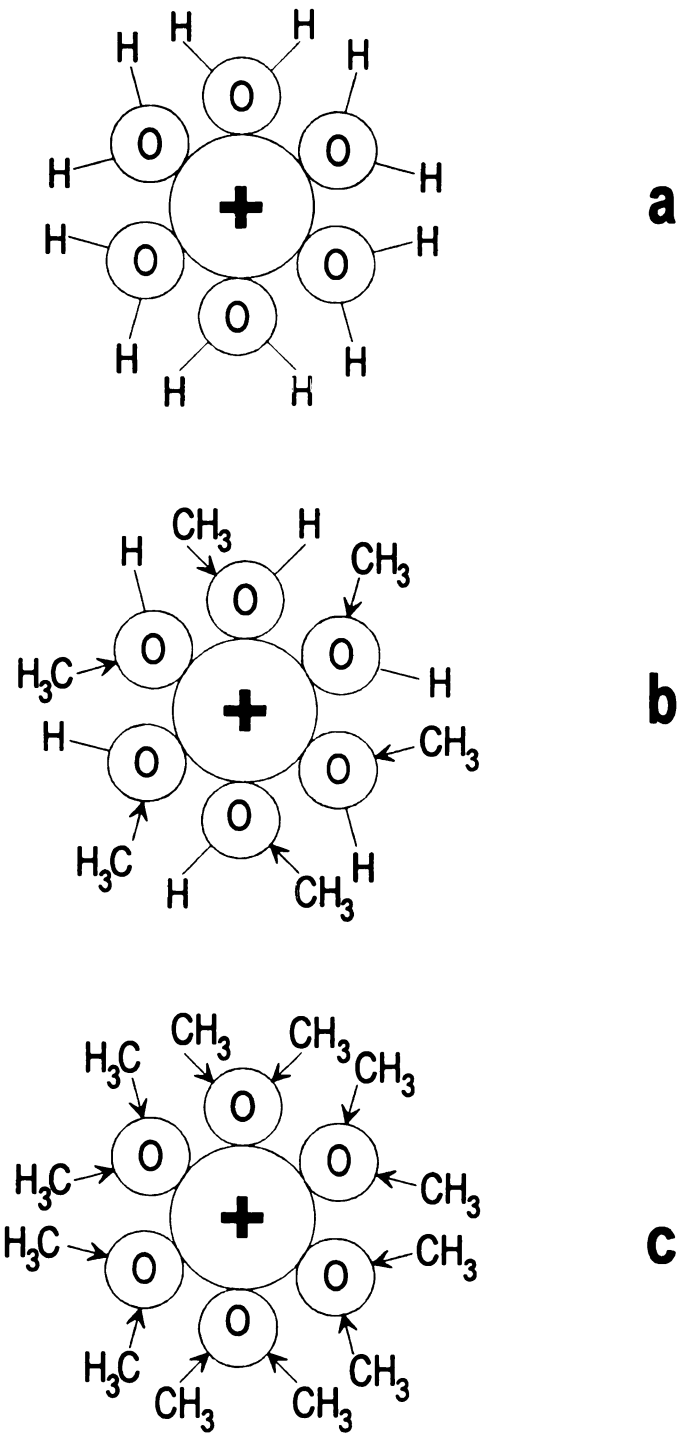

Figure 2.3 *Generic structures of primary solvation shells around an alkali-metal ion. Ligand: (a) water, (b) methanol, and (c) dimethylether*

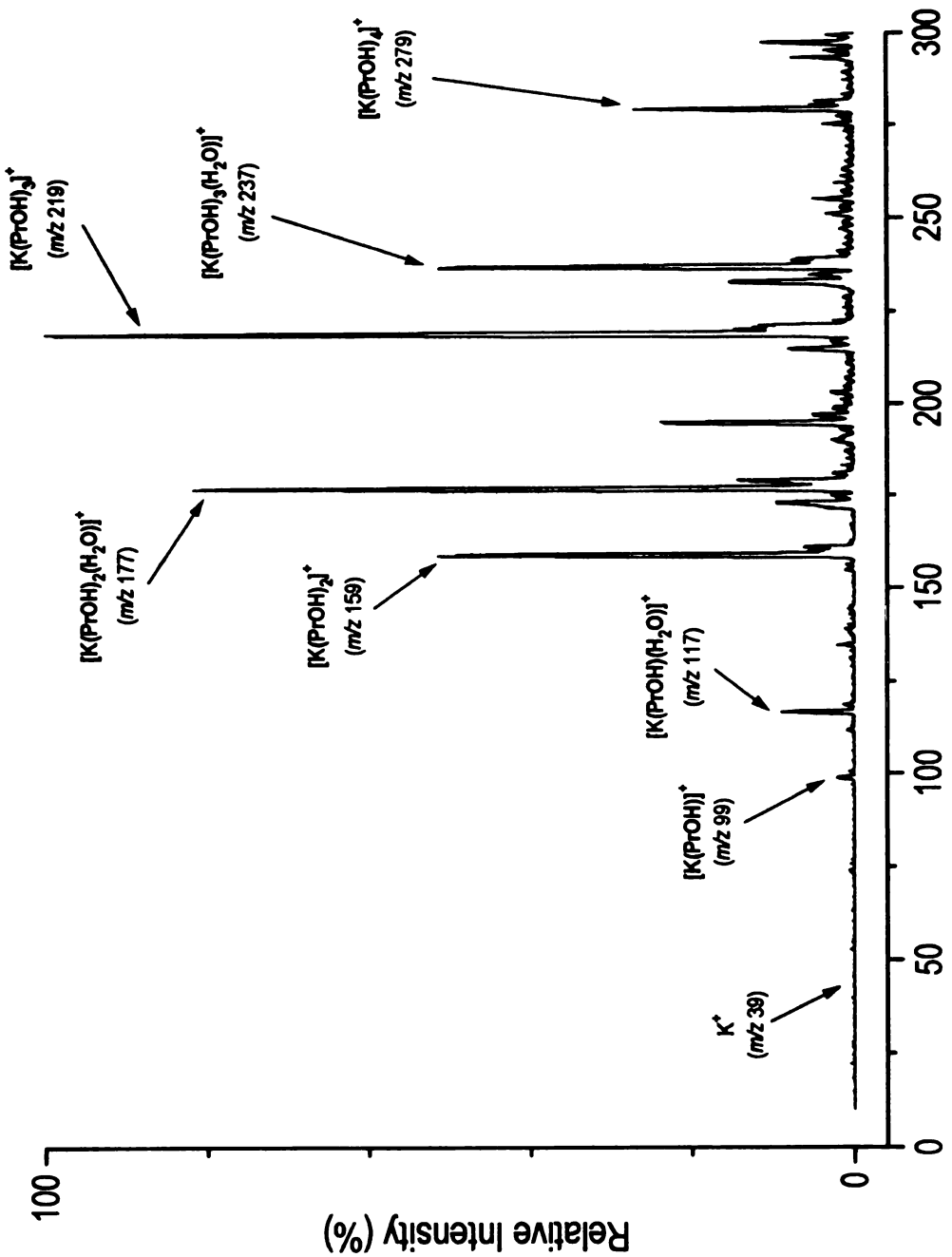

Figure 2.4 *ES-MS spectrum of KCl in 1-propanol. Capillary temperature = 120 C*

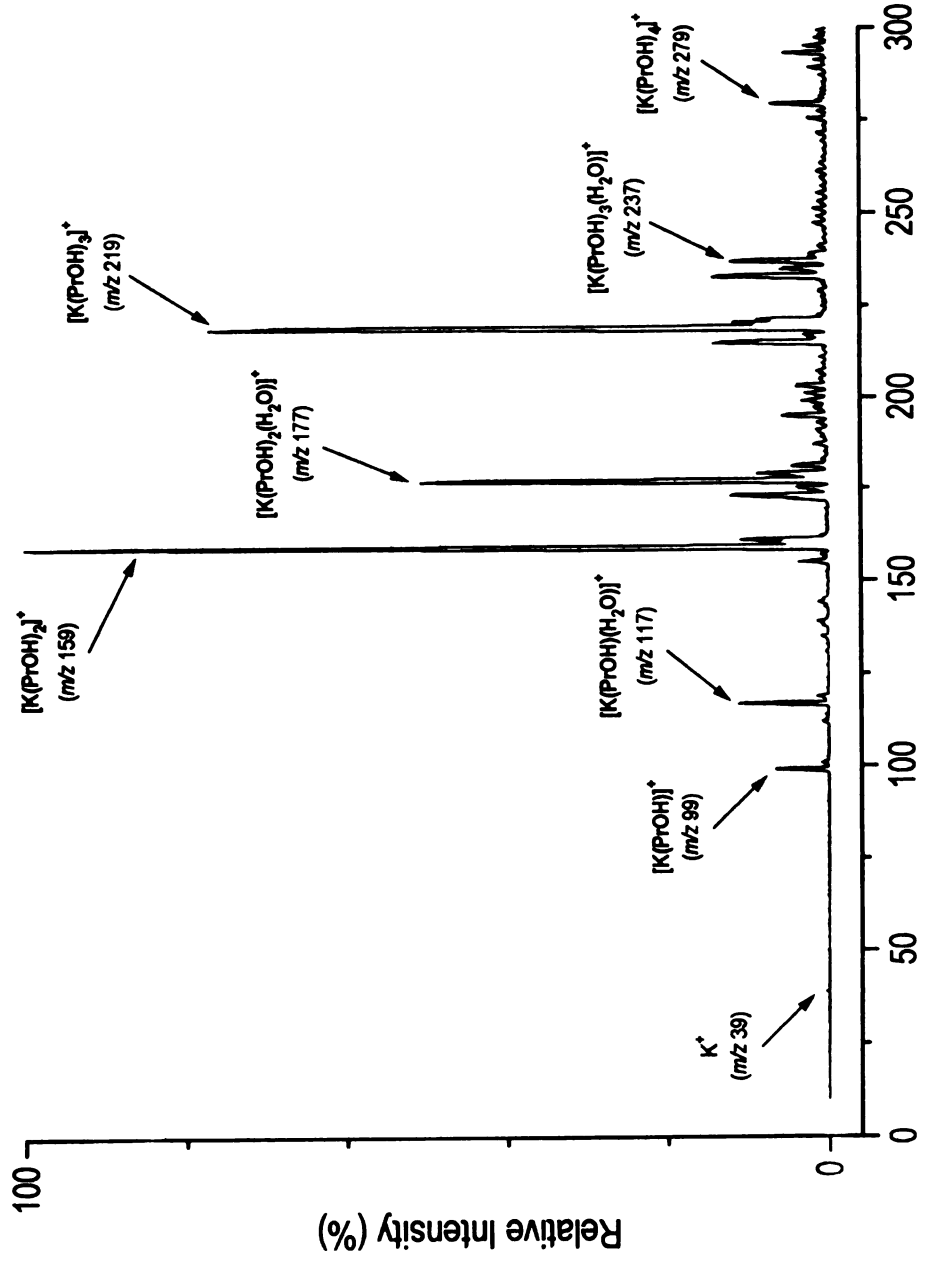

Figure 2.5 *ES-MS spectrum of KCl in 1-propanol. Capillary temperature = 160 C*

237, denote a lower "survival" rate of such species during their transfer through the electrospray interface. The relative intensities of all-propanol adducts, such as *m/z* 159 and *m/z* 219 increases, these ions being probably products of in-source, heat-induced dehydration of the species at *m/z* 177 and *m/z* 237, respectively. No quantitative correlation between the peak intensities and the extent of water loss from the coordination shells can be found, due to the fact that the solvation energies of the adducts involved are unknown. However, the qualitative conclusion regarding the binding strength between the metal ion and the two ligands is consistent with the difference in the donor character of water and 1-propanol.

$[K(PrOH)(H_2O)]^+$ (*m/z* 117) is an apparent exception to the above rationale, its ionic abundance slightly increasing with an increase in the capillary temperature, while the peak intensity of its immediate dehydration product $[K(PrOH)]^+$ (*m/z* 99) follows the trend. This is consistent with the assumption that, from a mechanistic point of view, $[K(PrOH)(H_2O)]^+$ is an intermediate in a multiple-step fragmentation of heavier propanol-water adducts, a process that ultimately leads to the formation of $[K(PrOH)]^+$ or even K^+.

Due to its versatility and relative simplicity, ES-MS is perfectly suited for studying the strength of such metal-ligand interactions in a variety of solvents. By modifying the operational parameters of electrospray and/or the interface voltage or temperature settings, various degrees of desolvation can

be achieved. Chapter 3 consists of a more detailed discussion about specific processes that occur during ion formation, desolvation, and transport.

References

1. Schulten, H. M. *Int. J. Mass Spectrom. Ion Phys.* **1979**, *32*, 97.
2. Budzikiewitz, H.; Linscheid, M. *Biomed. Mass Spectrom.* **1977**, *4*, 103.
3. Detter, L. D.; Walton, R. A. *Polyhedron*, **1986**, *5*, 1321.
4. Day, R. J.; Unger, S. E.; Cooks, R. G. *Anal. Chem.* **1980**, *52*, 557A.
5. Sundqvist, B.; McFarlane, R. D. *Mass Spectrom. Rev.* **1985**, *4*, 421.
6. Karas, M.; Killenkamp, F. *Anal. Chem.* **1988**, *60*, 2299.
7. Cochran, R. L. *Appl. Spectrosc. Rev.* **1986**, *22*, 137.
8. Miller, J. M. *Mass Spectrom. Rev.* **1989**, *9*, 319.
9. Hodges, R. V.; Beauchamp, J. L. *Anal. Chem.* **1976**, *48*, 825.
10. Allison, J.; Ridge, P. D. *J. Am. Chem. Soc.* **1979**, *101*, 4998.
11. Bombick, D.; Pinkston, J. D.; Allison, J. *Anal. Chem.* **1984**, *56*, 396.
12. Marcus, Y. *Ion Solvation*, John Wiley & Sons Ltd.: Chichester-New York-Brisbane-Toronto-Singapore, 1985, p 12.
13. Kebarle, P.; Davidson, W. R.; French, M.; Cumming, J. B.; McMahon, T. B. *Disc. Faraday Soc.* **1977**, *64*, 220.
14. Kebarle, P. Ann. Rev. *Phys. Chem.* **1977**, *28*, 445.
15. Agnes, G. R.; Horlick, G. *Appl. Spectrosc.* **1994**, *48*, 655.
16. Cheng, Z. L.; Siu, K. W. M.; Guevremont, R.; Berman, S. S. *J. Am. Soc. Mass Spectrom.* **1992**, *3*, 281.
17. Jayaweera, P.; Blades, A. T.; Ikonomou, M. G.; Kebarle, P. *J. Am. Chem. Soc.* **1990**, *112*, 2452.

18. Colton R.; Kläui, W. *Inorg. Chimica Acta* **1993**, *211*, 235.

19. Wahl, K. L.; Stromatt, R. W.; Blanchard, D. L. In *Proceedings of the 43rd ASMS Conference on Mass Spectrometry and Allied Topics*, Atlanta, GA, May 21-26, 1995.

20. Xu, Y.; Zhang, X.; Yergey, A. L. In *Proceedings of the 43rd ASMS Conference on Mass Spectrometry and Allied Topics*, Atlanta, GA, May 21-26, 1995.

21. Wang, J.; Ke, F.; Guevremont, R.; Siu, K. W. M. In *Proceedings of the 43rd ASMS Conference on Mass Spectrometry and Allied Topics*, Atlanta, GA, May 21-26, 1995.

22. Van Berkel, G. J.; McLuckey, S. A.; Glish, G. L. In *Proceedings of the 39th ASMS Conference on Mass Spectrometry and Allied Topics*, Nashville, TN, May 19-24, 1991.

23. Smith, R. M.; Martell, A. E. *Critical Stability Constants*, vol. 4: Inorganic Complexes; Plenum: New York, 1981, p 135.

24. *Handbook of Chemistry and Physics*, 65th ed.; CRC Press, Inc.: Boca Raton, Florida, 1984.

25. Schneider, H. In *Solute-Solvent Interactions*; Coetzee, J. F. and Ritchie, C. D., Eds.; Marcel Dekker: New York and London, 1969.

26. Grunwald, E.; Baughman, G.; Kohnstam, G. *J. Am. Chem. Soc.* **1960**, *82*, 5201.

Chapter 3

"Source CAD" - An Advantage or a Hindrance?

Introduction

As discussed in Chapter 2, in order to take advantage of the main feature of electrospray "ionization", namely, achieving minimum fragmentation of preexisting ionic species during their transfer from solution into the gas phase, all operational parameters must be carefully chosen and closely monitored. Electrospray voltage, solution flow rate, sheath and auxiliary gas flow rates, voltage and temperature on the interface components, the entire array of ion optics settings, and so on, all affect, in different ways and to various extents, the "deviation" of electrospray from perfection. In other words, they determine the closeness of the appearance of an ES-MS spectrum

to being an ideal reproduction of the ionic composition of a given analyte solution.

Depending on the purpose of a certain experiment, one can determine the most favorable set of parameters, usually at the expense of trading off other potential collateral experimental findings. Three positive-ion modes are common, a metal-ion mode, an ion cluster mode, and an intermediate mode [1], named for the type of information eventually available from the mass spectrum. For instance, for the elemental analysis of metal ions in a liquid matrix one would have to employ a procedure that strips metal adducts of their coordination shells, regardless of their structure and binding strength, to the maximum possible extent. In the ion cluster mode, which this chapter focuses on, the electrospray source is run under so-called "mild" conditions, and the mass spectra are quite complex since the ion-solvent cluster distribution generated during the ES process is preserved relatively intact. With this mode it is possible to determine the solution valence states of the cations, and the data obtained in this mode are generally more representative of solution speciation. The third mode consists of an intermediate approach in which partial declustering occurs, some of the ion clusters may contain counterions, and various species with reduced charge may be observed.

Structural Transformations within the Electrospray Source

A schematic of the dual-stage Finnigan MAT electrospray source is shown in Figure 3.1. Immediately after the liquid droplets emerge from the tip of the electrospray needle, the solvent begins to evaporate. Because of the pressure difference between the chambers at both ends of the transfer capillary, solvent evaporation, ion desolvation, and ion transport all occur during the relatively short time required for the transfer to the first pumping stage. At the end of the capillary, a "steering" voltage is applied, the ions being therefore accelerated. Various degrees of ion fragmentation occur in this stage, during the free jet expansion and ion acceleration, the process being analogous to some extent to CAD that takes place in the collision chamber of an MS/MS experimental arrangement. It was reported that the product ions generated during "source CAD" are more efficiently transferred into the quadrupole mass analyzer than the CAD products in a triple quadrupole tandem system [2].

Thus, the in-source fragmentation can be regarded as a hindrance reducing the ability of ES-MS to provide comprehensive solution chemistry elucidation, or it can be exploited as a tremendous advantage. Many ionic species that preexist in solution or are formed during ion desolvation and transport are very fragile, some are unobtainable through any other gas

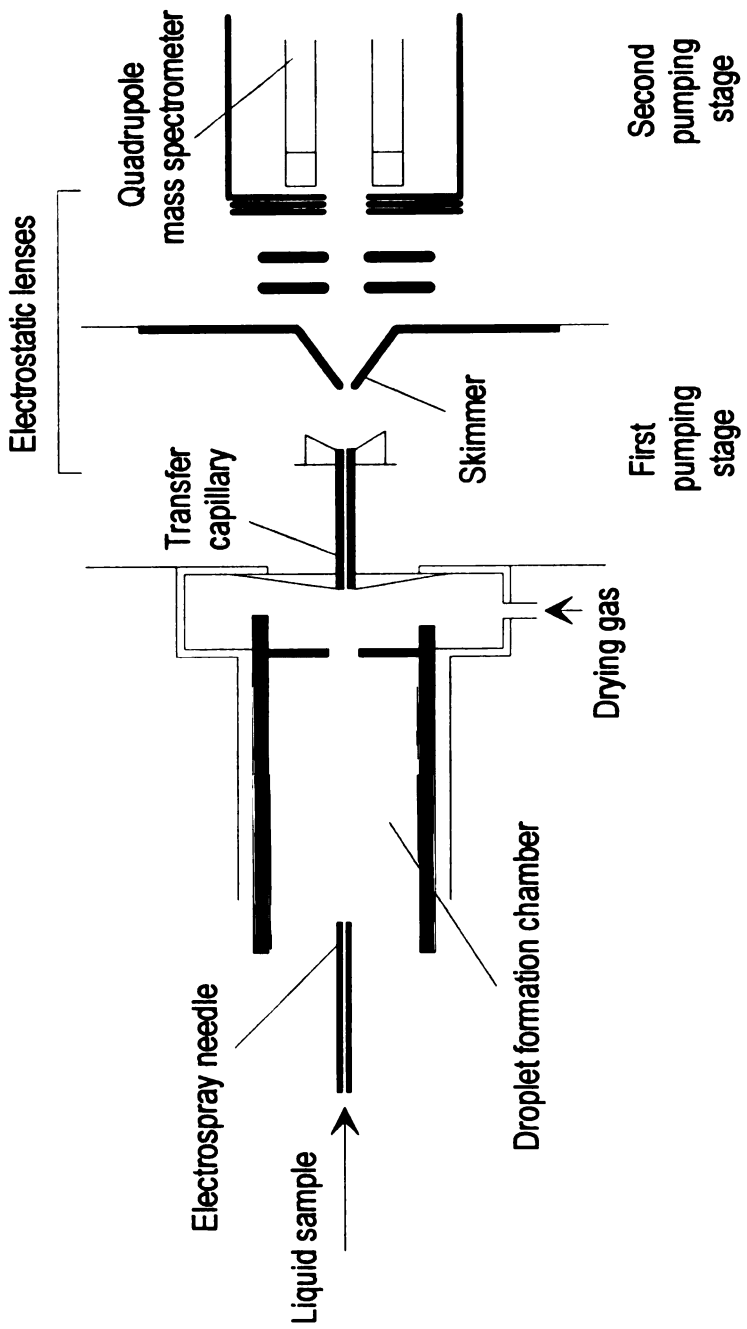

Figure 3.1 *The schematic of an electrospray - mass spectrometer interface*

phase processes, and only a careful and systematic investigation taking into account all processes and phenomena that occur in the electrospray source can be of benefit. This chapter deals with specific aspects and examples of a variety of structural transformations that occur within an electrospray source, including structure-reactivity relationships.

Metal Ion - Solvent Adducts

The ion adduct formation involving certain alkali-metal ions in solutions of two aliphatic alcohols was partially covered in Chapter 2, as a part of the general behavior of metal ions in the electrospray process. The reason one of the most common alcohols, ethanol, though not common in electrospray studies, was not employed in the general study is that it offered us a wealth of fascinating results, worth a separate, more detailed subchapter.

Experimental. Solutions of NaCl and KCl (0.1 M) respectively were made according to the general procedure, by dissolving the salt (ACS grade) in the minimum required amount of distilled water, followed by dilution with dehydrated absolute ethanol (McCormick Distilling Co.). The sample solutions were introduced continuously into the ES source with the aid of a syringe pump (Harvard Apparatus) at a flow rate of 5 μL/min. The electrospray voltage was maintained at 5 kV. The temperature of the transfer capillary was varied between 110 C and

220 C. Argon was used as the collision gas in the CAD experiments. Both ES-MS and MS-MS spectra were acquired using a signal averaging procedure, 60 spectra being averaged throughout the study.

Concerning their general appearance, both ES-MS spectra of NaCl and KCl in ethanol consist of much fewer outstanding peaks than the spectra of methanol solutions of both metals recorded under similar conditions (Figure 2.1 and 2.2). Most of the adducts of both metal ions have structurally identical ligand arrangements around the cation, significant differences being noticeable regarding the intensity of their peaks.

At a capillary temperature of 110 C the ES-MS spectrum of NaCl (Figure 3.2) is dominated by the peaks at *m/z* 147 and *m/z* 179. Other significant peaks present include Na^+ (*m/z* 23), $[Na(EtOH)]^+$ (*m/z* 69), and $[Na(EtOH)_2]^+$ (*m/z* 115). At this point it is not clear, based only on the appearance of ES-MS spectra whether the peak at *m/z* 179 represents a singly charged or a multiply charged ionic cluster. With an increase in the capillary temperature, significant changes in the relative intensities of these and other peaks take place, amid a slight decrease in the total ion current. At 160 C the peak at *m/z* 147 becomes the base peak (Figure 3.3), mainly due to the dramatic decrease in the relative intensity of *m/z* 179. Also, as the temperature of the transfer capillary is raised, the relative intensity of an apparently unexpected peak (*m/z* 287) increases steadily, becoming the base

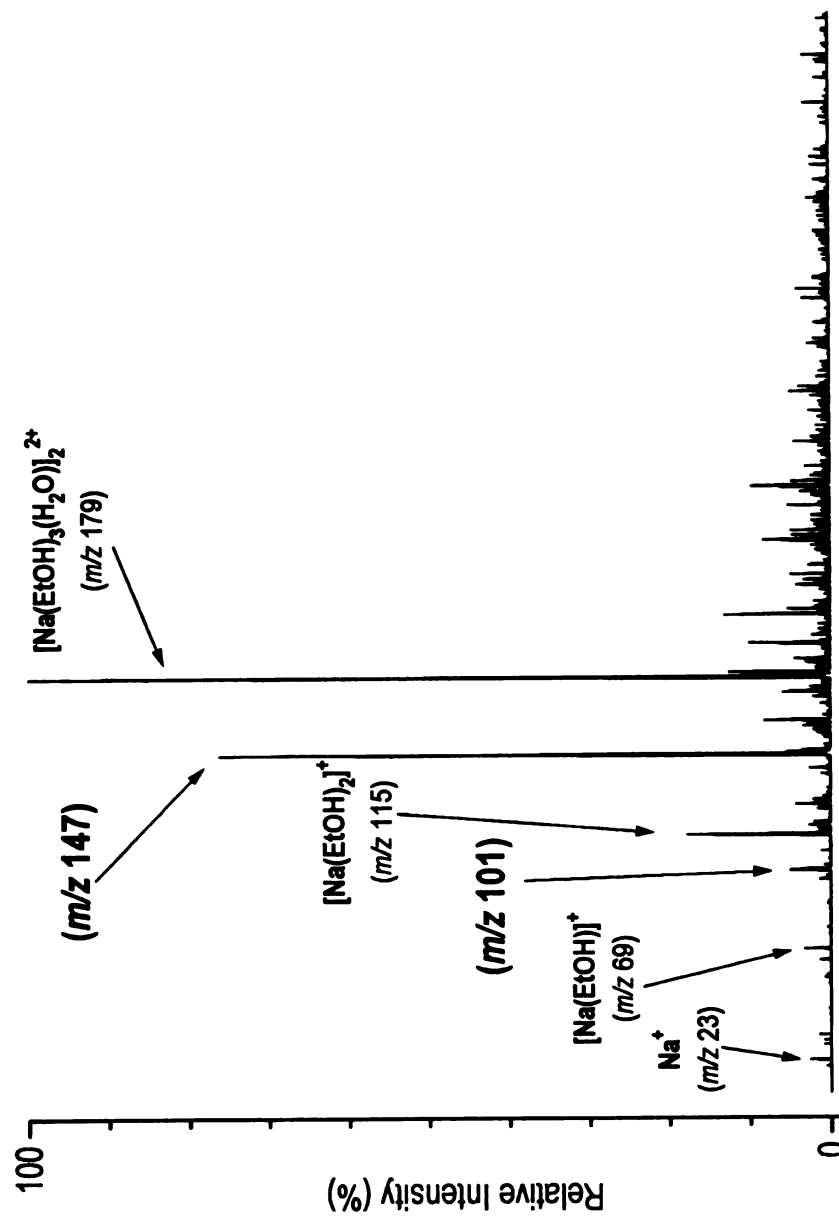

Figure 3.2 *ES-MS spectrum of NaCl in ethanol. Capillary temperature = 110 C*

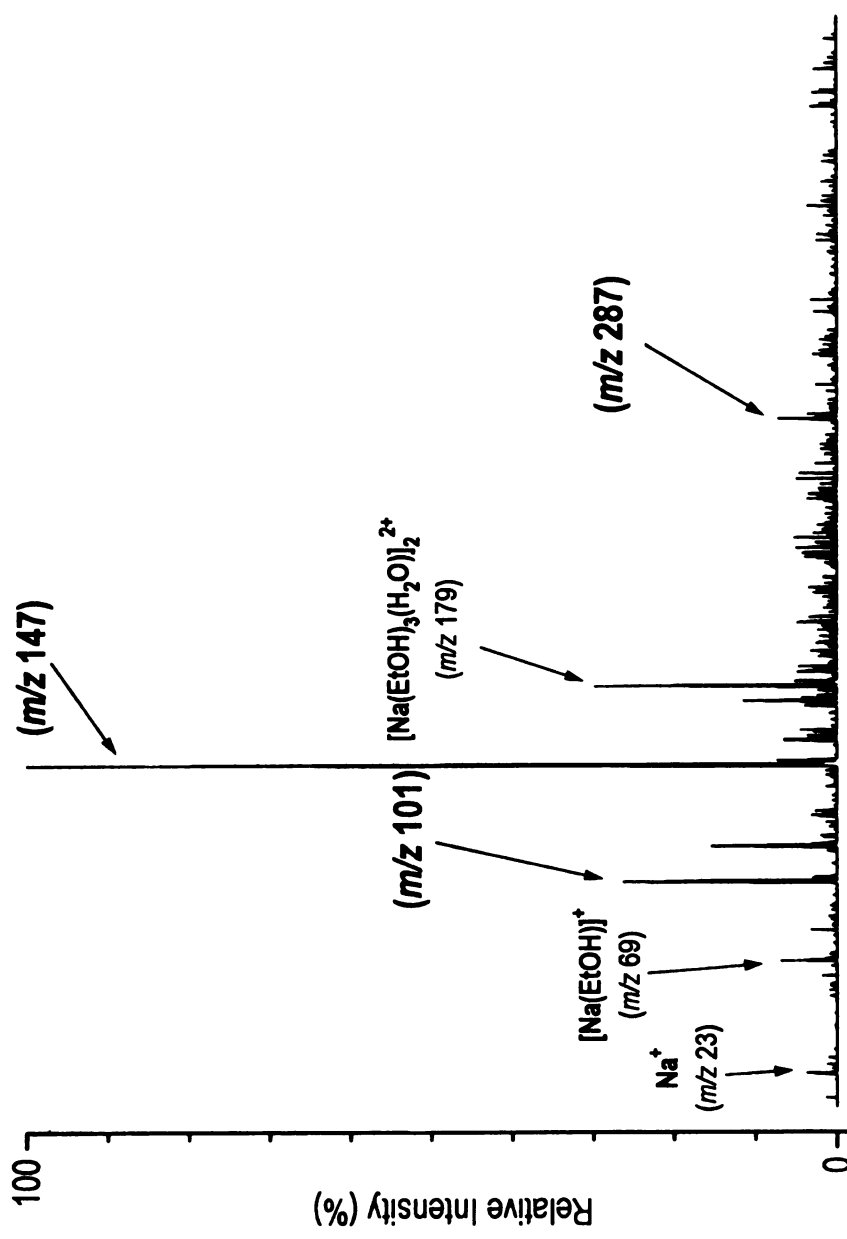

Figure 3.3 *ES-MS spectrum of NaCl in ethanol. Capillary temperature = 160 C*

peak at a temperature of 220 C (Figure 3.4). Again, for the determination of its structure a tandem mass analysis with precursor ion selection is necessary. The peak intensities corresponding to the predominant species in the spectra were rationalized to the total ion current for the entire scan range (*m/z* 10 to *m/z* 450) and are summarized in Table 3.1.

Overall, several conclusions can be drawn regarding the ES-MS spectra of sodium chloride in ethanol:

- The ion abundance of clusters containing water decreases with an increase in the capillary temperature relative to the anhydrous adducts. This is due to the fact that water is less strongly coordinated to the metal cation (see Chapter 2) compared to, for instance, an aliphatic alcohol;
- Adduct stripping is enhanced by a higher temperature, one of the effects being an increase in the peak intensity of Na^+ (*m/z* 23);
- The peak intensity of *m/z* 287 increases, absolutely and relatively, the ion being probably a product of an intermolecular collisionally activated reaction involving solvent molecules.

Potassium chloride solutions behave similarly under identical ES-MS experimental conditions (Table 3.2). There are, however, a few discrepancies between the spectra of potassium solutions versus sodium. The ion of *m/z* 195 (structurally analogous to *m/z* 179 in the ES-MS spectra of sodium

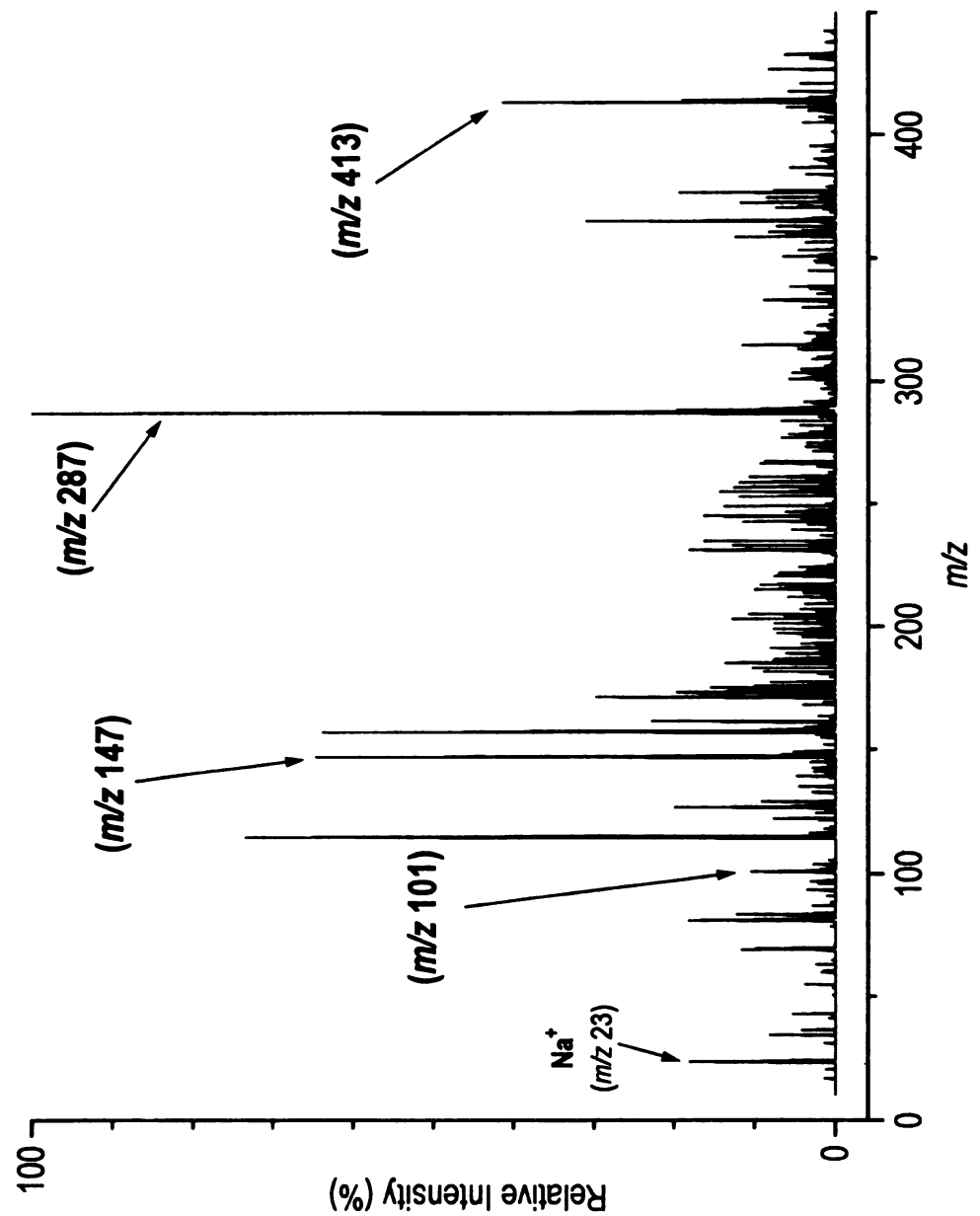

Figure 3.4 *ES-MS spectrum of NaCl in ethanol. Capillary temperature = 220 C*

Table 3.1 *Rationalized peak intensities for the predominant ions in the ES-MS spectrum of NaCl in ethanol, as a function of the transfer capillary temperature*

Capillary Temperature (C)	Rationalized Peak Intensity* (%)							
	m/z 23	m/z 69	m/z 101	m/z 115	m/z 147	m/z 179	m/z 287	m/z 413
110	1.2	1.5	2.2	7.8	33	44	1.1	0
140	1.9	1.3	9.0	5.2	35	40	4.6	0.5
160	1.8	3.4	12	7.1	49	15	3.5	1.5
170	3.3	2.6	11	7.8	42	10	5.3	2.9
180	4.3	2.8	8.9	14	47	5.7	5.1	2.1
200	2.8	3.1	6.4	25	26	1.5	11	2.7
220	3.8	2.4	2.2	15	14	0.5	21	8.7

* Denotes rationalizing the peak intensity to the total ion current for the scan range *m/z* 10 to *m/z* 450

Table 3.2 *Rationalized peak intensities for the predominant ions in the ES-MS spectrum of KCl in ethanol, as a function of the transfer capillary temperature*

Capillary Temperature (C)	Rationalized Peak Intensity* (%)							
	m/z 39	m/z 85	m/z 117	m/z 131	m/z 147	m/z 195	m/z 303	m/z 429
110	1.6	6.2	34	4.2	1.9	25	6.0	1.0
140	10	3.4	38	1.8	1.0	8.7	15	1.6
160	13	5.5	36	1.2	4.6	3.6	15	2.5
170	25	2.6	17	0.4	3.1	0.7	26	3.7
180	25	1.6	5.3	0.4	2.6	0.3	52	5.7
200	20	1.3	1.0	0	1.2	0	70	7.6
220	19	1.2	0.5	0	0.5	0	61	9.8

* Denotes rationalizing the peak intensity to the total ion current for the scan range *m/z* 10 to *m/z* 450

solutions) is depleting at a much faster rate as the temperature increases. This is due to the fact that the potassium adduct is probably less stable in the gas phase compared to its sodium counterpart. The surprising appearance of a possible product of an intermolecular collisionally activated reaction at *m/z* 287 in the case of sodium solutions is confirmed once again when potassium is involved. Furthermore, the peak intensity of the analogous ionic species at *m/z* 303 increases more steeply with the temperature of the transfer capillary (Figure 3.5, 3.6, and 3.7). Thus the hypothesis that an intermolecular condensation/dehydrogenation process involving probably six ethanol molecules may lead to the *in situ* formation of 18-crown-6 ether, known for its very high affinity for alkali-metal ions.

A tandem mass spectrometric experiment was performed in order to elucidate the charge states and structures of some unassigned peaks present in the ES-MS spectra. First, CAD of ions of *m/z* 195 was performed aiming at the determination of their fragmentation path and charge state. The product ion spectrum is shown in Figure 3.8. A very "clean" dissociation of the precursor ion generates a symmetrical fragmentation pattern, somewhat characteristic of doubly charged precursor ions (see Chapter 6). In this case however, the product ions are not symmetrically distributed on both sides of the precursor on the m/z scale, but they are both the result of an identical neutral loss, the difference between the two reaction pathways being the

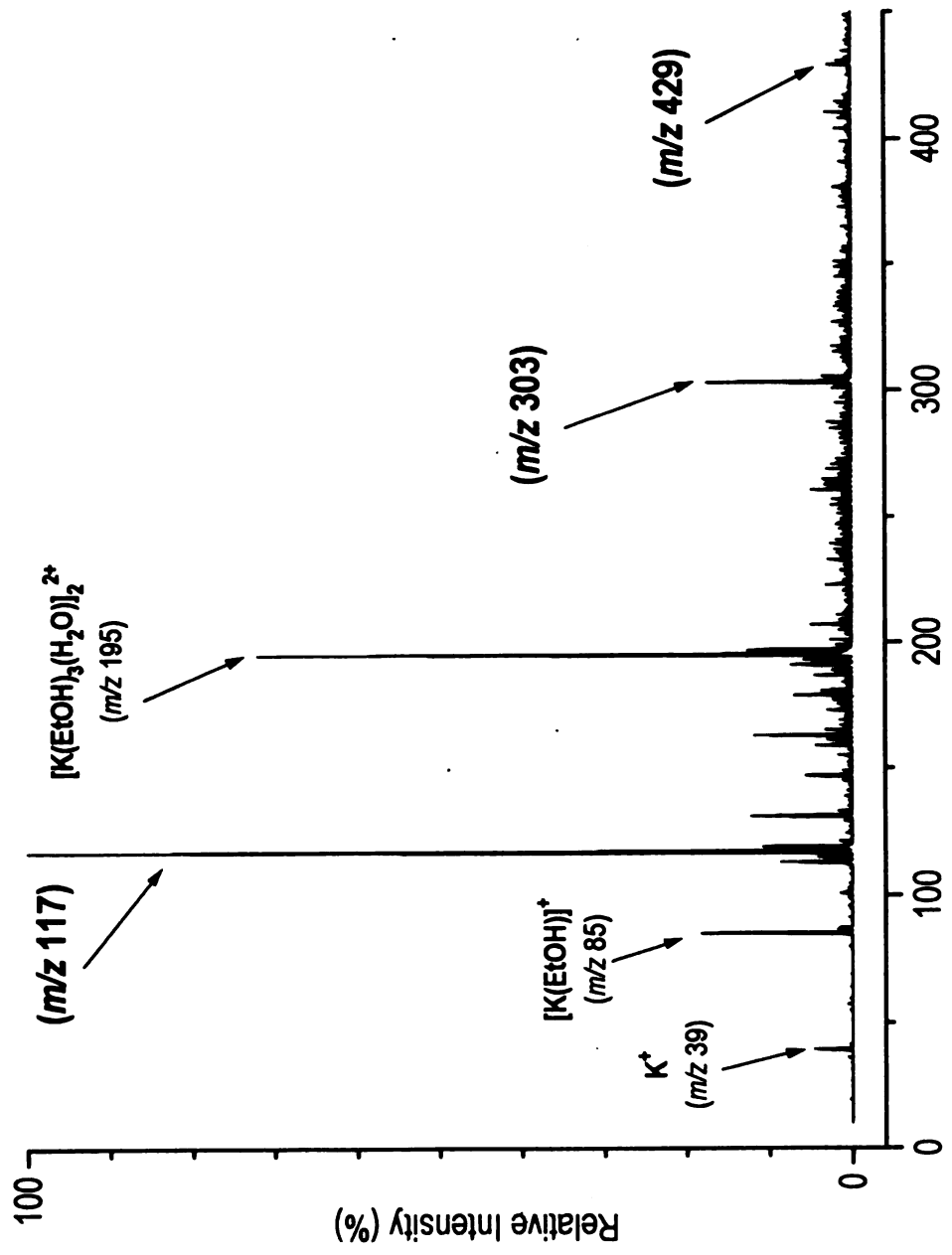

Figure 3.5 *ES-MS spectrum of KCl in ethanol. Capillary temperature = 110 C*

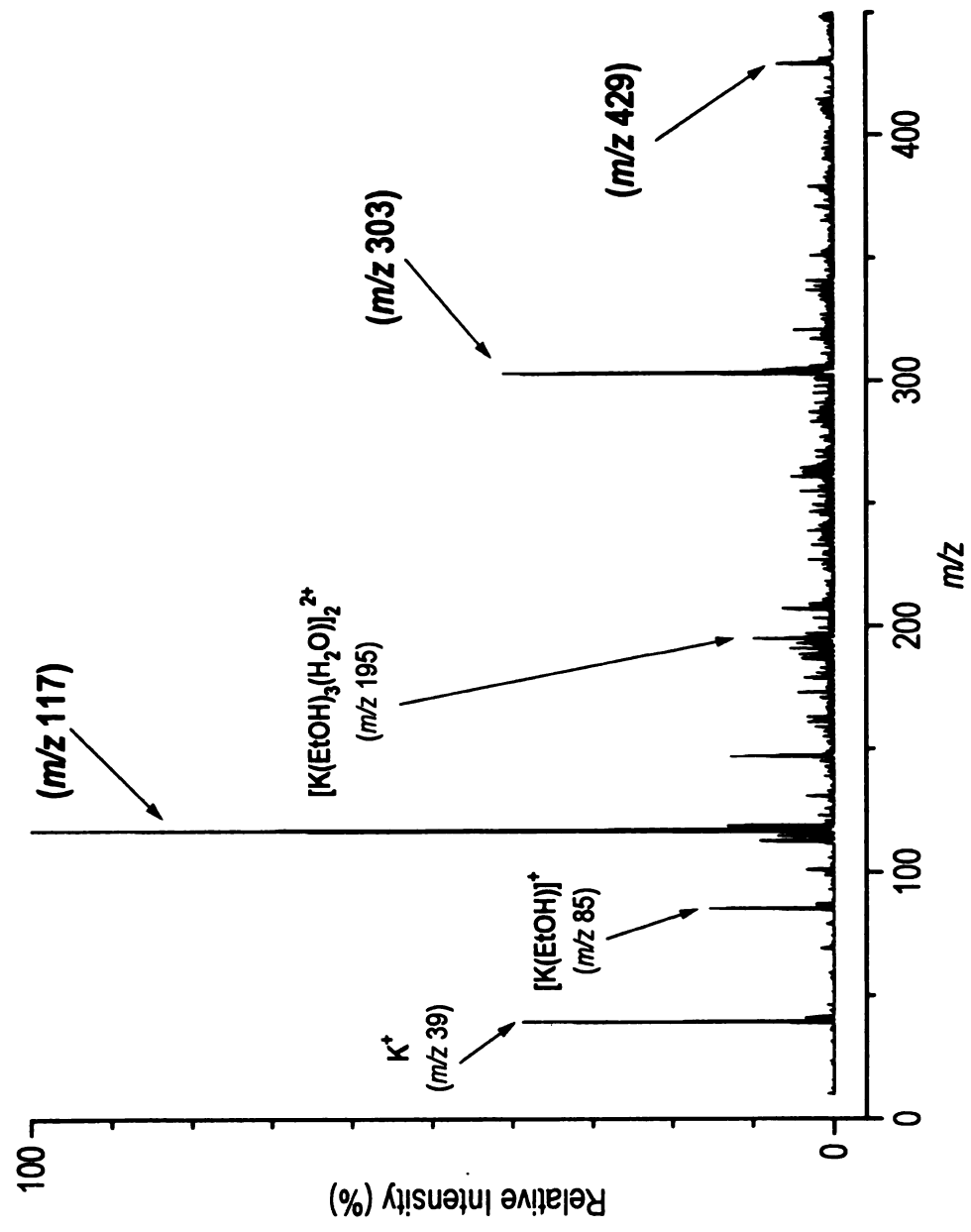

Figure 3.6 *ES-MS spectrum of KCl in ethanol. Capillary temperature = 160 C*

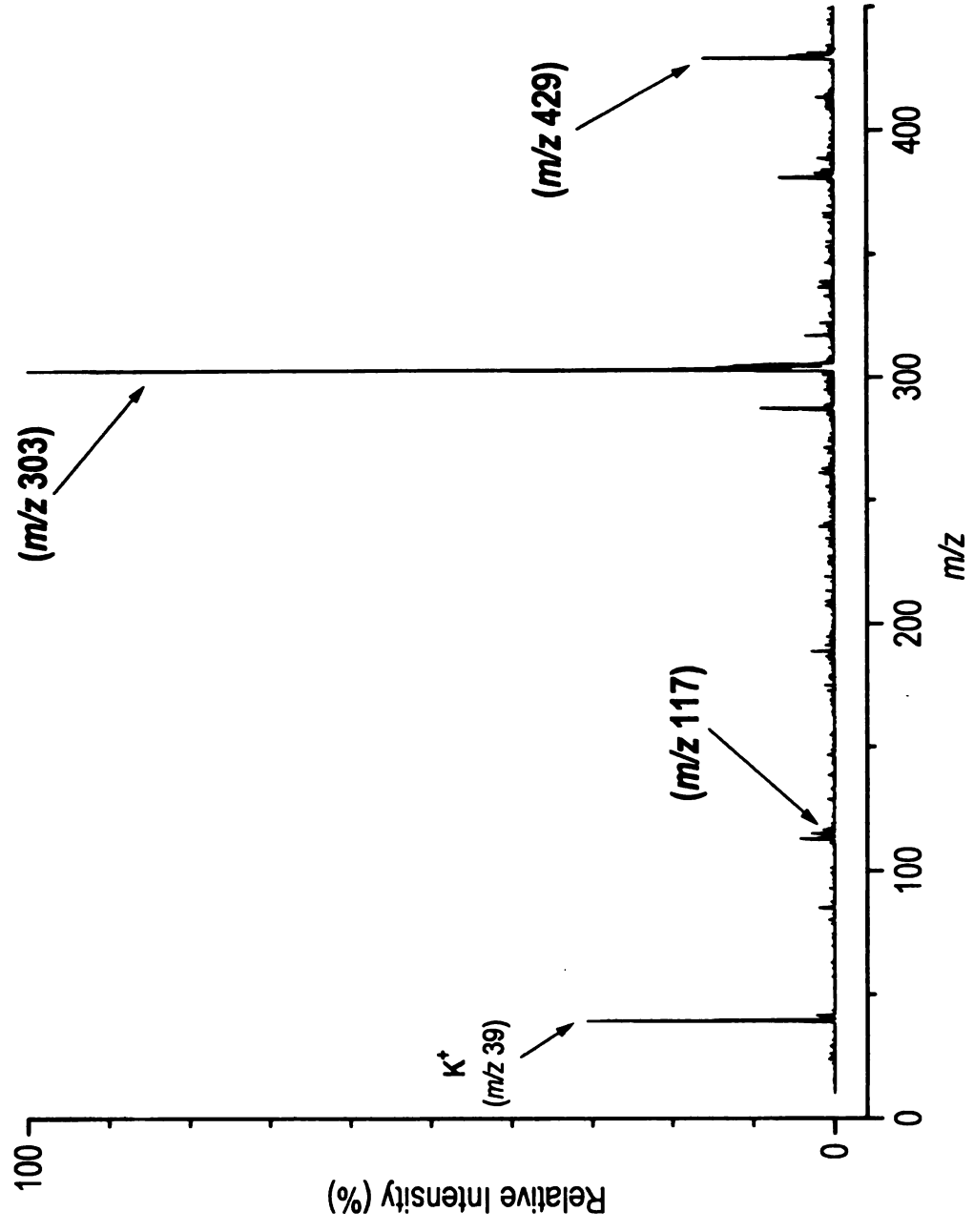

Figure 3.7 *ES-MS spectrum of KCl in ethanol. Capillary temperature = 220 C*

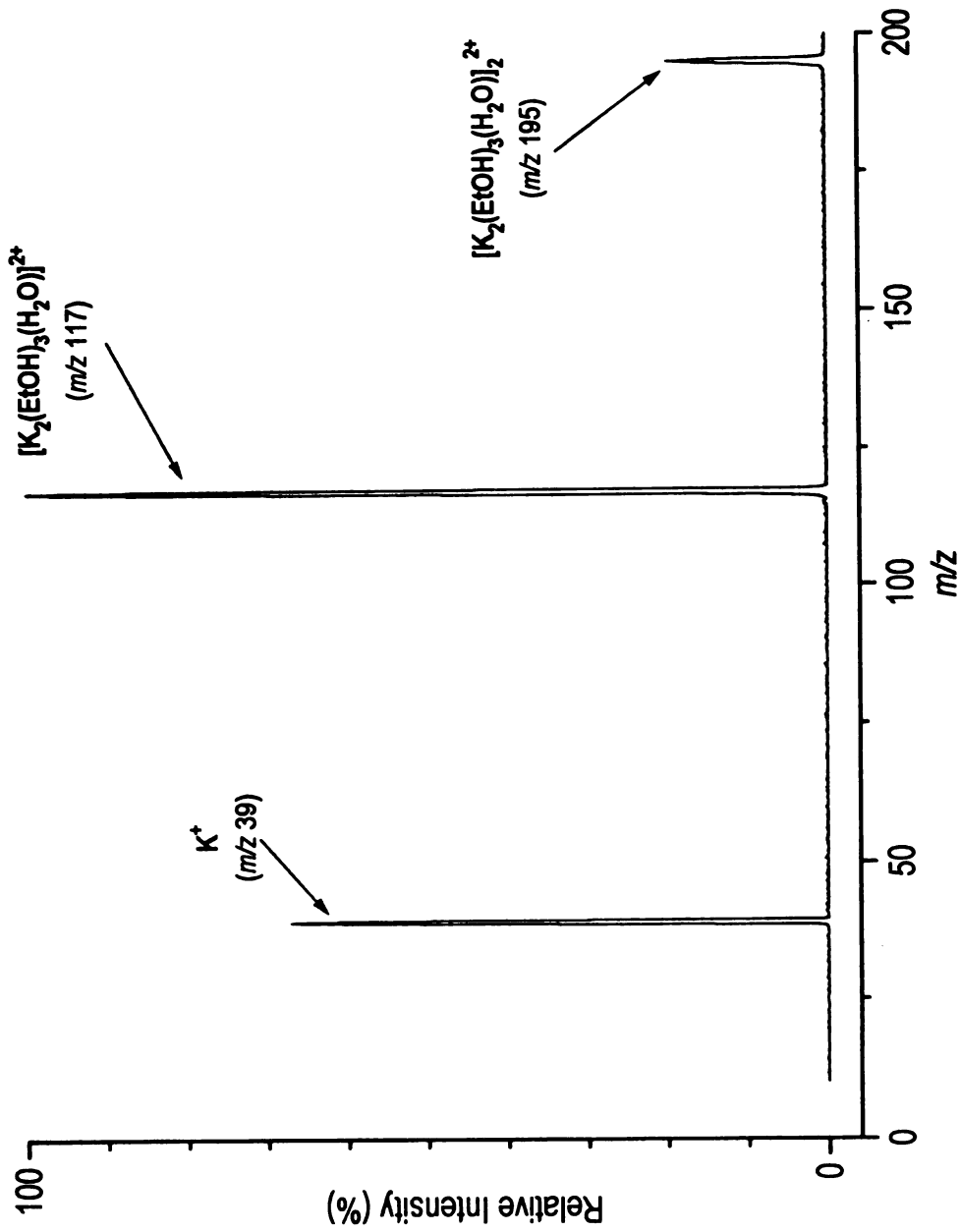

Figure 3.8 *MS/CAD/MS product ion spectrum of m/z 195*

occurrence of charge reduction. The proposed mechanism is given in Equations 3.1 and 3.2.

$$\underset{(m/z\ 195)}{[K(EtOH)_3(H_2O)]_2^{2+}} \longrightarrow \underset{(m/z\ 117)}{[K_2(EtOH)_3(H_2O)]^{2+}} + 3\ EtOH + H_2O \qquad (3.1)$$

$$\underset{(m/z\ 195)}{[K(EtOH)_3(H_2O)]_2^{2+}} \longrightarrow \underset{(m/z\ 39)}{2\ K^+} + 6\ EtOH + 2\ H_2O \qquad (3.2)$$

Thus, the peaks at *m/z* 117 and *m/z* 195 in the ES-MS spectra of KCl solutions in ethanol represent doubly charged ionic species that originate in solution. Additional proof is provided in the product ion spectrum that results in CAD of the ions of *m/z* 117 (Figure 3.9). The collision energy of the precursor ions was 20 eV, and the collision gas pressure 0.3 mTorr. The sole fragmentation product is the bare metal ion K^+ (*m/z* 39), in agreement to Equation 3.3.

$$\underset{(m/z\ 117)}{[K_2(EtOH)_3(H_2O)]^{2+}} \longrightarrow \underset{(m/z\ 39)}{2\ K^+} + 3\ EtOH + H_2O \qquad (3.3)$$

Apparently, according to our preliminary ion assignments, most of the adducts of interest contain the metal ions. Tandem mass spectrometry with CAD also provides a confirmation of this fact, by means of a "reverse" analysis approach, namely a product ion selection in conjunction to the mass analysis of its precursors. Therefore K^+ (*m/z* 39) was selected as the product

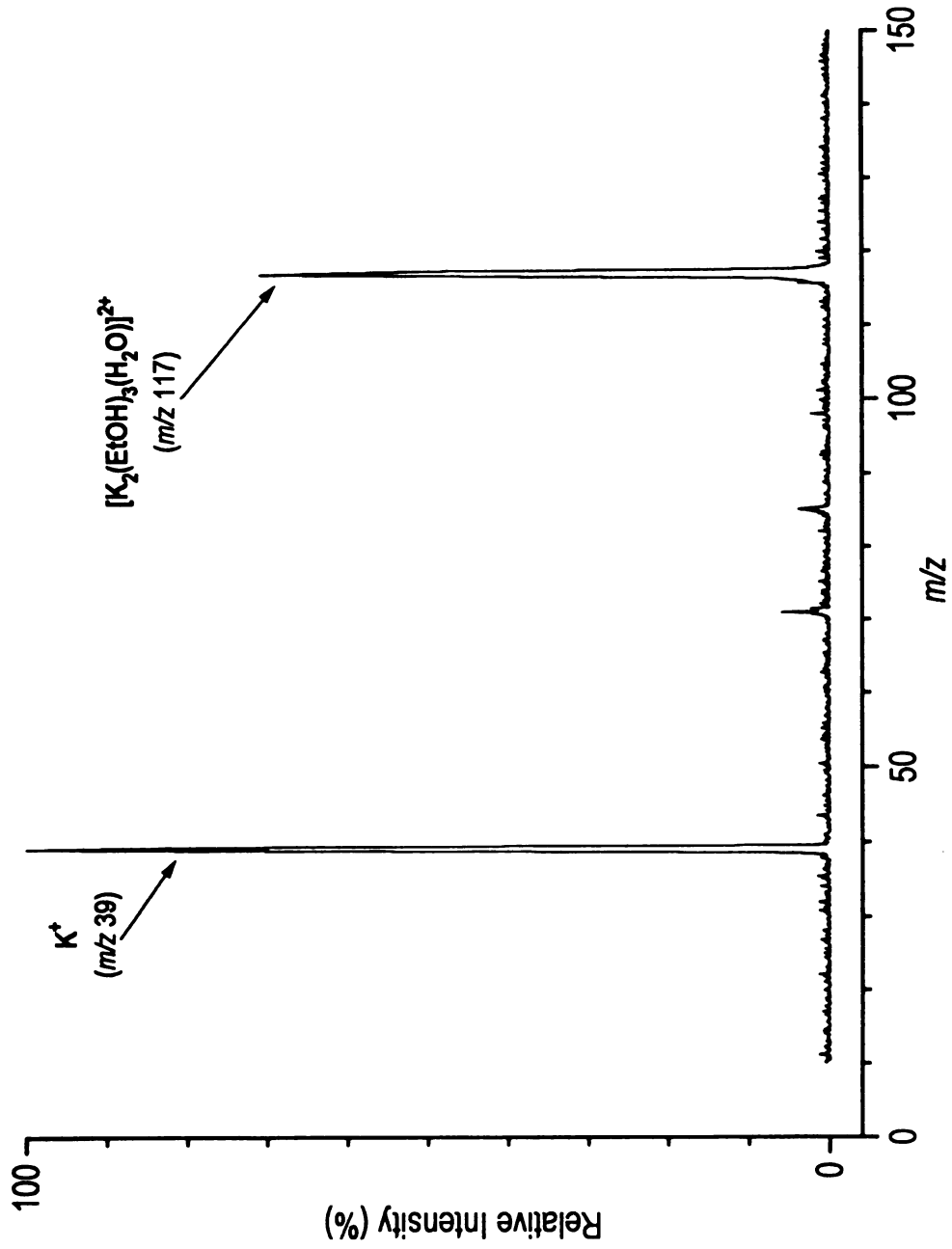

Figure 3.9 *MS/CAD/MS product ion spectrum of m/z 117*

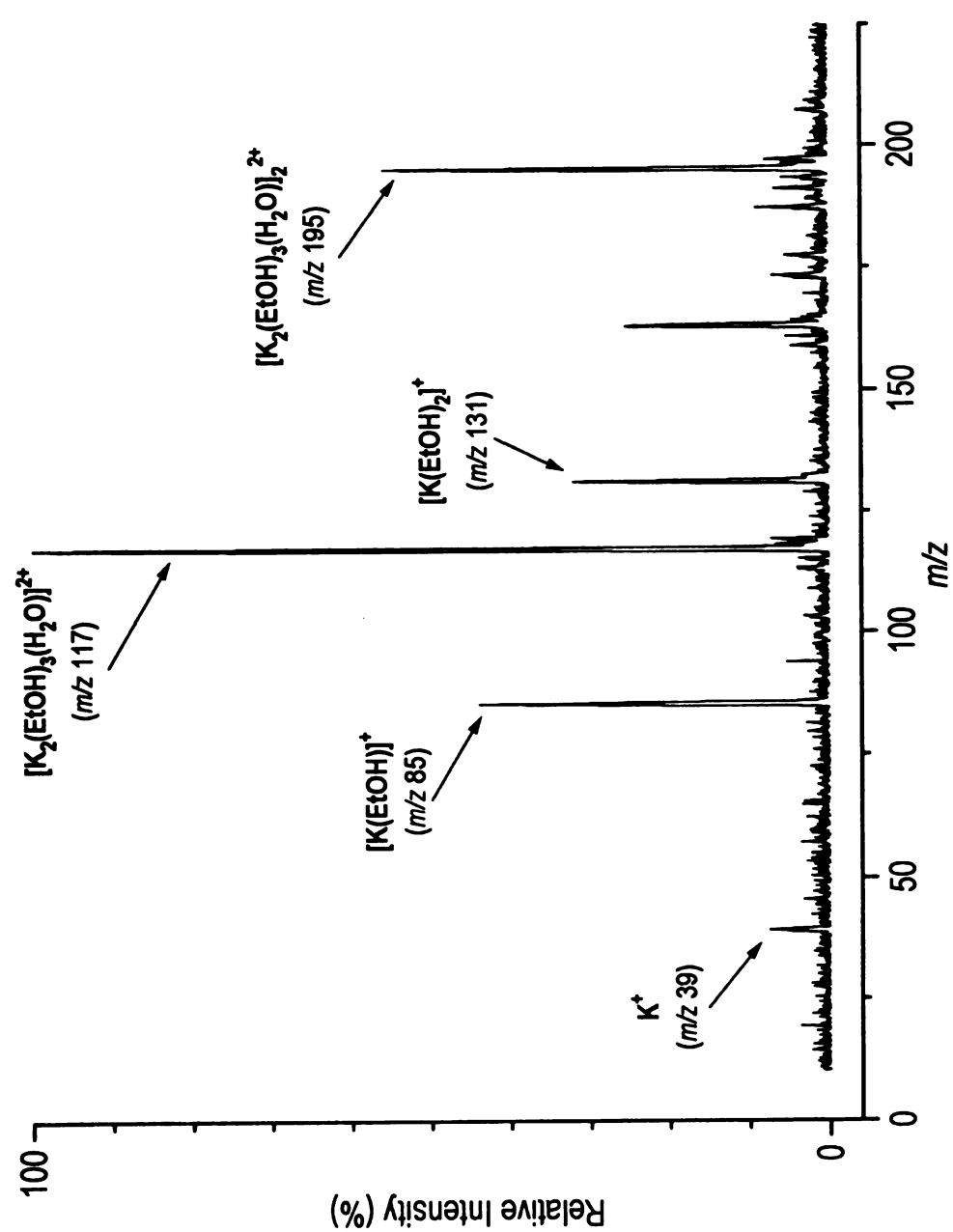

Figure 3.10 *MS/CAD/MS precursor ion spectrum of m/z 39*

ion of interest, and the CAD spectrum containing the precursor ions which were fragmented into K^+ is presented in Figure 3.10. The collision energy employed was 30 eV, and the collision gas pressure 0.4 mTorr. As it can be seen, all the adducts of *m/z* 85, *m/z* 117, *m/z* 131, *m/z* 163, and *m/z* 195 include potassium in their structures. The reason the peak at *m/z* 303 is not present in this precursor ion spectrum is not that it does not contain potassium, but rather that the dissociation did not occur under the specific conditions applied, the collisions induced being energetically insufficient for the fragmentation of a complex with a very high stability, exhibited both in solution and in the gas phase. A similar experiment for sodium results in the ruling that the ions of *m/z* 101 and *m/z* 179, respectively, are doubly charged as well, and structurally analogous to the potassium-containing ions of *m/z* 117 and *m/z* 195, respectively.

References

1. Agnes, G. R.; Horlick, G. *Appl. Spectrosc.* **1994**, *48*, 655.

2. Voyksner, R. D.; Pack, T. *Rapid Commun. Mass Spectrom.* **1991**, *5*, 263.

Chapter 4

Interaction of Metal Ions with Macrocyclic Ligands

Introduction

Although various aspects of metal ion-ligand interactions had been studied before 1974 [1,2], it was then that Cram [3] introduced the term "host-guest chemistry" to describe the developing field of synthetic complexation chemistry, exemplified by cryptands, crown ethers, and related structures. Host-guest chemistry is primarily concerned with elucidating the "rules of non-covalency" [4], involved in the recognition and binding of a guest by a specific receptor (host).

A host is usually a large and geometrically concave organic molecule that can non-covalently interact with and bind a guest. Hosts may be acyclic, macrocyclic, or oligomeric, and possess cavities or clefts into which the guest

fits. The host's recognition site or sites for the guest may be inherent in its normal structure or may be organized during the process of interaction. The binding sites may interact with guests by combinations of various non-covalent means, such as hydrogen-bonding, ion-ion, ion-dipole, π, van der Waals, electron donor-acceptor, and hydrophobic interactions. A certain degree of covalency may sometimes exist, along with non-covalent interactions, depending on the nature and structure of the guest and the particular coordination sites involved.

Guests are simpler organic or inorganic molecules or ions, whose epitopes present divergent binding sites complementary in charge and steric requirements to the host. The term "epitope" defines the part of the guest that actually interacts with the host, an extension of the use of the term in immunology, where the epitope is the portion of the antigen actually recognized by an antibody [4]. Typical guests include metal ions, ammonium ions, polar neutral species, hydrogen-bonding compounds, aromatic substrates, diazonium salts, halides, and many others. The interaction of a host with a guest produces a complex. One of the most significant properties of macrocyclic ligands, such as crown ethers and analogous structures is the formation of "host-guest"-type complexes with a wide variety of metal ions.

Crown Ethers and Aza-Analogs

The macrocyclic polyethers, termed "crown ethers" from their structural resemblance to crowns, were first synthesized by Pedersen [5] and since then cyclic polyethers containing up to twenty oxygen atoms have been prepared [6,7]. Crown ethers were among the first synthetic reagents found to bind strongly to alkali metal cations and they have been widely used to transfer alkali metal salts into non-aqueous phases, and in solvent extraction studies [4].

The structural features of polyether macrocyclic ligands are represented by systems containing the unsubstituted 1,4,7,10,13,16-hexaoxacyclooctadecane (L), commonly named 18-crown-6 (Figure 4.1).

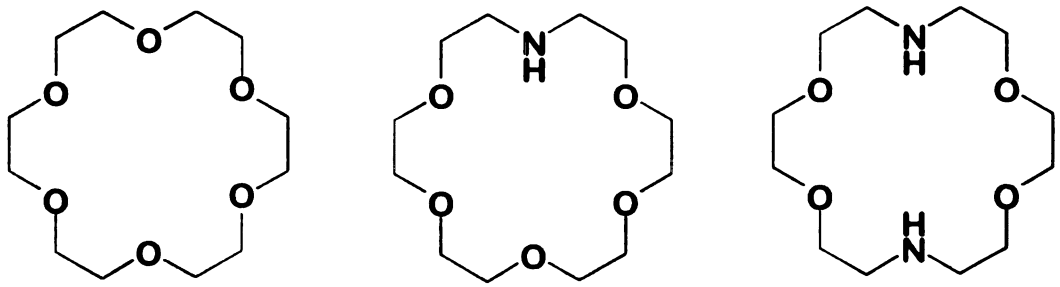

L L' L"

18-crown-6 aza-18-crown-6 diaza-18-crown-6

Figure 4.1 *The structures of the 18-member macrocyclic ligands considered in the present complexation studies*

Substituting one or more oxygen atoms with other heteroatoms, such as nitrogen or sulfur dramatically changes the complexation ability of the ligand and the properties of the resulting complexes, both in solution and in the gas phase [8]. Our comparative study focuses on the behavior of potassium and silver complexes with a series of macrocyclic systems having the 18-crown-6 hexaether skeleton, namely 18-crown-6 (L), aza-18-crown-6 (1,4,7,10,13-pentaoxa-16-azacyclooctadecane) (L'), and diaza-18-crown-6 (1,4,10,13-tetraoxa-7,16-diazacyclooctadecane) (L") (Figure 4.1).

While the steric compatibility between the cations and the cavity of the ligand is recognized as a key factor in complexation [9] the electronic structure of the metal ions also affects the selectivity of the macrocyclic ligands towards cations [10]. The stability constants for the interaction of potassium and silver with 18-crown-6 hexaether and its aza and diaza derivatives in solution (Table 4.1) show that the ligand affinity for K^+ decreases while that for Ag^+ increases in going from the oxa (L), to the aza (L'), and then diaza (L") ligand.

Table 4.1 *Comparison of log K_s values for the complexation of L, L', and L" with K^+ and Ag^+ in methanol* [11]

Cation	Ligand		
	L	L'	L"
K^+	6.29	4.18	1.80
Ag^+	4.05	6.03	9.99

As it will be further elaborated in this chapter, the relative peak intensities of the potassium and silver complexes, as well as their uncomplexed ligands in the ES-MS spectra follow, qualitatively, the trends expected from Table 4.1. Tandem mass spectrometry with collisionally activated dissociation (CAD) provides additional information regarding the contrasting behavior of the complexes of the two metals in the gas phase. The different dissociation patterns observed are direct consequences of the binding strength between the metal and the coordination sites, as well as the nature and distribution of the potential protonation centers within the complex structure. Also, the relative gas phase stabilities of the complexes considered can be qualitatively assessed based on the various degrees of induced fragmentation observed.

Interactions in Solution

Many solution studies have been performed on the relative stability of complexes of different metal cations with various crown ethers and aza-analogs with particular emphasis on discrimination between the metals [9,12]. However, determination of the stoichiometry of complexes in solution is significantly more difficult because the systems are very labile and especially because most of the techniques used give only average compositions. Christensen and co-workers [13] suggested that caution be

exercised in assessing the structures in solution from the solid state structures of crown ether complexes with metals.

The stability constants of complexes of macrocyclic ligands with a large number of metal cations were determined by using a wide variety of physico-chemical methods [14]. As a measure of the complexing strength between metal ions and ligands in solution, the stability constants are a function of ligand structure, cation size and type, and solvent.

In methanol solutions, the stability constants of the complexes studied follow opposite trends for potassium and silver, respectively [11]. The stability of potassium complexes in solution decreases with an increase in the number of nitrogen atoms in the ligands, whereas in the case of silver complexes, their stability increases with the number of nitrogen donors in the ligand. Potassium is an A-type, "hard" acceptor [15], and so it interacts most readily with A-type, "hard" donor atoms, like oxygen. Consequently, potassium complexes derived from ligands containing only oxygen atoms have high stability constants (K_s) values (Table 4.1). The introduction of B-type, "soft" donors such as nitrogen atoms in the ligand structure gives a destabilizing influence to the coordination process of "hard" cations. As shown in Table 4.1, the stability of the nitrogen-containing complexes of potassium, $(KL')^+$ and $(KL'')^+$ is much lower than the stability of their oxa-crown analog $(KL)^+$, while increased K_s values characterize the complexation of silver, a B-type, "soft" cation, with ligands containing nitrogen atoms.

Complexation of potassium is weakened appreciably by increasing the number of nitrogen atoms in the host. This is just as expected: as the negative charge on the binding site drops, the electrostatic attraction between it and the metal cation is diminished. The effects of nitrogen atoms on silver complexation are exactly the opposite: binding strength is greatly increased at these sites, although it is not electrostatic interaction that matters here, but rather an increased degree of covalent bonding, which is somewhat characteristic of silver complexation with amine functional groups.

The degree of covalency involved in the complexation of silver cannot be determined from solution chemistry alone. Neither can the contribution of electrostatic interactions to the stability of complexes be assessed. On the other hand, though it is highly unlikely that covalency plays any role in the complexation of potassium, solution chemistry studies do not rule that out either.

The technique of electrospray mass spectrometry (ES-MS) is well suited to complement existing methods for studying solutions of metal complexes with macrocyclic ligands. Unlike other forms of ionization, electrospray allows the preservation of most ionic structures that preexist in solution, and most of their characteristics during the transfer from solution into the gas phase.

Experimental. All solutions were made by dissolving KCl and $AgNO_3$ (ACS-grade) in minimum amount of water followed by dilution with

HPLC-grade methanol (Merck). The total metal ion concentrations were 1 mM, while the water content of each solution was kept around 0.3%. The ligands were used as supplied (Aldrich) and added to each metal salt solution to give a ligand concentration of 1 mM.

Positive ion electrospray mass spectra were obtained using a Finnigan MAT–TSQ® 7000 triple-stage quadrupole mass spectrometer system equipped with an electrospray source (Finnigan MAT, San Jose, CA). The solutions, prepared as described, were directly introduced into the electrospray source using a syringe pump (Harvard Apparatus) at a flow rate of 5 μL/min. The electrospray voltage was 5 kV and the temperature of the transfer capillary was maintained at 200 C.

For the MS/MS study, argon was used as collision gas, its collision cell pressure being 1 mTorr. The laboratory collision energy (E_{LAB}) of the precursor ions was adjusted according to their mass to provide similar center-of-mass collision energy (E_{CM}), for consistency. Hence, E_{LAB} was set and maintained at 22 eV for potassium complexes and 26 eV for silver complexes, E_{CM} being, in both cases, approximately equal to 2.5 eV. The ion selection stage, that is, the first quadrupole analyzer, was tuned to unit mass resolution to allow for unambiguous precursor selection. Typically, 60 signal-averaged spectra were acquired for both full and product spectra throughout the study.

Interactions in the Gas Phase

ES-MS

In the full ES-MS spectra of the potassium complexes (Figure 4.2) the predominant ions are K^+ (*m/z* 39), and the singly charged intact (1:1) complexes, KL^+ (*m/z* 303), $(KL')^+$ (*m/z* 302), and $(KL'')^+$ (*m/z* 301) respectively. In the case of the oxa-crown potassium complex $(KL)^+$ (Figure 4.2.a) no protonated uncomplexed ligand ions are observed. The peak intensity of protonated nitrogen-containing uncomplexed ligands, $(L'H)^+$ (*m/z* 264) and $(L''H)^+$ (*m/z* 263) was found to increase with the number of nitrogen atoms involved in coordination. Furthermore, in the case of the potassium complex of L'', the doubly protonated uncomplexed ligand $(L''+2H)^{2+}$ (*m/z* 132) is present in the spectrum (Figure 4.2.c). The peaks at *m/z* 346 (Figure 4.2.b) and *m/z* 347 (Figure 4.2.c) are due to the complexation of potassium by the aza and diaza analogs of 21-crown-7 ether, present as impurities in aza-18-crown-6 and diaza-18-crown-6, respectively.

The nitrogen heteroatoms act, therefore, as more favorable protonation sites than the oxygen atoms. According to the variation in the peak intensities of species derived from uncomplexed ligands, the amount of uncomplexed ligand available for protonation was found to increase with an increase in the number of nitrogen atoms in the ligand. Considering the

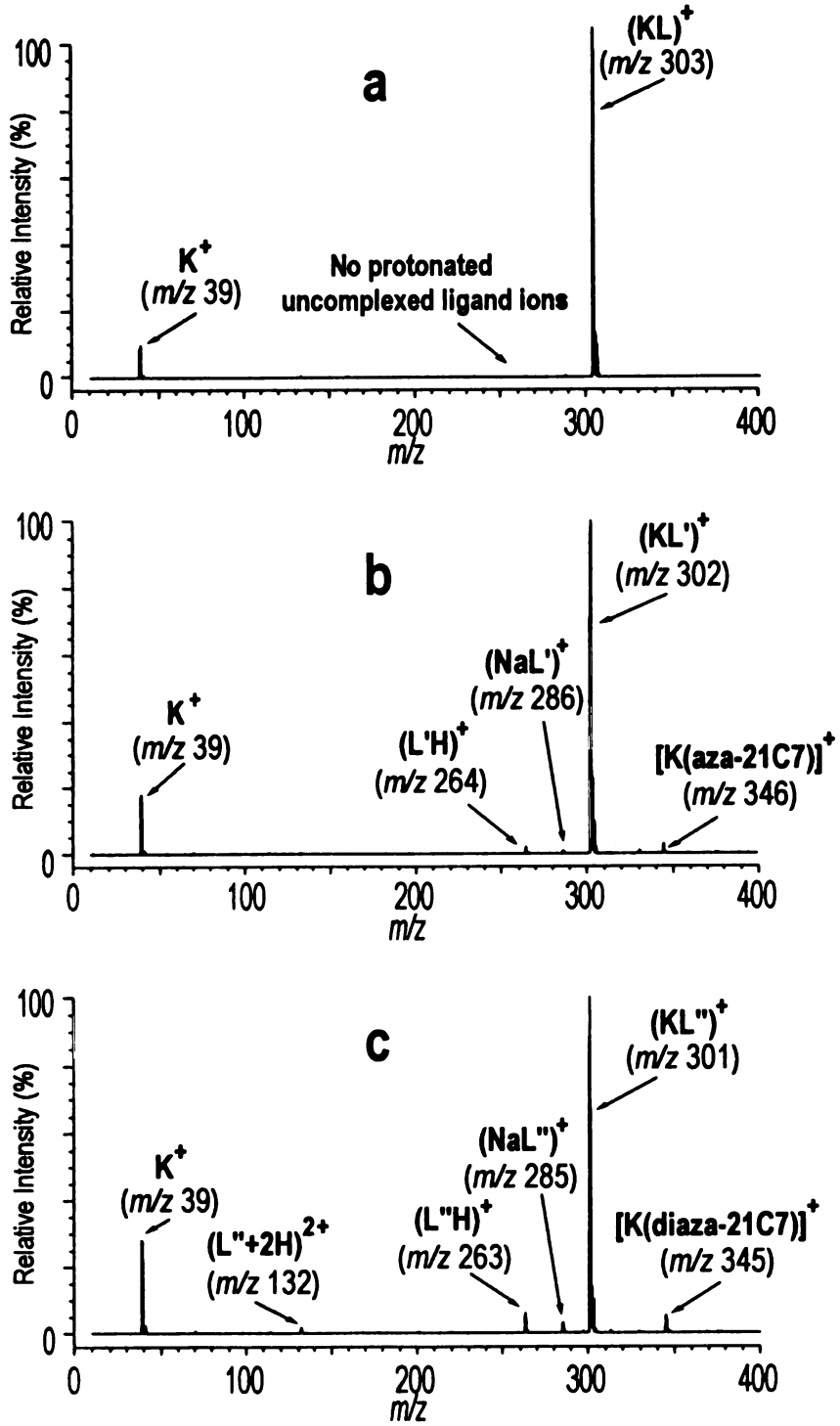

Figure 4.2 *ES-MS spectra of: a) Potassium complex of 18-crown-6 $(KL)^+$*
b) Potassium complex of aza-18-crown-6 $(KL')^+$
c) Potassium complex of diaza-18-crown-6 $(KL'')^+$

solution equilibria and stability of $(KL)^+$, $(KL')^+$, and $(KL'')^+$ respectively [11,15], the concentration of free ligand in solution is consistent with the appearance and peak intensities of protonated ligands in the ES-MS spectra.

Unlike the potassium complexes discussed above, the ES-MS spectra of silver complexes (Figure 4.3), recorded under identical experimental conditions, do not contain the bare metal ion Ag^+. The ions representing the intact (1:1) complexes, $(AgL)^+$ (*m/z* 371), $(AgL')^+$ (*m/z* 370), and $(AgL'')^+$ (*m/z* 369) are still predominant, but more fragments derived from uncomplexed ligands are present. Protonation of uncomplexed oxa-crown ligand (L) is not noticeable in the ES-MS spectrum of AgL. In addition to the protonated aza and diaza ligands $(L'H)^+$ (*m/z* 264), $(L''H)^+$ (*m/z* 263), and $(L''+2H)^{2+}$ (*m/z* 132), when protonation is accompanied by hydrogen loss, ions of *m/z* 262 (Figure 4.3.b) and *m/z* 261 (Figure 4.3.c) are formed and present in the ES-MS spectra of $(AgL')^+$ and $(AgL'')^+$, respectively.

The absence of Ag^+ is expected considering its high ionization potential (7.576 eV) [16] and its low charge affinity. Hence, it is more likely that other species with higher proton affinity (i.e., uncomplexed ligand) would preferentially win the competition for the excess charge generated during the ion formation process and therefore appear in the spectrum. The ES-MS response factors for various ionic species are also strongly dependent on their relative solvation energies [17]. In other words, the formation of bare K^+ ions is favored compared to the formation of bare Ag^+ ions during the electrospray

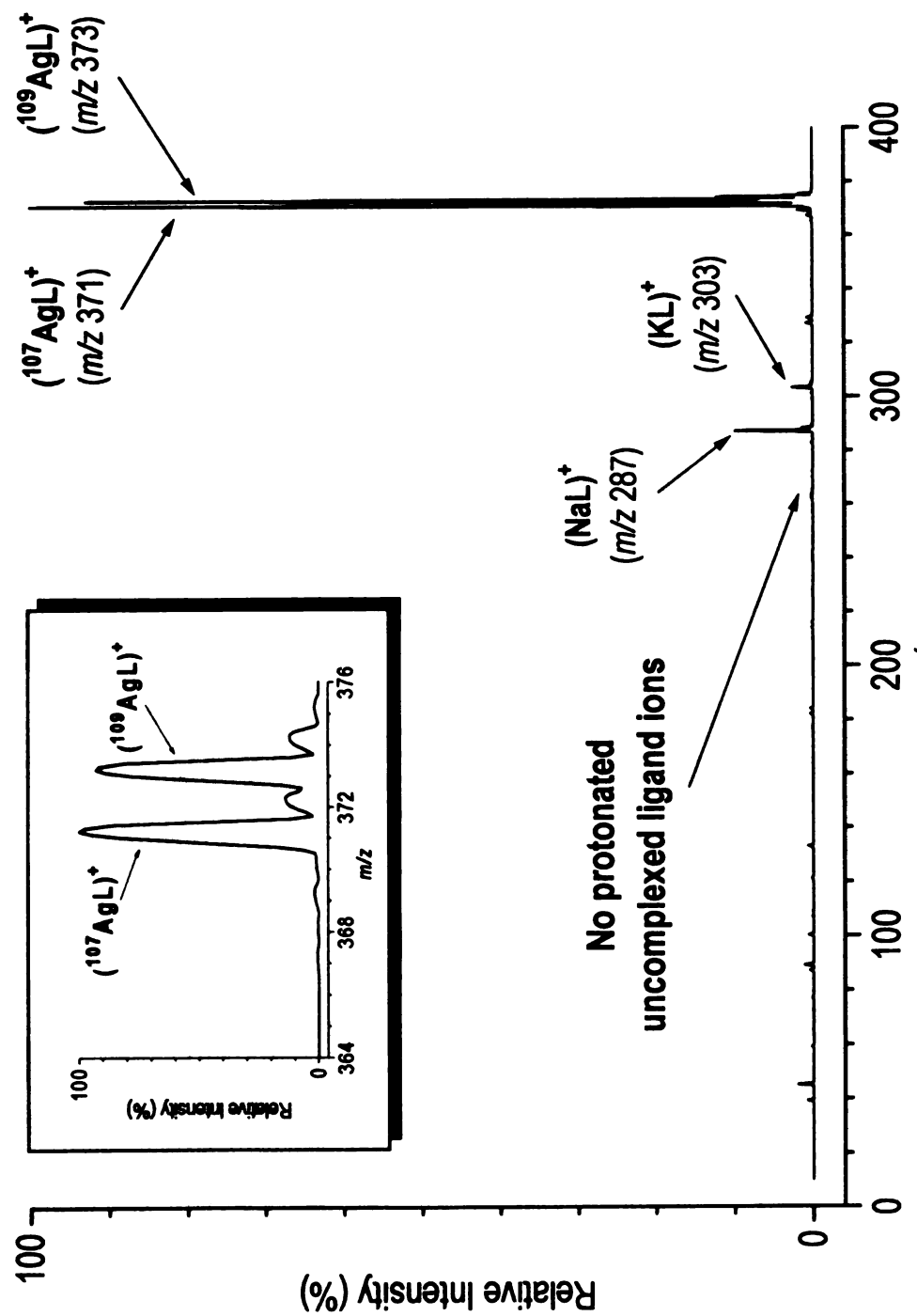

Figure 4.3.a *ES-MS spectrum of the silver complex of 18-crown-6 $(AgL)^+$*

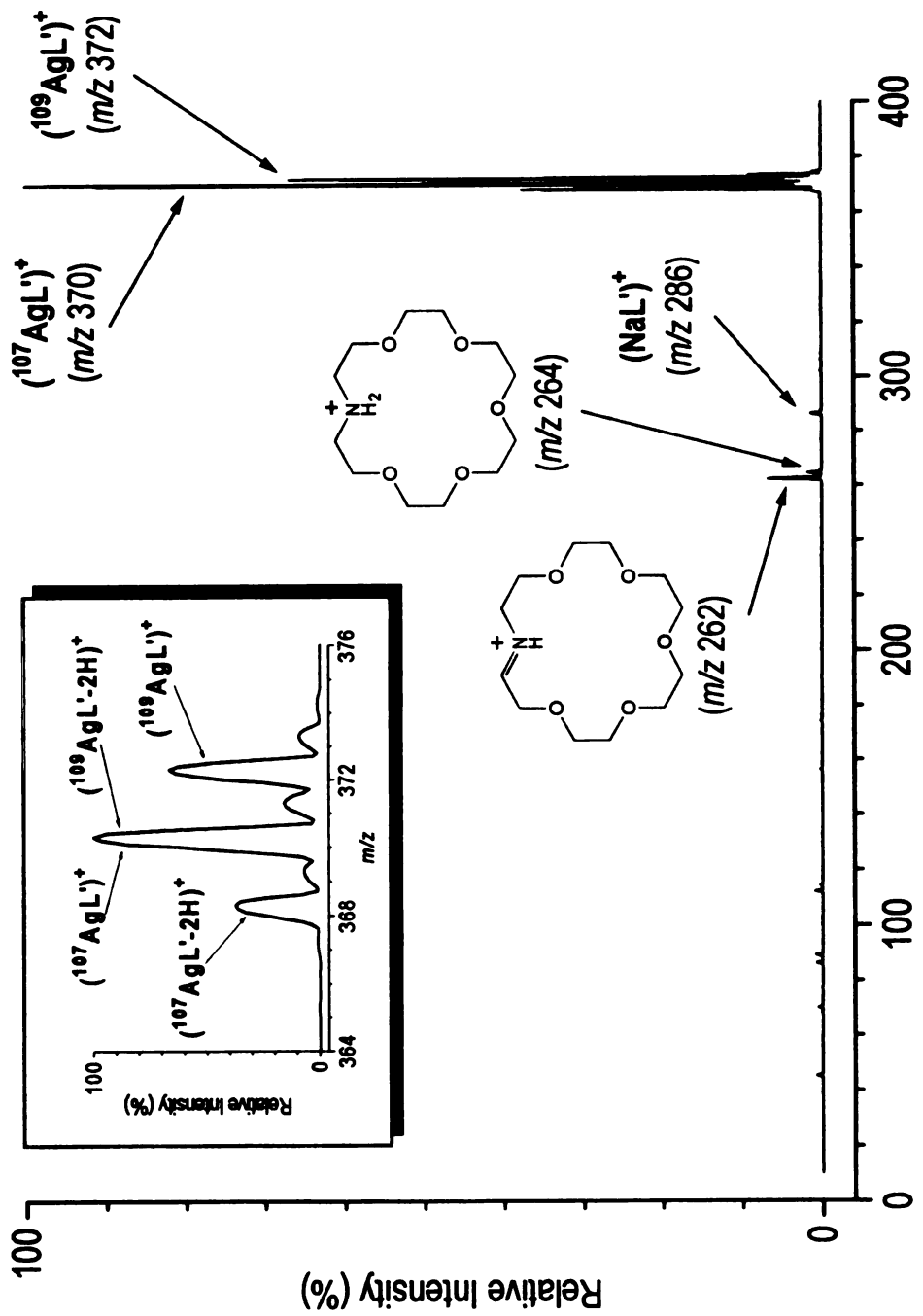

Figure 4.3.b *ES-MS spectrum of the silver complex of aza-18-crown-6 $(AgL')^+$*

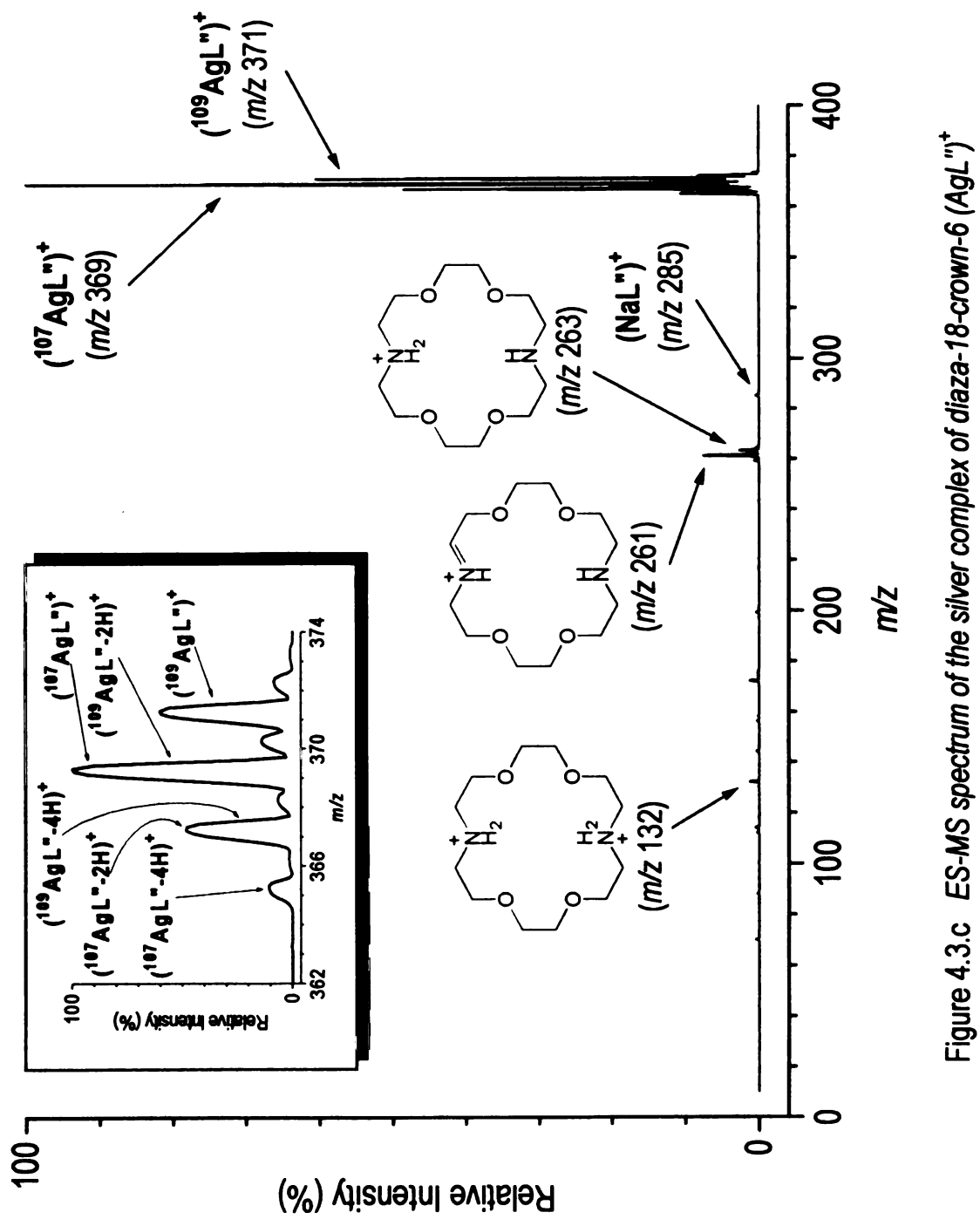

Figure 4.3.c *ES-MS spectrum of the silver complex of diaza-18-crown-6 (AgL")*$^+$

process. The appearance of $(NaL)^+$ (m/z 287) and $(KL)^+$ (m/z 303) in the spectrum (Figure 4.3.a), is not surprising, being consistent with the very high affinity of the oxa macrocycle for alkali-metal ions [18] which exist as impurities in the solution matrix. However, the intensity of the peaks corresponding to complexes of L, L', and L" with alkali-metal impurities decreases with the increasing number of nitrogen atoms in the ligand, the trend following, once again, the stability sequence of potassium complexes in solution [11]. The complexation of silver with the nitrogen-containing ligands L' and L" generates characteristic ion patterns in the (1:1) intact complex ion region (Figure 4.3.b and 4.3.c). These patterns are the result of superimposing the characteristic isotope patterns of silver, and the patterns due to the successive dehydrogenation (i.e., 2 m/z units for each loss of two hydrogen atoms) (Figure 4.4).

The deconvolution of the ions represented by these patterns is necessary in order to avoid ambiguity in subsequent MS/MS experiments involving especially the ions of m/z 367 and m/z 369 as selected precursors in CAD processes. Based on the natural abundances of silver isotopes (^{107}Ag = 51.84% and ^{109}Ag = 48.16%) and the assumption that all reaction mechanisms and yields are identical for the two isotopes, the deconvolution of the predominant peaks in the ES-MS spectrum of AgL" resulted in the data shown in Table 4.2.

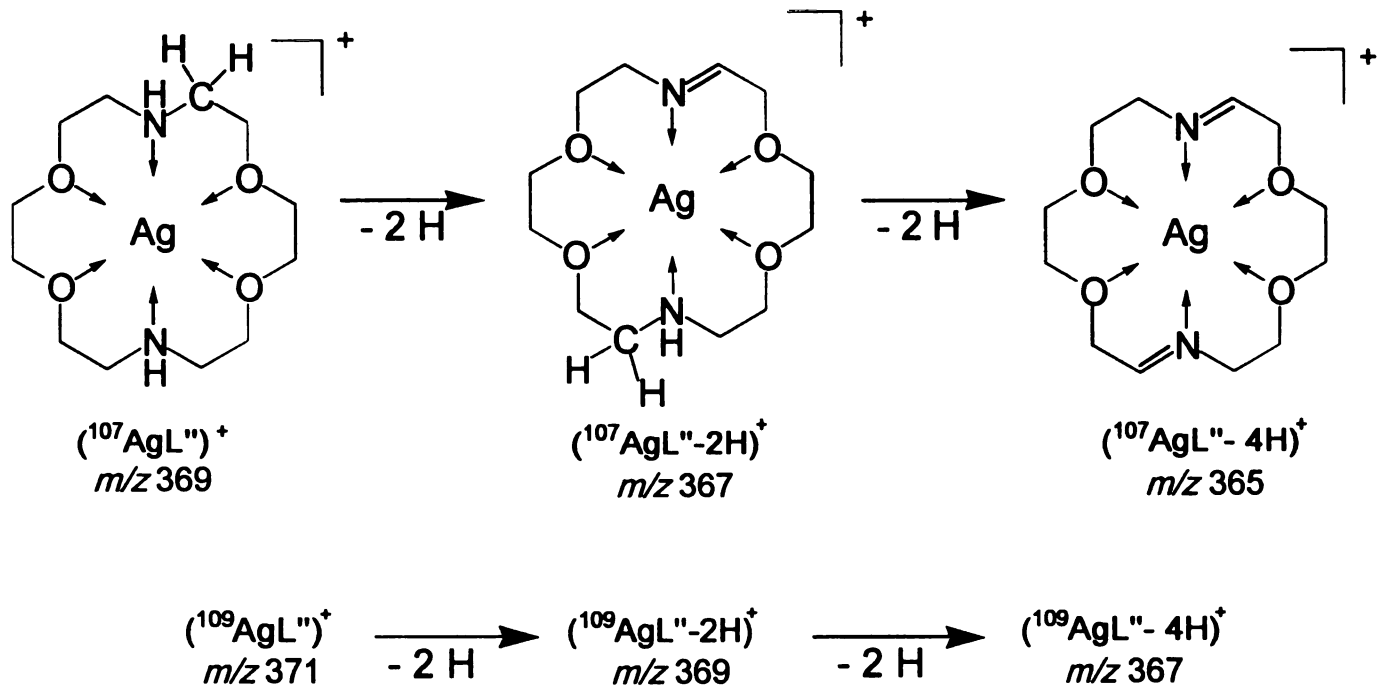

Figure 4.4 *Proposed scheme for the dehydrogenation of the silver complex of diaza-18-crown-6 (AgL")$^{+}$ during the electrospray process*

Table 4.2 *Absolute and relative peak intensities of the predominant ions in the ES-MS spectrum of AgL"*

Ion		Absolute Intensity (counts × 10^7)	Relative Intensity (% of base peak)
m/z	Species		
371	$(^{109}AgL")^+$	8.5	60
369	$(^{109}AgL" - 2H)^+$	9.2	
	$(^{107}AgL")^+$	5.0	
	Total	14	100
367	$(^{109}AgL" - 4H)^+$	5.4	
	$(^{107}AgL" - 2H)^+$	1.6	
	Total	6.9	49
365	$(^{107}AgL" - 4H)^+$	1.5	11

ES-MS/MS

Unlike ES-MS experiments, which generate information about the solution chemistry and processes that occur at the interface between solution and gas phase, CAD is a much "cleaner" gas phase experiment. The MS/CAD/MS product spectra also exhibit substantial differences between the complexes of the two cations. The dissociation of $(KL)^+$, $(KL')^+$, and $(KL")^+$ follows a one-step pathway, the process resulting in a unique product ion, K^+ (*m/z* 39) (Figure 4.5). Therefore, only two ionic species, the precursor complex ion and K^+ as the sole product are present in the spectra.

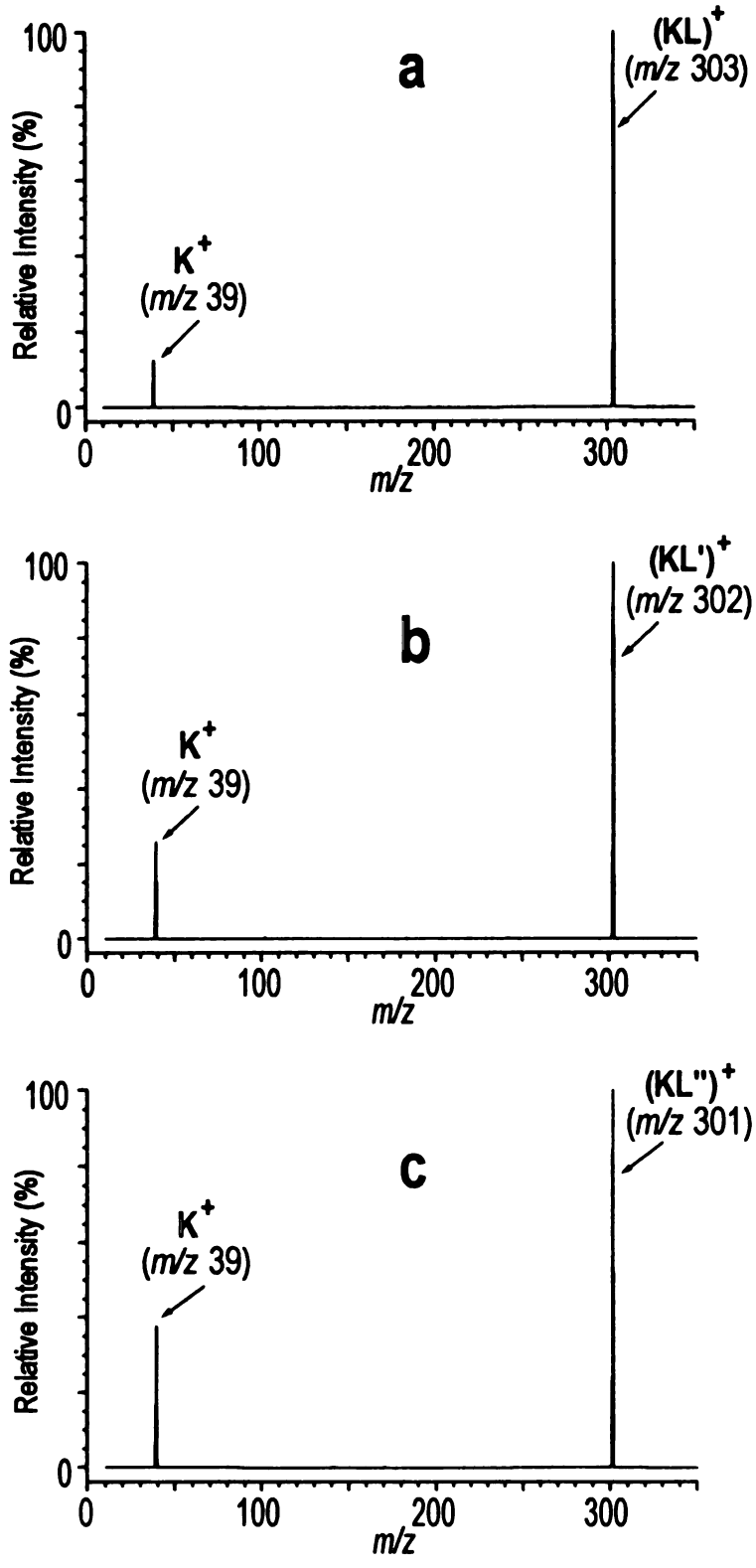

Figure 4.5 *MS/CAD/MS spectra of: a) Potassium complex of 18-crown-6 $(KL)^+$*
b) Potassium complex of aza-18-crown-6 $(KL')^+$
c) Potassium complex of diaza-18-crown-6 $(KL")^+$

The ratios of peak intensities of the precursor ion and K^+ are qualitatively indicative of the relative affinities of the three ligands, L, L', and L" respectively, for the potassium ions. This conclusion is in agreement with the observations of Brodbelt *et al.* [19] regarding the gas phase stabilities of alkali-metal complexes with a variety of macrocyclic ligands. The trend depicted in Figure 4.5 suggests a similar stability sequence to the stability of potassium complexes in solution (Table 4.1), although no quantitative correlation between the relative peak intensities and the stability constants in solution can be found based solely on this experiment.

The relative peak intensity of these ions is also a function of the collision energy and the collision gas pressure. An increase in either of these two parameters leads to a greater fragmentation, that is, a larger relative peak intensity of the bare metal ion. Chapter 5 deals extensively with CAD of alkali-metal complexes and the effect of various operational parameters on their gas phase stability. Under identical experimental conditions the complexes containing a larger number of "soft" nitrogen donor sites involved in complexation, that is, complexes of K^+ with aza and diaza ligands generate larger abundances of the bare metal ion.

The silver complex precursor ions undergo different dissociation pathways. The CAD spectrum of $(AgL)^+$ contains the fragment ions Ag^+ (m/z 107), ligand fragments (e.g., m/z 45), and silver-containing complex fragments (e.g., m/z 182) (Figure 4.6.a). Following collisions with target gas

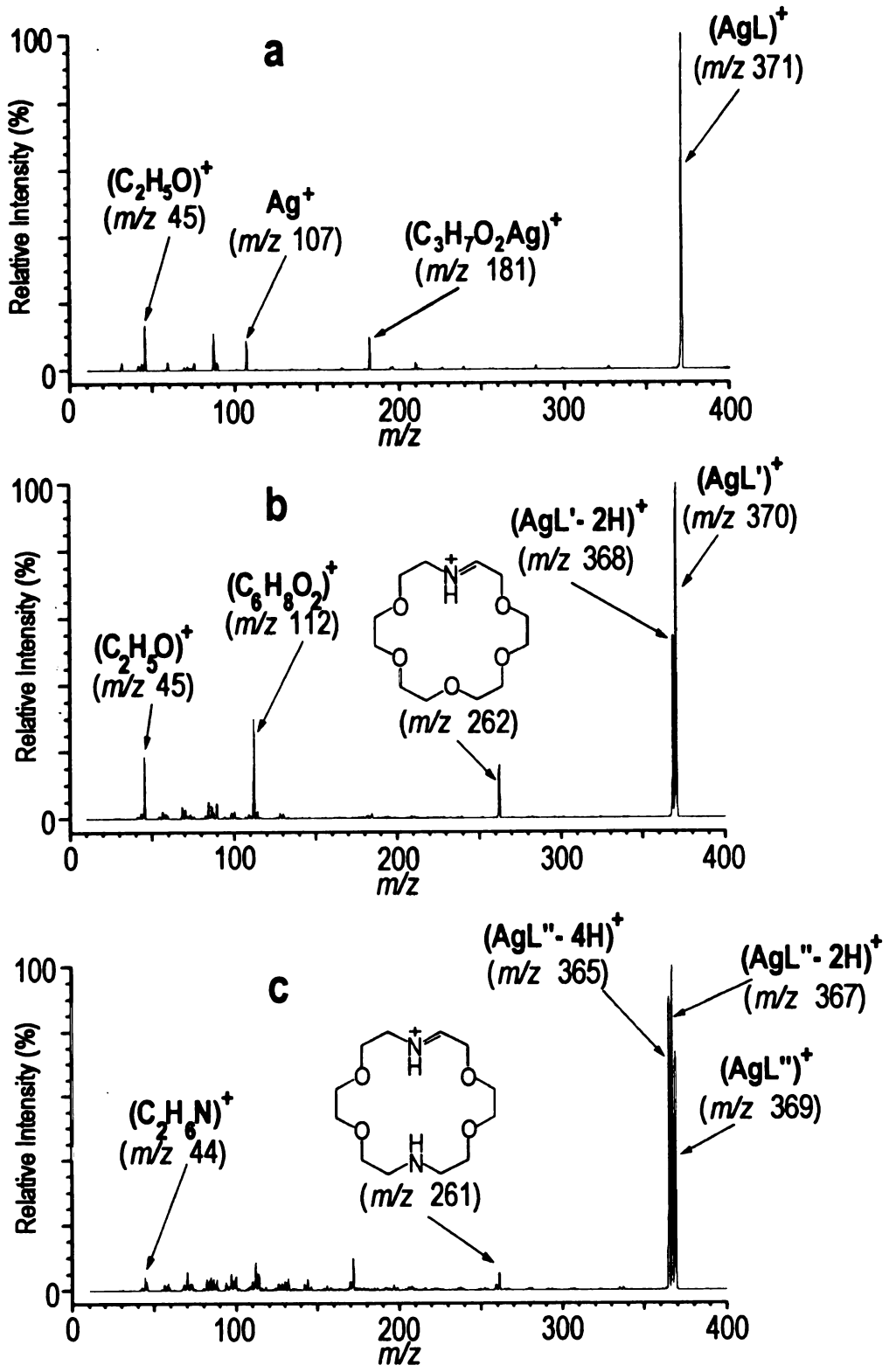

Figure 4.6 *MS/CAD/MS spectra of: a) Silver complex of 18-crown-6 $(AgL)^+$*
b) Silver complex of aza-18-crown-6 $(AgL')^+$
c) Silver complex of diaza-18-crown-6 $(AgL'')^+$

molecules, the nitrogen-containing precursor ions $(AgL')^+$ and $(AgL'')^+$ do not form Ag^+. Instead, these complex ions release silver in the form of a neutral product, AgH, a process characteristic of the precursor ions $(AgL')^+$ (*m/z* 370) (Figure 4.6.b), and $(AgL'')^+$ (*m/z* 369) (Figure 4.6.c). Except for the ions formed by dehydrogenation, no other product ions containing silver are present in the MS/MS spectrum.

Hydrogen loss involving the nitrogen atom sites is a significant process characteristic of CAD of $(AgL')^+$ and $(AgL'')^+$. This process can occur during either "in-source fragmentation" during electrospray ion formation (Figure 4.3.b and 4.3.c) or it can be induced by CAD of selected precursor complex ions. For instance, CAD of ions of *m/z* 371, *m/z* 369, *m/z* 367, and *m/z* 365, ions that exist in the ES-MS spectrum of AgL" (Figure 4.3.c) provides crucial information about silver binding within the complex as a function of structural changes in the ligand constitution. The selection of ions of *m/z* 365 and *m/z* 371 as precursors presents no problem, the peaks representing unique ionic species, $(^{107}AgL''\text{-}4H)^+$ and $(^{109}AgL'')^+$ respectively. Tuning the first mass analyzer to unit mass resolution allows therefore for unambiguous precursor ion selection. The analysis of the product ions resulting in CAD of species of *m/z* 367 and *m/z* 369, which consist of overlapped peaks, is however more complicated, involving the deconvolution of both the precursor and product ions. Based on the peak intensities of the product ions of interest, which are summarized in Table 4.3, we conclude that the second

Table 4.3 *Absolute peak intensities of the precursor and product ions for the CAD of $(AgL")^+$, $(AgL"-2H)^+$, and $(AgL"-4H)^+$*

Precursor Ion		Absolute Peak Intensity (counts × 10^5)				
m/z	Species	M	M - 2H	M - 4H	M - AgH	M - 2H - AgH
371	$(^{109}AgL")^+$	12	8.5	13	0.7	0.1
369	$(^{109}AgL" - 2H)^+$	1.6	7.8	-	0.2	-
	$(^{107}AgL")^+$	13	9.1	15	0.7	0.1
	Total	14	17	15	0.9	0.1
367	$(^{109}AgL" - 4H)^+$	5.9	-	-	-	-
	$(^{107}AgL" - 2H)^+$	1.7	0.9	-	0.1	-
	Total	7.6	0.9	-	0.1	
365	$(^{107}AgL" - 4H)^+$	5.8	-	-	-	-

dehydrogenation step (k_2) is favored compared to the first step (k_1) (Figure 4.7).

The loss of AgH occurs when intact complex ions (e.g., $(AgL")^+$) collide with target gas molecules (Figure 4.7.a). The loss of AgH from $(AgL")^+$ during CAD is dependent upon the degree of previous dehydrogenation, as shown in Table 4.3. The release of AgH from ions that have previously lost two hydrogen atoms (e.g., $(AgL"-2H)^+$) is significantly hindered with respect to that from $(AgL")^+$ (Figure 4.7.b and 4.7.c), and silver hydride is not released at all from ions that have already lost four hydrogen atoms (e.g., $(AgL"-4H)^+$) (Figure 4.7.d).

The formation of double bonds following dehydrogenation has a tremendous effect on the coordination of silver. The degree of covalency involved in silver binding is dramatically increased by the contribution of carbon-nitrogen double bonds formed (Figure 4.7.a). Therefore, the interaction of silver with the ligand is enhanced, making the neutral loss of AgH more difficult when associated with an increased degree of dehydrogenation.

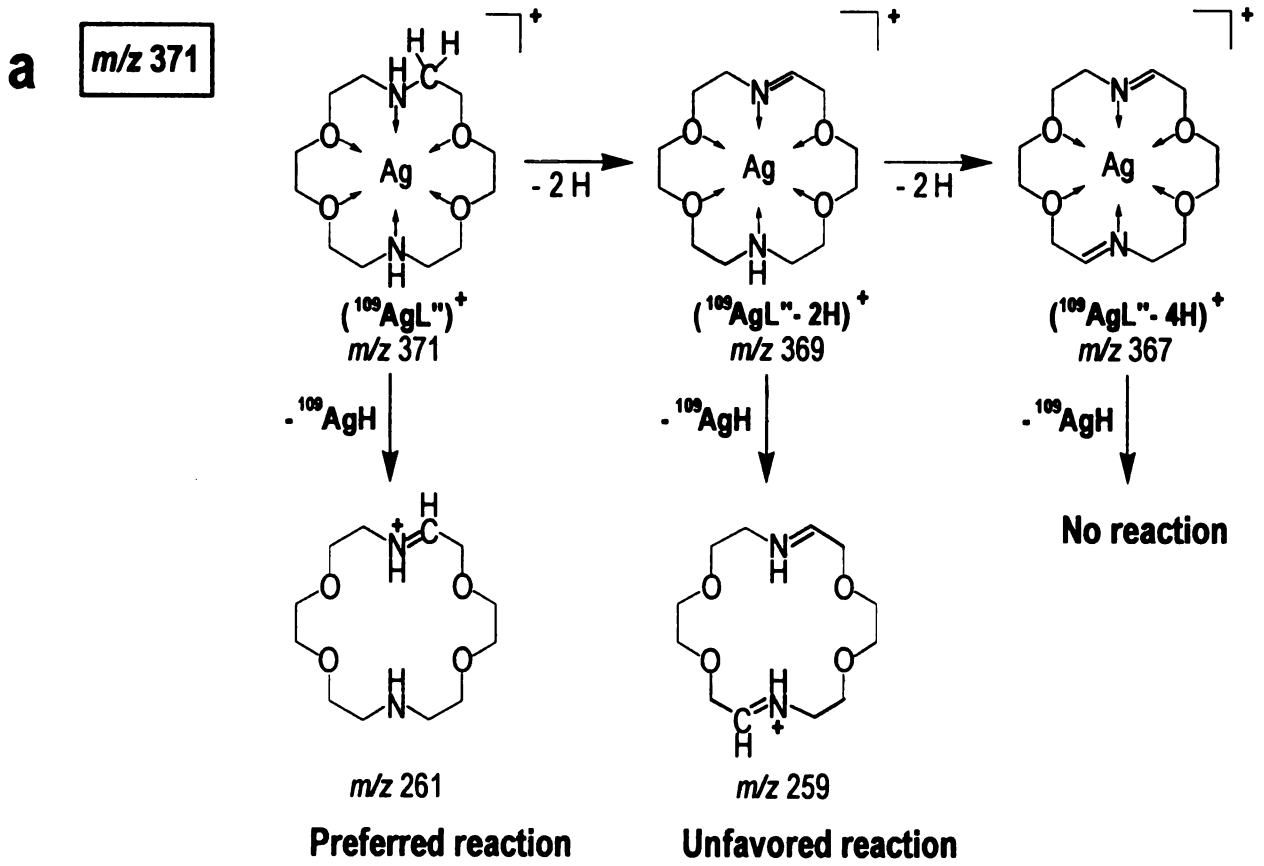

Figure 4.7 *Proposed mechanism for dehydrogenation and loss of silver hydride (AgH) during CAD of ions of: (a) m/z 371, (b) m/z 369, (c) m/z 367, and (d) m/z 365* *(continued on page 78)*

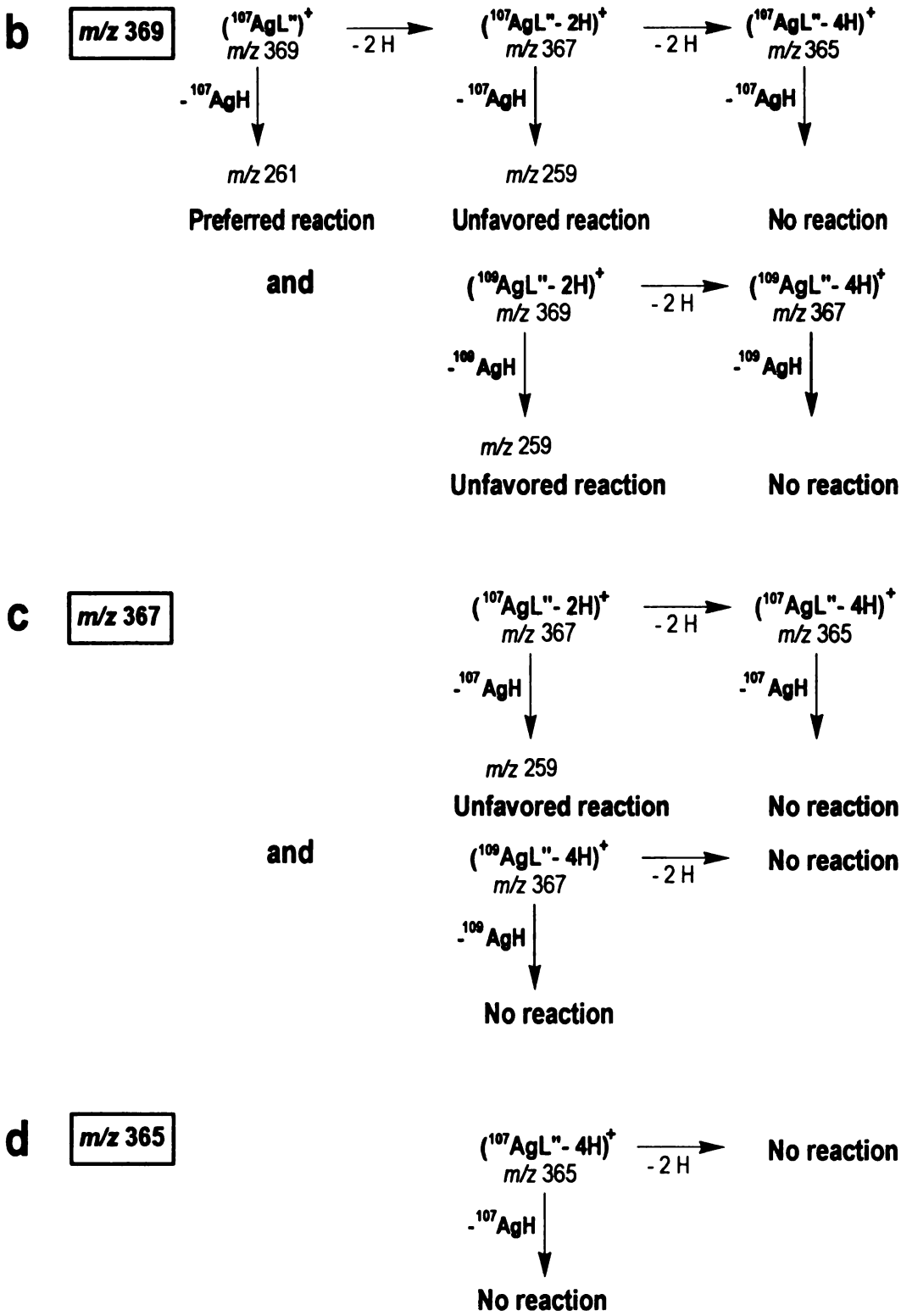

Figure 4.7 (continued from page 77)

Summary

The stability of potassium and silver complexes in solution strictly follows the theoretical considerations regarding preferential "hard-hard" and "soft-soft" interactions between the metal ions and the coordination sites in the ligand, respectively. Hence, the interaction strength of potassium with L, L', and L" is weakened with an increase in the number of nitrogen atoms, trend which is qualitatively evident in both ES-MS and CAD spectra of the complexes chosen.

In the electrospray spectra, similar trends in the stability of the complexes were noticed, although a quantitative correlation, regarding the extent to which the appearance of the ES-MS spectra of the compounds considered resembles their equilibrium concentrations in solution was not readily observable. The complex processes behind the electrospray ion formation, desolvation, and transport prevent making an immediate correlation between relative peak intensities and the relative concentrations of those ionic species in solution. Solvent evaporation and ion desolvation occur differently for different ionic species, so that the ES-MS spectra are not quantitatively representative of their solution chemistry. A quantitative study would only be possible if the solvation energies of all species involved were identical or known. However, the qualitative observations are on more

solid ground; at least some of the ionic species present in the ES-MS spectra do exist in solution.

The ES-MS spectra of silver and potassium complexes with the macrocyclic ligands chosen illustrate their contrasting behavior. Silver does not generally have a preference for charge retention, therefore Ag^+ is not present in the ES-MS spectra, especially when nitrogen-containing ligands are involved. The nitrogen atoms in the ligands are more favored protonation sites than the oxygen atoms, so that protonation of L' and L" may occur at every nitrogen atom available (Figure 4.3.b and 4.3.c). Potassium, however, is always present as K^+ (m/z 39) in the ES-MS spectra, regardless the nature and the number of donor sites in the ligands. Very limited protonation of nitrogen-containing ligands was observed in the presence of potassium, clearly indicating the greater ability of potassium to retain the charge in competition with various coexisting species. This is further illustrated in the CAD spectra of potassium complexes, where a single dissociation product, K^+, prevails over any other fragment that might be formed during the collision processes in the gas phase.

Electrospray combined with tandem mass spectrometry could be further employed in studying complexes of transition metals with macrocyclic and chelating ligands. Not only does electrospray provide qualitative data about the ionic species that exist in solution, but CAD with tandem mass spectrometry complements this information with observations regarding

their gas phase chemistry. The assessment of preferential metal-ligand binding, and especially the interaction strength between metal ions and various coordination sites are research objectives that may be reached by using ES-MS/MS.

References

1. Harrigan, E. T.; Hirota, N. *Chem. Phys. Lett.* **1967**, *1*, 281.

2. Andretti, G. D.; Cavalca, L.; Sgarabotto, P. *Gazz. Chim. Ital.* **1970**, *100*, 697.

3. Cram, D. J.; Cram, J. M. *Science* **1974**, *183*, 803.

4. Weber, E.; Toner, J. L.; Goldberg, I.; Vögtle, F.; Laidler, D. A.; Stoddart, J. F.; Bartsch, R. A.; Liotta, C. L. In *Crown Ethers and Analogs*, S. Patai and Z. Rappoport, Eds.; John Wiley & Sons: Chichester-New York-Brisbane-Toronto-Singapore, 1989.

5. Pedersen, C. J. *J. Am. Chem. Soc.* **1967**, *89*, 7017.

6. Izatt, R. M.; Christensen, J. J. In *Synthetic Multidentate Macrocyclic Compounds*; Academic Press: New York, 1978.

7. Gokel, G. W.; Durst, H. D. *Synthesis* **1976**, *3*, 168.

8. Frensdorff, H. K. *J. Am. Chem. Soc.* **1971**, *93*, 600.

9. Man, V. F.; Dale Lin, J.; Cook, K. D. *J. Am. Chem. Soc.* **1985**, *107*, 4635.

10. Gokel, G. W.; Goli, D. M.; Minganti, C.; Echegoyen, L. *J. Am. Chem. Soc.* **1983**, *105*, 6786.

11. Stroka, J.; Ossowski, T.; Cox, B. G.; Thaler, A.; Schneider, H. *Inorg. Chimica Acta* **1994**, *219*, 31.

12. Boss, R. D.; Popov, A. I. *Inorg. Chem.* **1985**, *24*, 3660.

13. Christensen, J. J.; Eatough, D. J.; Izatt, R. M. *Chem. Rev.* **1974**, *74*, 351.

14. Izatt, R. M.; Pawlak, K.; Bradshaw, J. S. *Chem. Rev.* **1991**, *91*, 1721.

15. Pearson, R. G.; *J. Am. Chem. Soc.* **1963**, *85*, 3533.

16. *Handbook of Chemistry and Physics*, 65th ed.; CRC Press, Inc.: Boca Raton, FL, 1984.

17. Dupont, A.; Leize, E.; Marquis-Rigault, A.; Funeriu, D.; Lehn, J.-M.; Van Dorsselaer, A. In *Proceedings of the 43rd ASMS Conference on Mass Spectrometry and Allied Topics*, Atlanta, GA, 1995; p 250.

18. Coxon, A. C.; Laidler, D. A.; Pettman, R. B.; Stoddart, J. F. *J. Am. Chem. Soc.* **1978**, *100*, 8260.

19. Maleknia, S.; Brodbelt, J. *J. Am. Chem. Soc.* **1992**, *114*, 4295.

Chapter 5

Stability Studies in the Gas Phase by Tandem Mass Spectrometry

Introduction

Tandem mass spectrometry is entering its third decade of application in the area of complex mixture analysis and its fourth decade of use in basic studies of ion chemistry in the gas phase [1]. One of the most exciting and rewarding areas in mass spectrometry is selected ion fragmentation, in which an ion is mass-selected, fragmented, and the resulting fragment ions are mass-analyzed. The most widely used process to obtain fragmentation of ions, which can be initially produced in a large variety of ionization processes is collisionally activated dissociation (CAD), also known as collision-induced dissociation (CID) [2].

CAD has grown dramatically in the past decade as an important method for ion structure determination and complex mixture analysis [3,4], especially with the development of new ionization techniques, such as fast atom bombardment and electrospray, both capable of producing ions from large molecules. Current applications of CAD include polypeptide sequencing [5], characterization of oligosaccharides [6], drug metabolites [7], inorganic coordination compounds [8], etc. The CAD process involves activation of ions following collisions with neutral gas molecules, or sometimes a surface, the latter being called surface-induced dissociation (SID) [9]. Subsequent fragmentation of activated ions to various product ions depends upon the amount of energy transferred into the ion.

The experimental methods used to study CAD have lately evolved significantly. Tandem arrays of momentum and energy analyzers and differentially pumped collision chambers provide a convenient means of selecting ions of interest, colliding these ions with neutral gas particles in cells located in field-free regions and conducting mass/energy analyses of the product ions. Sectors [2,10], quadrupoles [11], ion cyclotron resonance [12], time-of-flight [13], and ion traps [14] have all been used alone or in various combinations to suit individual requirements.

Collisionally Activated Dissociation in a Triple Quadrupole Mass Spectrometer

CAD of polyatomic ions occurs according to a two-step mechanism. Collisional activation (Equation 5.1), where a fraction of the kinetic energy of the target ion is transferred into internal energy, is followed by the dissociation of the internally excited ion (Equation 5.2).

$$M_1^+ + M_2 \longrightarrow M_1^{+*} + M_2 \qquad (5.1)$$

$$M_1^{+*} \longrightarrow M_3^+ + M_4 \qquad (5.2)$$

The essence of this model is that the collision time is short compared to the dissociation time, thus separating the activation and dissociation in time. During this time delay, internal energy is redistributed among various internal degrees of freedom of the ion. The mode of energy deposition in collision and the extent of internal energy redistribution are essential mechanistic issues in CAD of polyatomic ions.

Most commonly, a target mass (precursor ion) is selected in a primary mass analyzer (first quadrupole) and accelerated into the collision chamber at modestly elevated pressure. The collision chamber is commonly named "second quadrupole", even though it is built as an octapole in most of the

modern commercial instruments (Figure 5.1). The fragment ions formed in the collision chamber are subsequently mass discriminated and analyzed in the second analyzer (third quadrupole). These CAD fragments are known as "product ions". Although routinely referred to as MS/MS, tandem mass spectrometry involving collisionally activated dissociation is in fact MS/CAD/MS.

Unlike reactions induced in the condensed phase, including but not limited to electrospray ionization, CAD allows for "cleaner" gas phase studies, conducted in a solvent-free environment. The comparative study presented in Chapter 4 deals specifically with the complexes of two metal ions, K^+ and Ag^+ with three particular ligands, and their solution and gas phase chemistry. This chapter focuses to a greater extent on aspects of the gas phase stability of several alkali-metal ion complexes with 18-crown-6 (L) under CAD conditions. The effect of experimental CAD parameters is also discussed.

Experimental. The analyte, a solution of 0.1 M CsCl (Aldrich) in methanol was prepared according to the general procedure. The ligand used was 18-crown-6 (L), and it was added to the solution such as its concentration was 0.2 M. The electrospray voltage was 5 kV, and the temperature of the transfer capillary was 110 C. Argon was used as the collision gas in the CAD experiments. Both ES-MS and MS/MS spectra were acquired using a signal averaging procedure, 60 spectra being averaged throughout the experiments.

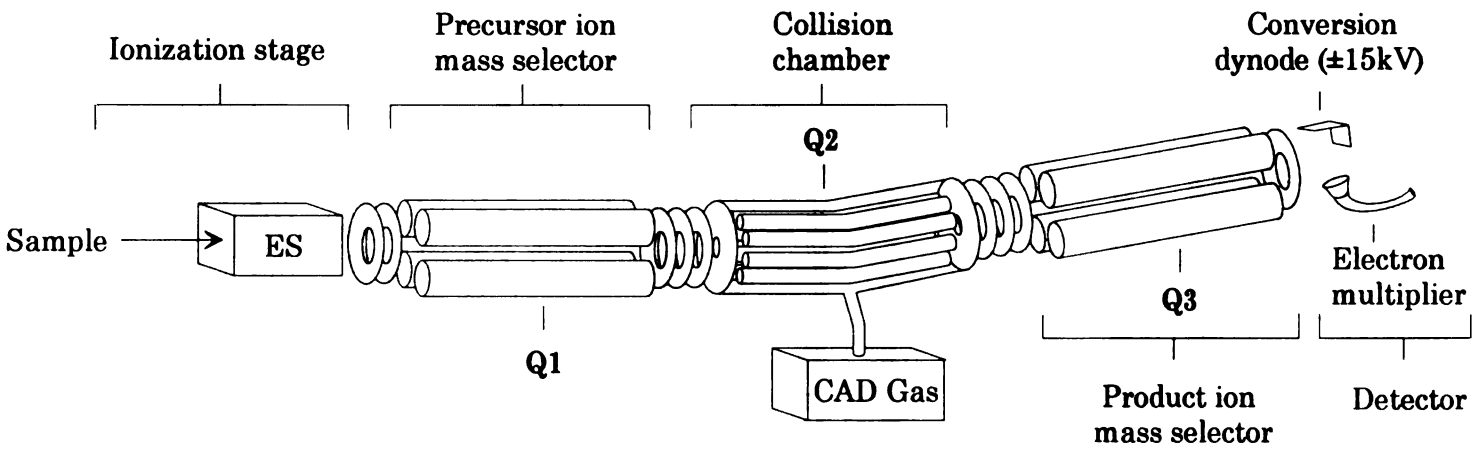

Figure 5.1 *The block diagram of the TSQ-7000 mass spectrometer (courtesy of Eric Hemenway)*

The ES-MS spectrum of the species that result in the complexation of Cs^+ with 18-crown-6 is shown in Figure 5.2. The experimental conditions were chosen such as the peak intensity of the "sandwich" $(CsL_2)^+$ complex was at a maximum. Even though a lower temperature of the transfer capillary would have probably yielded a larger amount of $(CsL_2)^+$ (see Chapter 3), its operation at at least 110 C was necessary to ensure the complete solvent evaporation from the emerging analyte solution droplets.

For the MS/MS operation $(CsL_2)^+$ (*m/z* 661) was selected as precursor in the first mass analyzer. Regardless the values of collision energy (E_{coll}) and collision gas pressure (P_{coll}), the general fragmentation pathway led to the exclusive formation of $(CsL)^+$ (*m/z* 397) and Cs^+ (*m/z* 133). The extent of the fragmentation was a function of the collision parameters. The specific influence of these variables is presented in detail in the present chapter.

Effect of Collision Energy

With the collision gas pressure set and maintained at approximately 0.4 mTorr, the voltage offset of Q2 was varied from -2 to -50 V and the peak intensities for the product ions that result in the CAD of $(CsL_2)^+$ monitored (Table 5.1). Typical MS/MS spectra, for two sets of experimental parameters are shown in Figure 5.3. For consistency, the relative peak intensities in spectra recorded under different sets of experimental parameters were

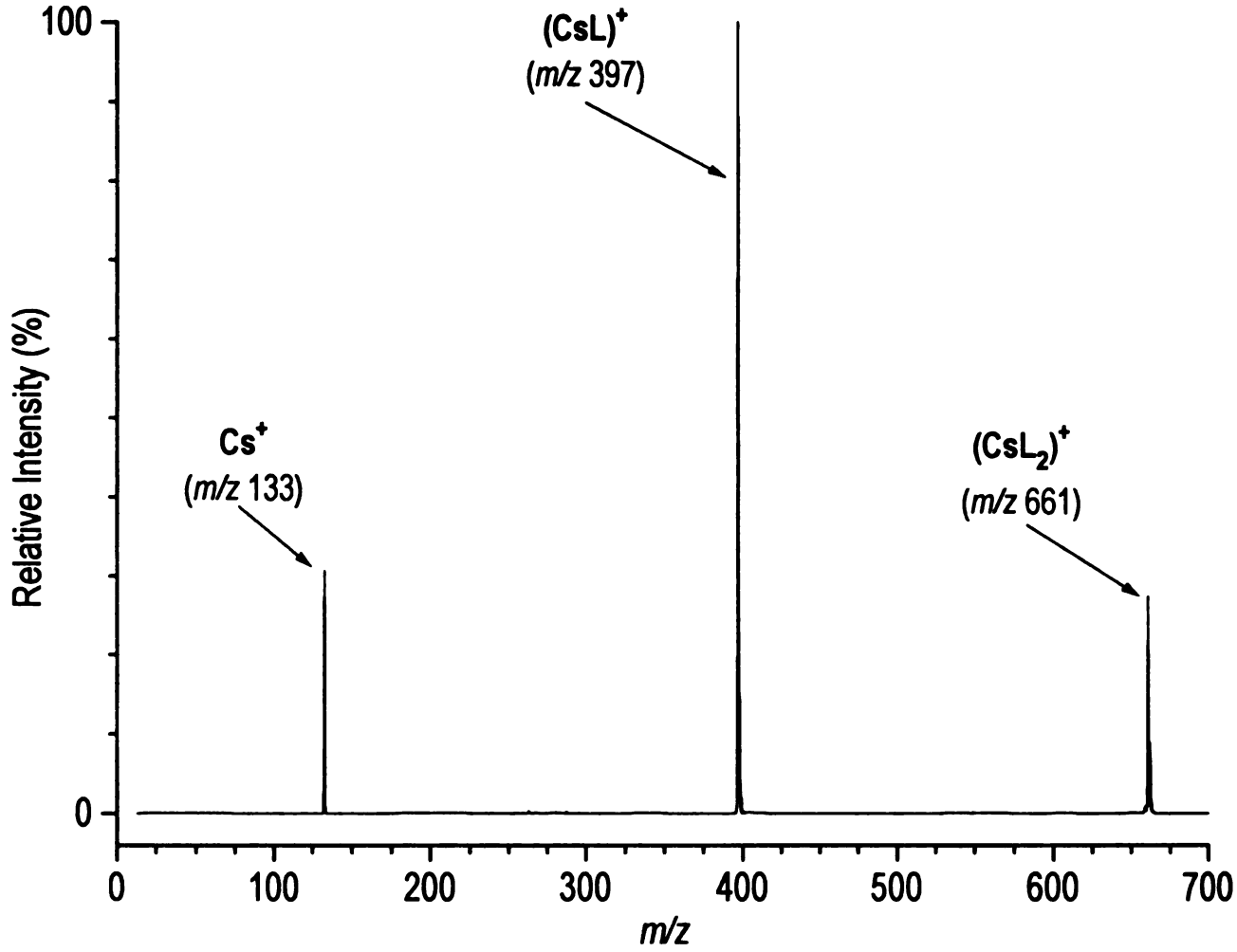

Figure 5.2 *ES-MS spectrum of a CsCl : L (1:2) solution in methanol. Capillary temperature = 110 C*

Table 5.1 *Effect of collision energy (E_{coll}) on the relative intensity of product ions of $(CsL_2)^+$ (m/z 661); Collision gas pressure = 0.40 mTorr*

Collision energy (eV)	Relative Intensity (%)		
	Cs^+ m/z 133	$(CsL)^+$ m/z 397	$(CsL_2)^+$ m/z 661
2	0	18	100
3	0	23	100
4	0	26	100
5	0	32	100
6	0	39	100
7	0	47	100
8	0	56	100
9	0	72	100
10	0	90	100
11	0	100	85
12	0	100	72
14	0	100	54
16	0	100	38
18	0	100	32
20	0.23	100	26
22	0.35	100	21
24	0.39	100	19
26	0.43	100	18
28	0.45	100	16
30	0.69	100	15
32	1.1	100	13
34	1.5	100	12
38	2.4	100	11
42	4.1	100	9.0
46	6.3	100	7.1
50	8.2	100	5.0

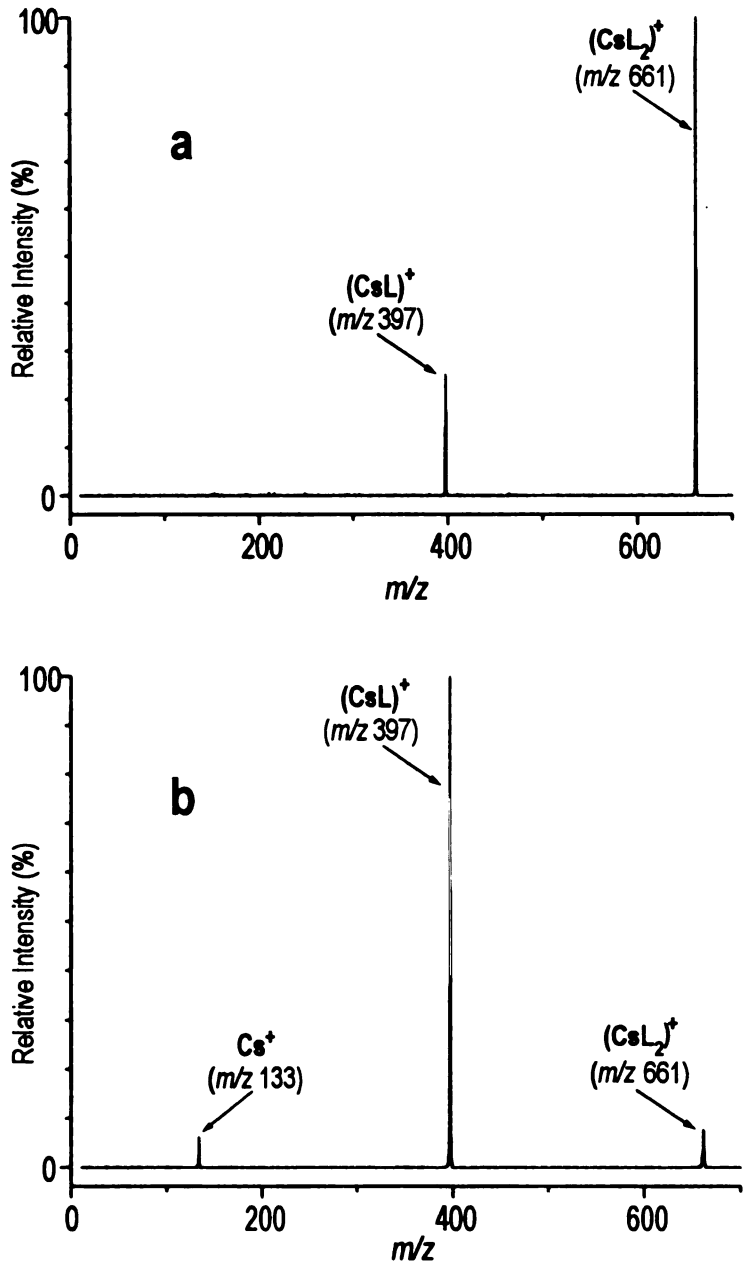

Figure 5.3 *MS/CAD/MS product ion spectra of $(CsL_2)^+$ (m/z 661). Collision gas pressure = 0.40 mTorr; Collision energy: (a) 4 eV, (b) 46 eV*

rationalized to the summed intensity of all the peaks present in the spectrum (Figure 5.4). As the collision energy increases from 2 eV to approximately 20 eV, a sharp decrease in the relative intensity of CsL_2^+ peak is evident, while a mirror-like increase is noticed in the relative intensity of $(CsL)^+$. The appearance energy of $(CsL)^+$ is therefore very low, according to the trend depicted in Figure 5.4. The appearance energy of Cs^+ (m/z 133) is approximately 20 eV, and its peak becomes more intense as the collision energy further increases. Even though the increase in Cs^+ peak intensity is qualitatively parallel with a decrease in the intensity of the precursor ion, the fragmentation mechanism (i.e., whether single or multiple-collision dissociations are involved) can not be studied based solely on the assessment of the collision energy effect.

Effect of Collision Gas Pressure

The conclusions drawn from the appearance of ES-MS spectra and from studying the effect of collision energy on fragmentation do not provide answers to crucial issues regarding various dissociation mechanisms and reaction pathways. There are several possible fragmentation mechanisms that govern CAD of complex ions. The reaction pathways, as well as the distribution of the product ions depend on the structure of the precursor ion,

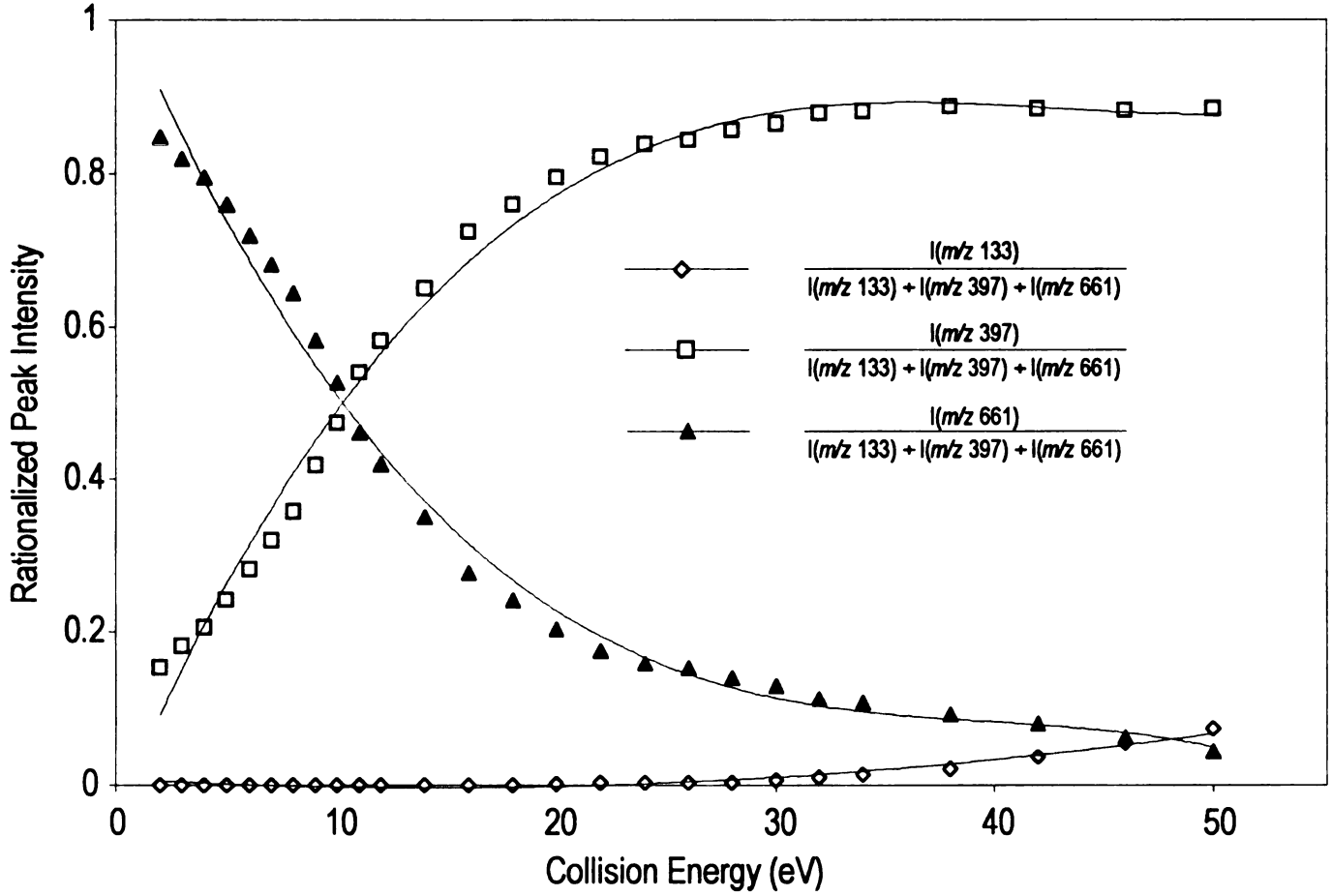

Figure 5.4 *Rationalized peak intensities of product ion Cs^+ (◇) , $(CsL)^+$ (□) , and $(CsL_2)^+$ (▲) in the CAD of $(CsL_2)^+$ (m/z 661) as a function of collision energy. Collision gas pressure = 0.40 mTorr.*

the range of collision energies applied, and a series of other factors among which the collision gas pressure is particularly important.

The fragmentation of $(CsL_2)^+$ (*m/z* 661) can occur according to the following mechanisms:

a) $(CsL_2)^+ + G \longrightarrow Cs^+ + 2L + G$ (5.3)
(*m/z* 661) (*m/z* 133)

b) $(CsL_2)^+ + G \longrightarrow (CsL)^+ + L + G$ (5.4.1)
(*m/z* 661) (*m/z* 397)

$(CsL)^+ + G \longrightarrow Cs^+ + L + G$ (5.4.2)
(*m/z* 397) (*m/z* 133)

The general equation describing the formation of Cs^+ (*m/z* 133) in either of the two instances above is:

$$\frac{d[Cs^+]}{dt} = k[(CsL_2)^+]^a P_{coll}^b \quad (5.5)$$

where P_{coll} is the collision gas (G) pressure in mTorr, (a) is the reaction order in CsL_2^+, and (b) is the reaction order in G.

The mechanism described by Equation 5.3 implies fragmentation occuring as a result of a single collision between the precursor ion and a target gas molecule, while Equation 5.4 describes a multiple-collision dissociation. According to the Equation 5.5, the rate of formation of Cs^+ from precursors depends on the collision gas pressure.

CAD of $(CsL)^+$ (*m/z* 397) is a good example of a single-collision fragmentation. The relative peak intensities of the only two ionic species present in the spectra (Figure 5.5) are presented in Table 5.2. The

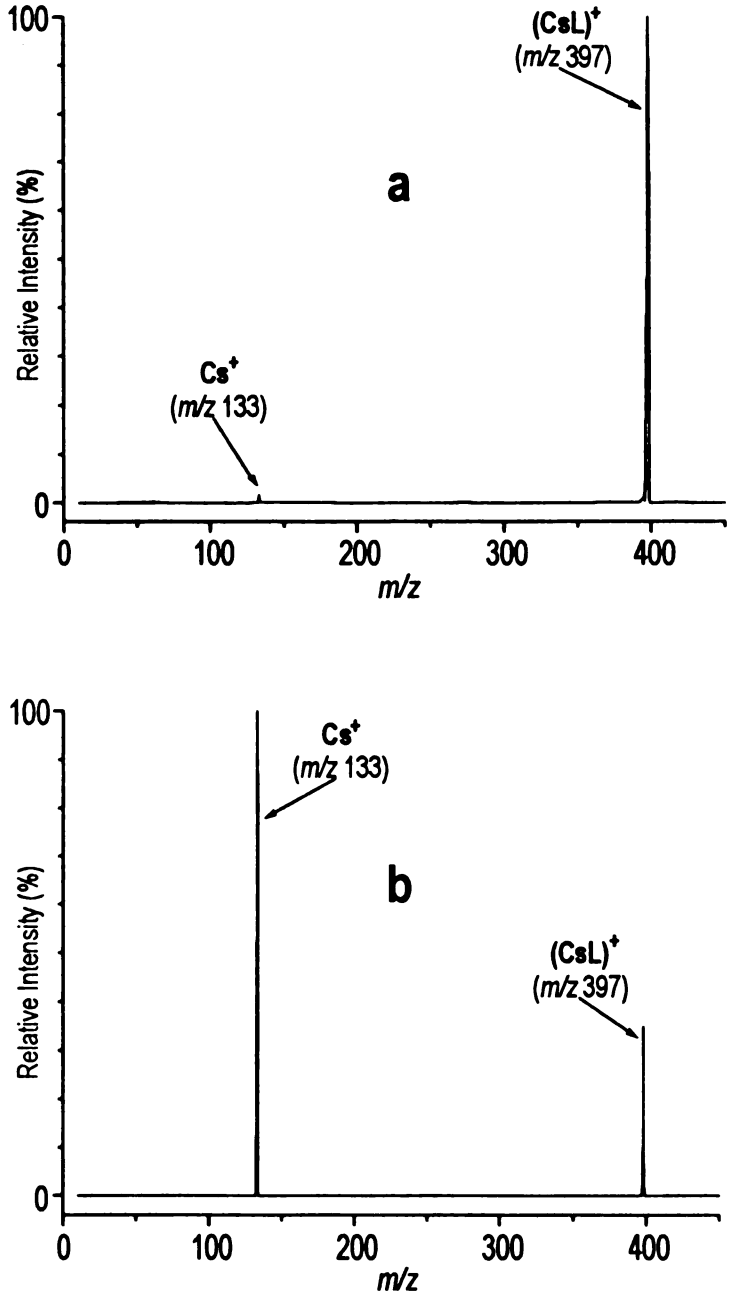

Figure 5.5 *MS/CAD/MS product ion spectra of $(CsL)^+$ (m/z 397). Collision energy = 20 eV; Collision gas pressure: (a) 0.10 mTorr, (b) 2.20 mTorr*

Table 5.2 *Effect of collision gas pressure (P_{coll}) on the relative intensities of product ions of $(CsL)^+$ (m/z 397); Collision energy = 20 eV*

Collision pressure (mTorr)	Relative Intensity (%)	
	Cs^+ *m/z* 133	$(CsL)^+$ *m/z* 397
0.10	1.7	100
0.21	5.4	100
0.28	8.1	100
0.35	11	100
0.42	16	100
0.46	20	100
0.50	21	100
0.61	30	100
0.65	31	100
0.71	34	100
0.80	35	100
0.86	45	100
0.94	58	100
1.0	62	100
1.1	67	100
1.2	83	100
1.3	92	100
1.5	100	86
1.6	100	75
1.8	100	66
1.9	100	54
2.1	100	40
2.2	100	35

rationalized peak intensity for the bare cesium ion (m/z 133) varies linearly with the collision gas pressure (Figure 5.6). Therefore, the fragmentation of $(CsL)^+$ follows a mechanism that is first order in G (Equation 5.4.2), which denotes a single-collision dissociation. Deviations from linearity were observed for collision pressures larger than 2 mTorr, amid an overall decrease in the total intensity of the peaks in the spectra.

Unlike the CAD of the (1:1) complex ion, the collision-induced fragmentation of the "sandwich" complex $(CsL_2)^+$ (m/z 661) yields three predominant product ions. Their relative peak intensities are summarized in Table 5.3. The appearance of the MS/MS spectra varies as a function of collision gas pressure, two examples being presented in Figure 5.7. By rationalizing the peak intensities of Cs^+ (m/z 133), $(CsL)^+$ (m/z 397), and $(CsL_2)^+$ (m/z 661) to the total peak intensities in the spectra, it can be noted that the abundance of the precursor ion follows a decreasing trend, while the abundance of the bare metal ion increases with an increase in collision gas pressure (Figure 5.8). The rationalized peak intensity of the (1:1) complex ion reaches a maximum (at P_{coll} = 0.35 mTorr), and its variation suggests the role of $(CsL)^+$ as an intermediate in a multiple-step fragmentation mechanism (Equations 5.4.1 and 5.4.2).

Indeed, the rationalized peak intensity of Cs^+ as a function of collision gas pressure follows a power trendline (Figure 5.9). Curve fitting of

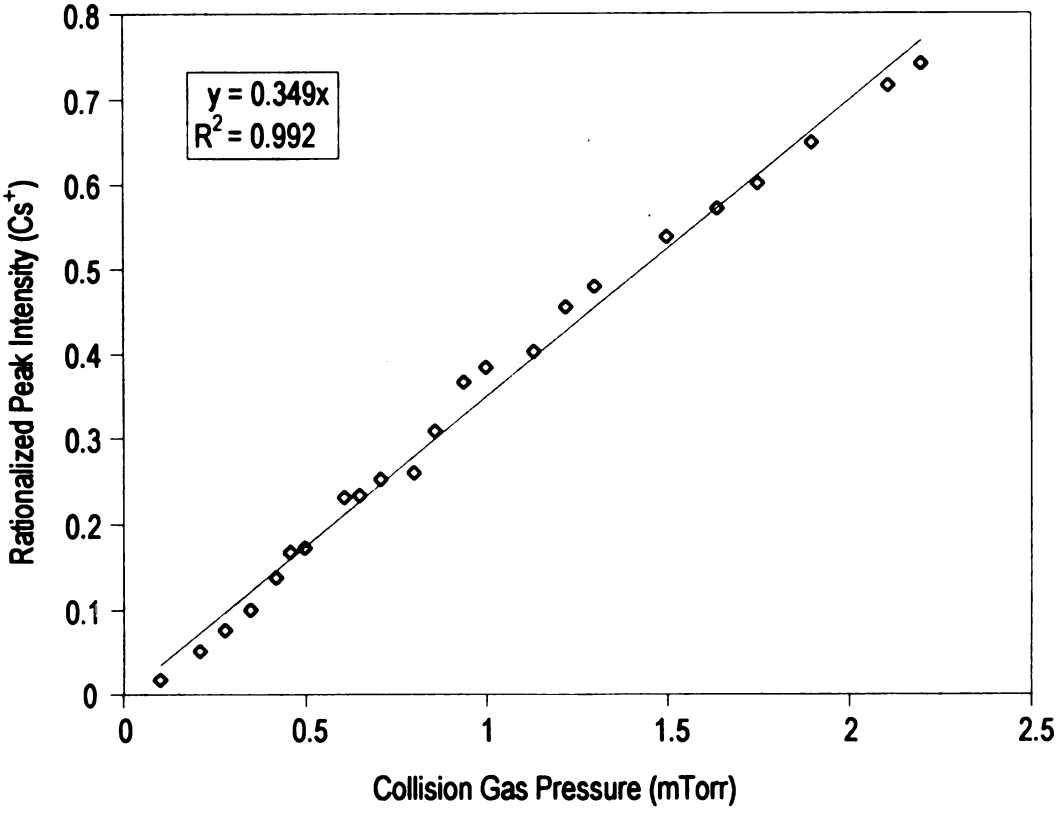

Figure 5.6 *Rationalized peak intensity of product ion Cs^+ (m/z 133) in the CAD of $(CsL)^+$ (m/z 397) as a function of collision gas pressure. Collision energy = 20 eV*

Table 5.3 *Effect of collision gas pressure (P_{coll}) on the relative intensities of product ions of $(CsL_2)^+$ (m/z 661). Collision energy = 60 eV.*

Collision pressure (mTorr)	Relative Intensity (%)		
	Cs^+ *m/z* 133	$(CsL)^+$ *m/z* 397	$(CsL_2)^+$ *m/z* 661
0.12	0.60	100	75
0.12	0.54	100	74
0.14	0.71	100	71
0.17	1.1	100	45
0.20	1.5	100	32
0.21	1.3	100	29
0.24	2.0	100	21
0.26	2.9	100	18
0.30	4.8	100	13
0.31	4.4	100	13
0.32	4.6	100	13
0.35	5.1	100	7.9
0.41	7.1	100	4.0
0.41	6.9	100	4.1
0.49	13	100	2.2
0.54	18	100	1.1
0.55	17	100	1.1
0.62	29	100	0.99
0.64	31	100	0.91
0.70	46	100	0.77
0.75	61	100	0.65
0.81	83	100	0.58

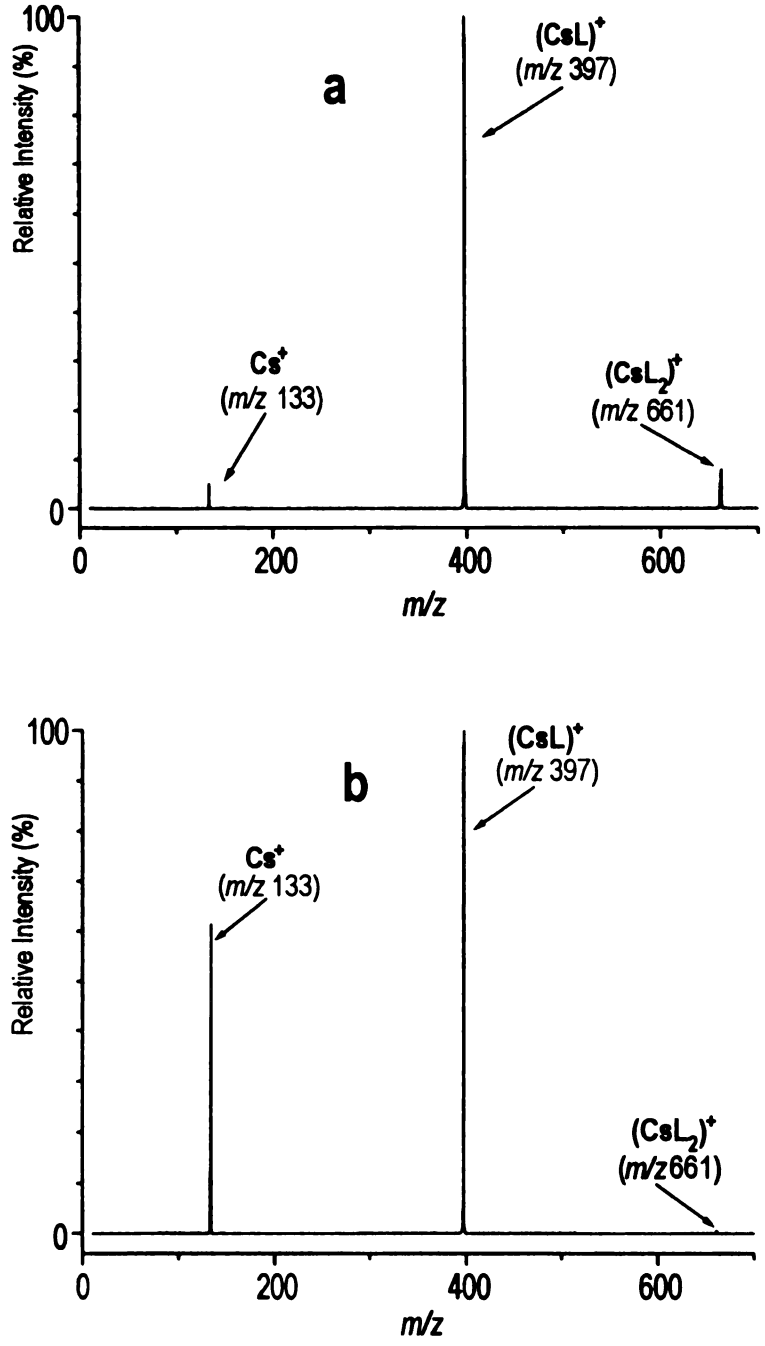

Figure 5.7 *MS/CAD/MS product ion spectra of $(CsL_2)^+$ (m/z 661). Collision energy = 60 eV; Collision gas pressure: (a) 0.35 mTorr, (b) 0.75 mTorr*

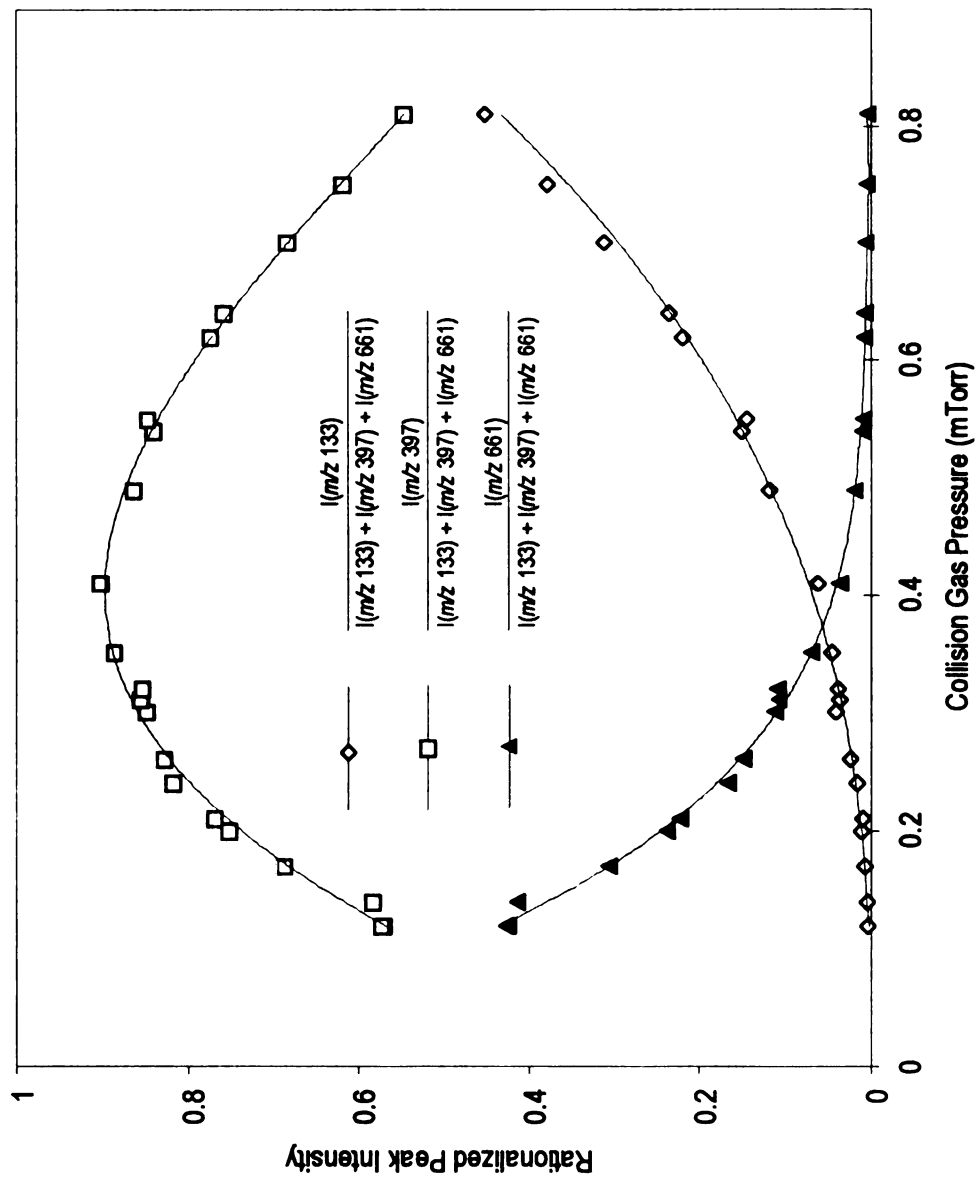

Figure 5.8 *Rationalized peak intensities of product ions Cs^+ (◇), $(CsL)^+$ (□), and $(CsL_2)^+$ (▲) in the CAD of $(CsL_2)^+$ (m/z 661) as a function of collision energy. Collision gas pressure = 0.40 mTorr.*

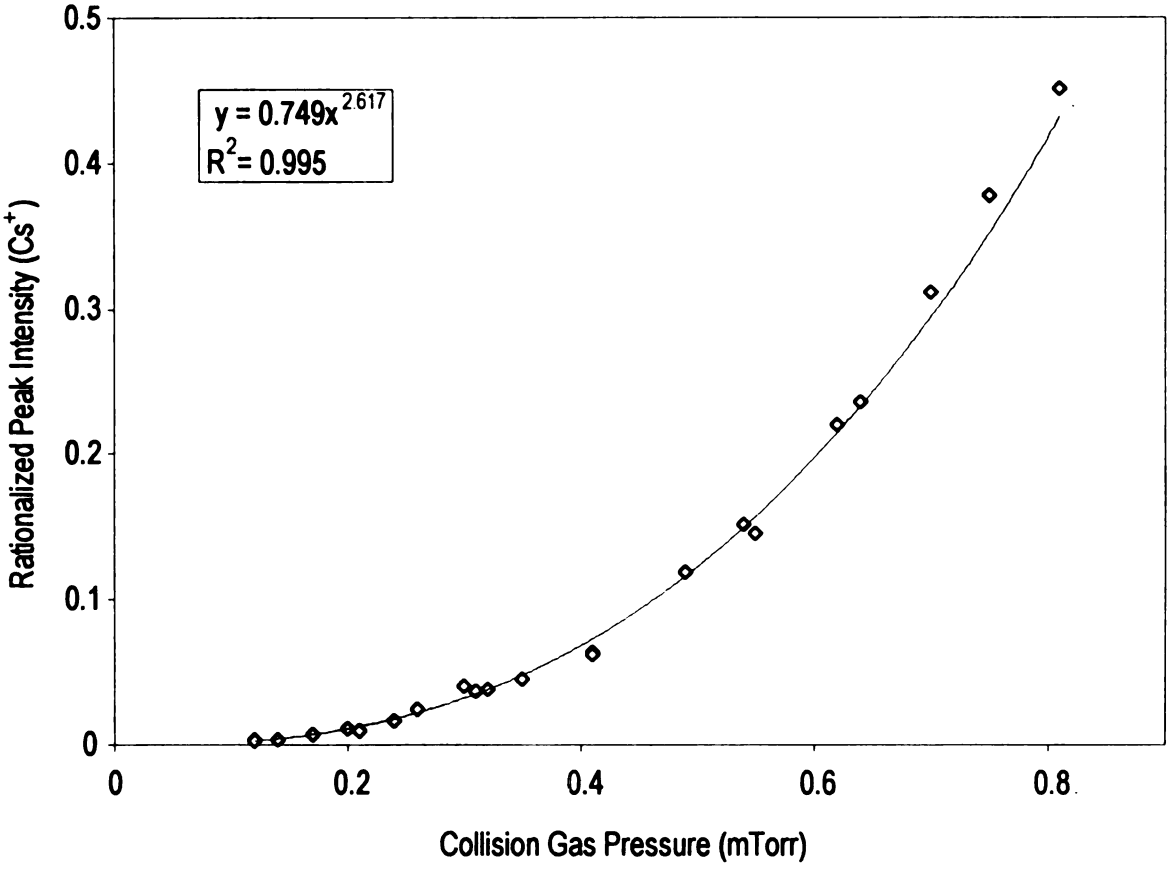

Figure 5.9 *Rationalized peak intensity of product ion Cs^+ (m/z 133) in the CAD of $(CsL_2)^+$ (m/z 661) as a function of collision gas pressure. Collision energy = 60 eV*

experimental points results in a power equation with an order of 2.6. According to Equation 5.5, the rate of formation of Cs^+ in CAD of $(CsL_2)^+$ has an apparent order of reaction of $b = 2.6$, a consequence of multiple collisions with argon molecules in the collision cell. Even though theoretically the reaction order in G should be 2, as a result of two collisions occurring per reaction, the higher apparent order is due to a deviation from ideality, namely, a certain amount of energy lost by the incident precursor ion following the first collision.

Comparison of Relative Stability of Alkali-Metal Complexes

In order to evaluate the intrinsic binding interactions involved in host-guest complexation of macrocyclic ligands with alkali-metal ions, a solvent-free environment appears to be a necessary experimental condition. Gas phase selectivities of crown ethers for various metal ions were previously determined by application of the kinetic method [15].

Experimental. An equiformular solution of NaCl, KCl, RbCl, CsCl (0.1 M) and 18-crown-6 ether in methanol was used as the analyte for the ES-MS investigation. All reagents were used as supplied. A syringe pump (Harvard Apparatus) was used for sample introduction, the solution flow rate being 5 μL/min. The electrospray voltage was 5 kV and the temperature of the transfer capillary 200 C.

The ES-MS spectrum of the (1:1) complexes of Na^+, K^+, Rb^+, and Cs^+ with 18-crown-6 (L) is shown in Figure 5.10. The ES-MS intensities for the peaks corresponding to the uncomplexed metals are in agreement with their solvation energies [16]. As mentioned in Chapter 4, no quantitative correlation can be made between the peak intensities of the complex and metal ions and their equilibrium concentrations in solution, even though the latter are generally known. A comprehensive quantitative interpretation of the ES-MS spectra can be done only if the solvation energies of all the ionic species involved are similar or known.

Tandem mass spectrometry is once again useful in this relative analysis within a series of complexes, allowing for the evaluation of the relative gas phase stabilities of the complexes of the four alkali-metal ions considered. The (1:1) complexes (ML^+), present in relatively large abundance in the ES-MS spectrum (Figure 5.10) were successively selected as precursor ions. The collision gas (Ar) pressure was set at 0.40 mTorr, and the collision energy (E_{LAB}) adjusted such as the center-of-mass collision energy (E_{CM}) was identical for each precursor ion selected, for consistency. The product ions present in each MS/MS spectrum were the bare metal ion, and the intact complex ion, the fragmentation being, as determined earlier, a single-collision process. The CAD collison energies and the peak intensities in the MS/MS spectra are summarized in Table 5.4.

Based on the relative intensities of the bare metal ion peaks with respect to their precursors, a qualitative conclusion about the gas phase

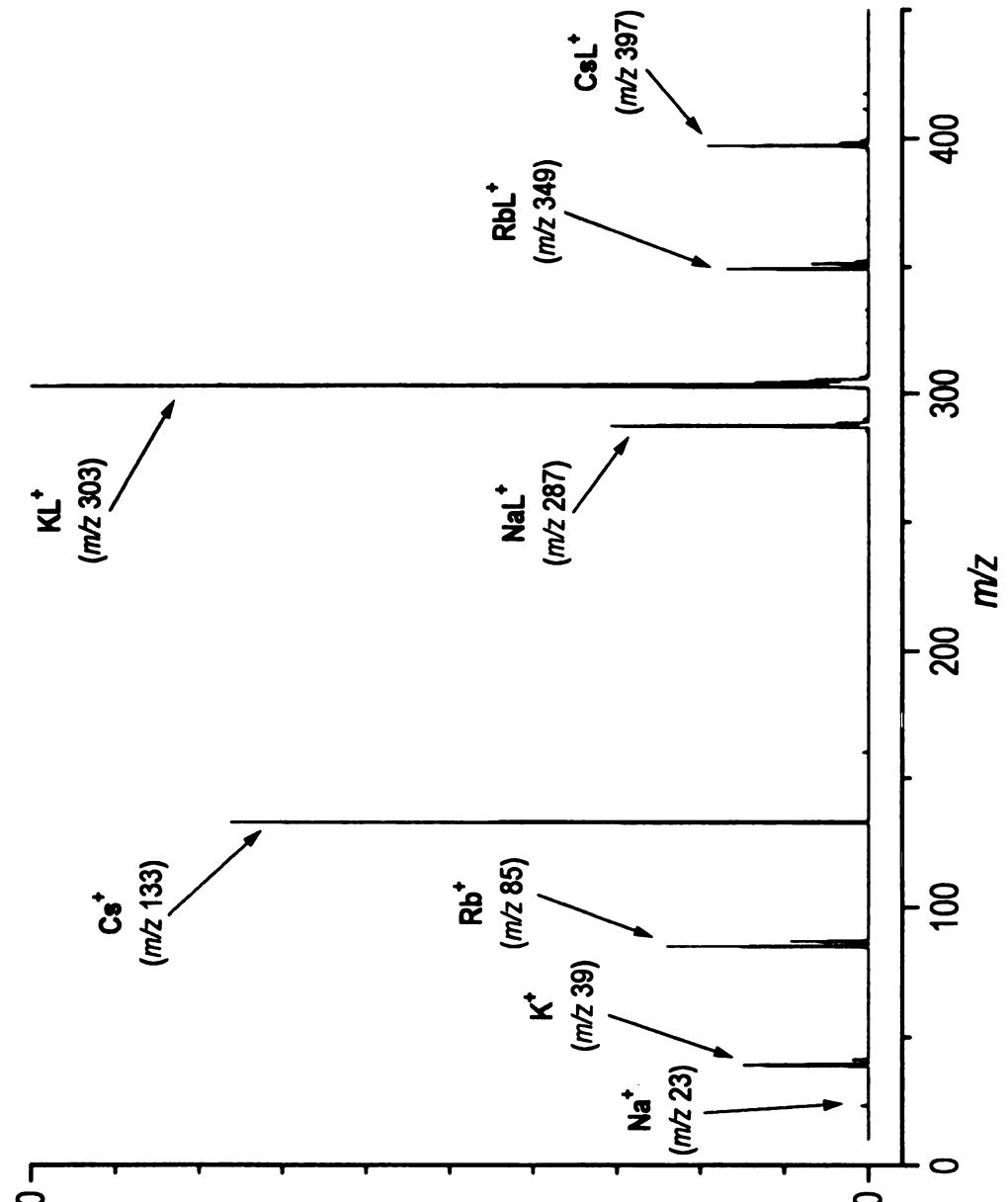

Figure 5.10 *ES-MS spectrum of an equifomular mixture of $(NaL)^+$, $(KL)^+$, $(RbL)^+$, and $(CsL)^+$. Capillary temperature = 200 C*

Table 5.4 *Relative intensities of the product ions in the CAD of complexes of alkali-metals with 18-crown-6 (L) Collision energy (E_{CM} = 4 eV)*

Metal Ion	Collision Energy (E_{LAB}) (eV)	Relative Intensity (%)	
		M^+	$(ML)^+$
Na^+	33	3.5	100
K^+	34	23	100
Rb^+	39	39	100
Cs^+	44	52	100

while the least stable, CsL^+, produces the largest abundance of its metal ion "core". Therefore, the stability sequence in the gas phase is:

$$(NaL)^+ > (KL)^+ > (RbL)^+ > (CsL)^+$$

Unlike in solution, where the stability sequence is, according to the complex equilibria, $(KL)^+ > (NaL)^+ > (RbL)^+ > (CsL)^+$, and is governed by the "best fit" concept between the cation size and the ligand cavity [17,18] the concept of "maximum contact point" [15] best describes the gas phase chemistry of these complexes.

Summary

The gas phase chemistry of coordination compounds can be studied, at least to a certain extent, by performing MS/CAD/MS experiments in a triple quadrupole mass spectrometer. The introduction of intact non-volatile inorganic species into the mass spectrometer had been a problem until the implementation of electrospray. The method has a double duty as a "launch pad" for tandem mass spectrometric analyses. ES does not only serve as a sample introduction means, ensuring the transfer into the gas phase of virtually any solvated ionic coordination compound, regardless its (non)volatility, but this transfer occurs with little or no fragmentation, even for unstable and thermally fragile ionic species.

Collisionally activated dissociation processes are strongly dependent on the reaction conditions, such as collision gas pressure and collision energy. Careful monitoring of instrumental parameters allows for mechanistic and relative structural studies, involving selected ions, in the gas phase.

References

1. Busch, K. L.; Glish, G. L.; McLuckey, S. A. *Mass Spectrometry/Mass Spectrometry: Techniques and Applications of Tandem Mass Spectrometry*; VCH Publishers: New York, 1988.

2. Jennings, K.R. *Int. J. Mass Spectrom. Ion Phys.* **1968**, *1*, 227.

3. Cooks, R. G. In *Collision Spectroscopy*, R. G. Cooks, Ed.; Plenum: New York, 1978.

4. *Tandem Mass Spectrometry*; F. W. McLafferty, Ed.; John Wiley & Sons: New York, 1983.

5. Carr, S. A.; Roberts, G. D.; Hermier, M. E. In *Mass Spectrometry of Biological Materials*; C. McEwen and B. Larsen, Eds.; Marcel Dekker: New York, 1990.

6. Domon, B.; Costello, C. E.; *Biochemistry*, **1988**, *27*, 1534.

7. Haroldsen, P. E.; Reilly, M. H.; Huges, H.; Gaskell, S. J.; Porter, C. *J. Biomed. Environ. Mass Spectrom.* **1988**, *15*, 615.

8. Znamirovschi, C. G.; Enke, C. G. *J. Am. Soc. Mass Spectrom.* (in press).

9. Mabud, Md. A.; Dekrey, M. J.; Cooks, R. G. *Int. J. Mass Spectrom. Ion Processes* 1985, 67, 285.

10. Hadden, W. F.; McLafferty, F. W. *J. Am. Chem. Soc.* **1968**, *90*, 4745.

11. Yost, R. A.; Enke, C. G. *J. Am. Chem. Soc.* **1978**, *100*, 2274.

12. Cody, R. B.; Freiser, B. S. *Int. J. Mass Spectrom. Ion Phys.* **1982**, *41*, 199.

13. Schey, K.; Cooks, R. G.; Grix, R.; Wollnik, H. *Int. J. Mass Spectrom. Ion Processes* **1987**, *77*, 49.

14. Louris, J. N.; Cooks, R. G.; Syka, J. E. P.; Kelley, P. E.; Reynolds, W. E.; Todd, J. F. J. *Anal. Chem.* **1987**, *59*, 1677.

15. Maleknia, S.; Brodbelt, J. *J. Am. Chem. Soc.* **1992**, *114*, 4295.

16. Dupont, A.; Leize, E.; Marquis-Rigault, A.; Funeriu, D.; Lehn, J.-M.; Van Doesselaer, A. In *Proceedings of the 43rd ASMS Conference on Mass Spectrometry and Allied Topics*, Atlanta, GA, May 21-26, 1995.

17. Gokel, G. W.; Doli, D. M.; Minganti, C.; Echegoyen, L. *J. Am. Chem. Soc.* **1983**, *105*, 6786.

18. Zhang, H.; Chu, I.-H.; Leming, S.; Dearden, D. V. *J. Am. Chem. Soc.* **1991**, *113*, 7415.

Chapter 6

Metal Complexes of a Novel Macrocyclic Ligand

Introduction

Electrospray mass spectrometry applied to coordination and organometallic systems has recently become a preferred tool for inorganic analytical and synthetic chemists. ES-MS operation in either positive or negative mode, coupled or not with tandem mass analysis, allows for structural and mechanistic investigations not approachable through most other means. Colton and co-workers have successfully applied the technique of electrospray to a wide variety of organometallic systems [1-3] as well as coordination complexes [4].

In the present study we applied electrospray mass spectrometry to the study of a novel polydentate, macrocylic ligand, hexahomotriazacalix[3]arene

(H_3L) (Figure 6.1), synthesized by Hampton and co-workers [5]. Calixarenes and related macrocycles have recently received considerable attention for their host-guest chemistry and for their coordination chemistry with metals [6,7]. The hexahomotriazacalix[3]arene which this study focuses on is the first structurally characterized compound of its kind. Following comprehensive structural studies of its complexation in solution [8], we attempted to acquire additional information about its host-guest coordination chemistry involving transition metal ions such as scandium (III), yttrium (III), and lanthanum (III) by means of electrospray mass spectrometry.

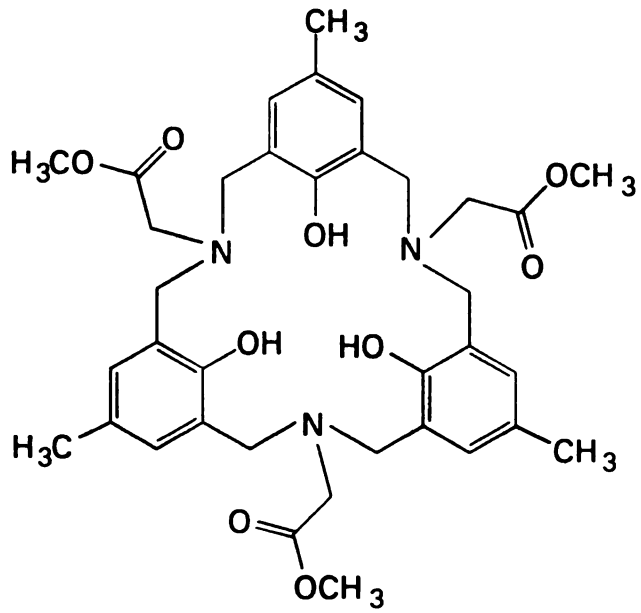

Figure 6.1 *The structure of hexahomotriazacalix[3]arene (H_3L)*

Complexes with Scandium (III), Yttrium (III), and Lanthanum (III)

Experimental. Solutions of $ScCl_3$, YCl_3, and $LaCl_3$ (ACS-grade) were prepared in accordance with the procedure previously described. Equivalent amounts of H_3L were added to each solution such as the concentrations of both the metal ion and the ligand were 0.1 M. The solvents used were HPLC-grade methanol or acetonitrile (Merck). The solutions were introduced in the electrospray source using a syringe pump, at a flow rate of 5 μL /min. The electrospray voltage was set at 5 kV, and the temperature of the transfer capillary was maintained at 200 C. For the CAD study, argon was used as collision gas. Data acquisition was done by means of a signal averaging procedure.

The ES-MS spectrum of the scandium complex in acetonitrile is shown in Figure 6.2. The protonated uncomplexed ligand $(H_4L)^+$ accounts for the base peak (*m/z* 664), while various ligand fragments are also present in the spectrum, in large abundances. The structure of the macrocyclic ligand consists of three monomeric entities (L'), each of them having one pendant arm (P) attached. The protonated trimer (*m/z* 664) does not lose any of the three pendant arms during the electrospray process, fact that denotes its greater stability compared to the protonated monomer (*m/z* 222) and the

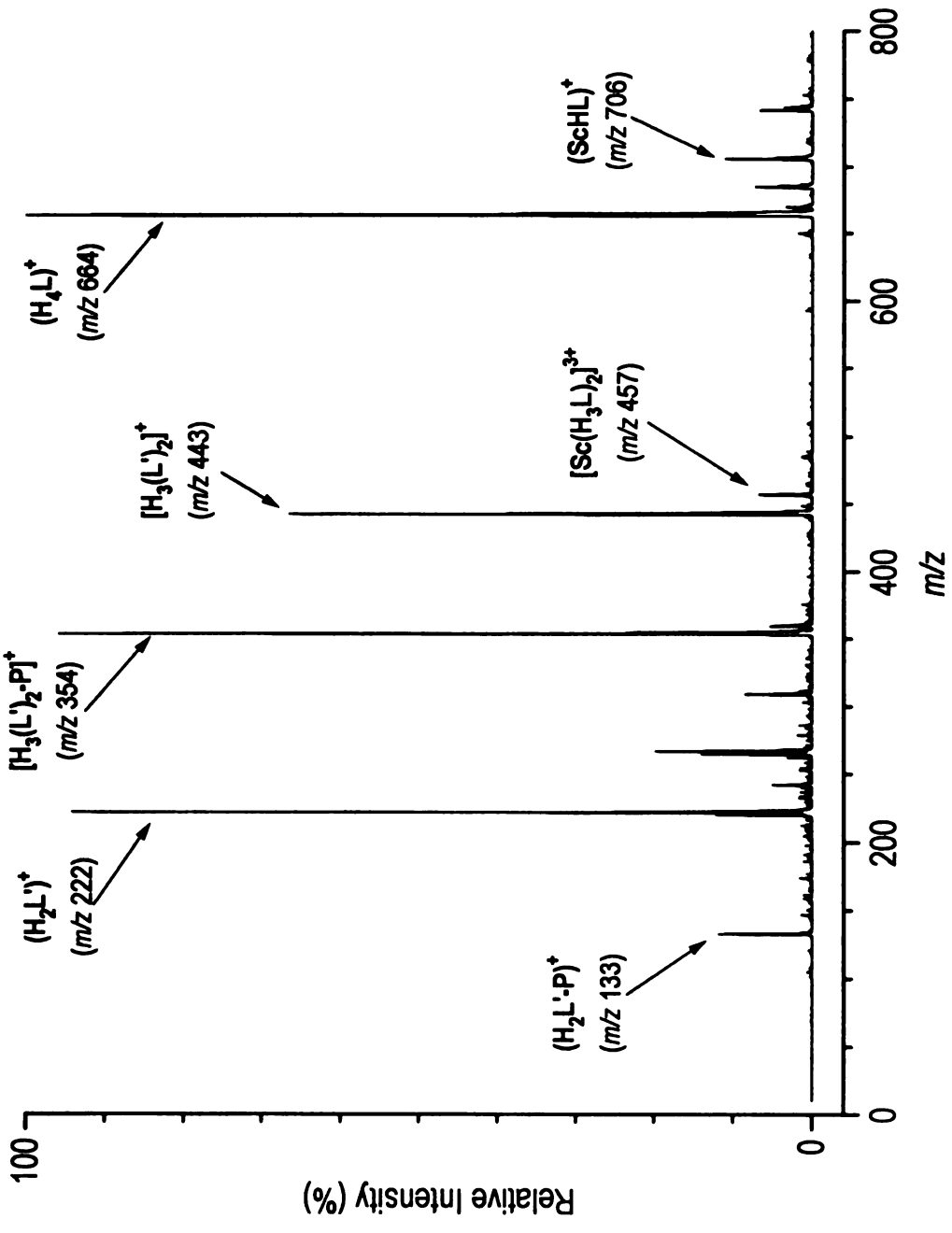

Figure 6.2 *ES-MS spectrum of a Sc^{3+} : H_3 L (1:1) solution in acetonitrile. Capillary temperature = 200 C*

protonated dimer (*m/z* 443), respectively. The loss of a pendant arm accounts for the neutral loss of 89 m/z units, for singly charged ionic species, the appearance of peaks at *m/z* 133 and *m/z* 354 being direct consequences of such in-source fragmentation processes. Scandium ions are complexed only to a little extent, according to the low intensities of the peaks at *m/z* 706 and *m/z* 457, respectively.

However, the peak at *m/z* 457 suggests a structure that was not determined as a part of the complexation studies in solution. The appearance of this triply charged (1:2) "sandwich" complex is surprising, especially taking into account the widely recognized difficulty of generating multiply charged ions in the gas phase [9,10].

When complexation occurred in a different solvent (methanol), the appearance of the ES-MS spectra changed significantly (Figure 6.3). More scandium-containing ions are present, leading to the conclusion that methanol is a more favorable medium for this particular complexation reaction in solution. The singly charged (1:1) complex ion $(ScHL)^+$ (*m/z* 706) is now the base peak in the spectrum, while the triply charged ion of *m/z* 457 is more abundant than in the acetonitrile solution. For the assignment of the peak at *m/z* 309, CAD was the experimental method of choice. The ion of *m/z* 309 was selected as a precursor, fragmentation being induced by collisions with argon in the collision chamber of a triple quadrupole experimental arrangement. The product ion spectrum is shown in Figure 6.4.

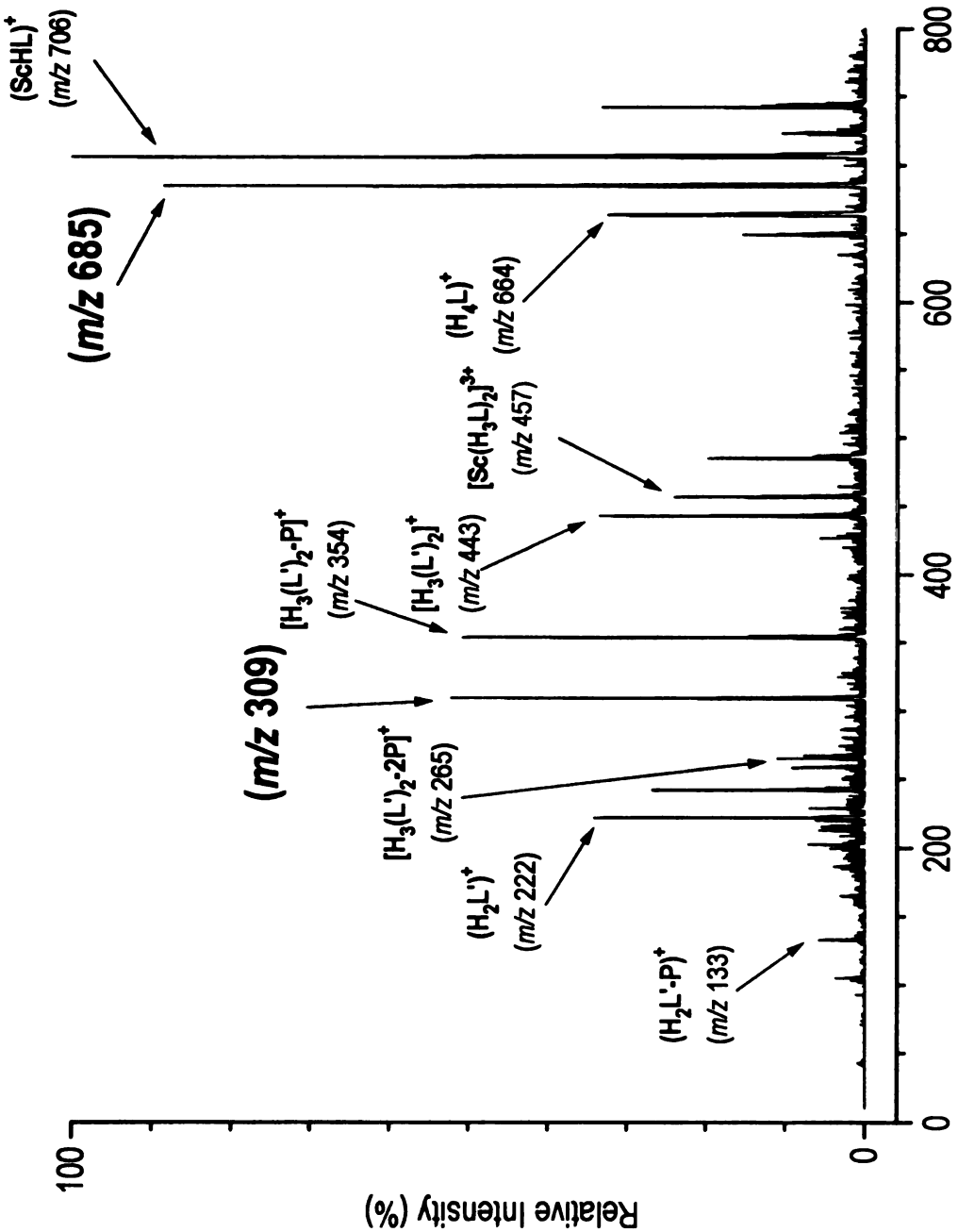

Figure 6.3 *ES-MS spectrum of a Sc^{3+} : H_3 L (1:1) solution in methanol (t = 200 C)*

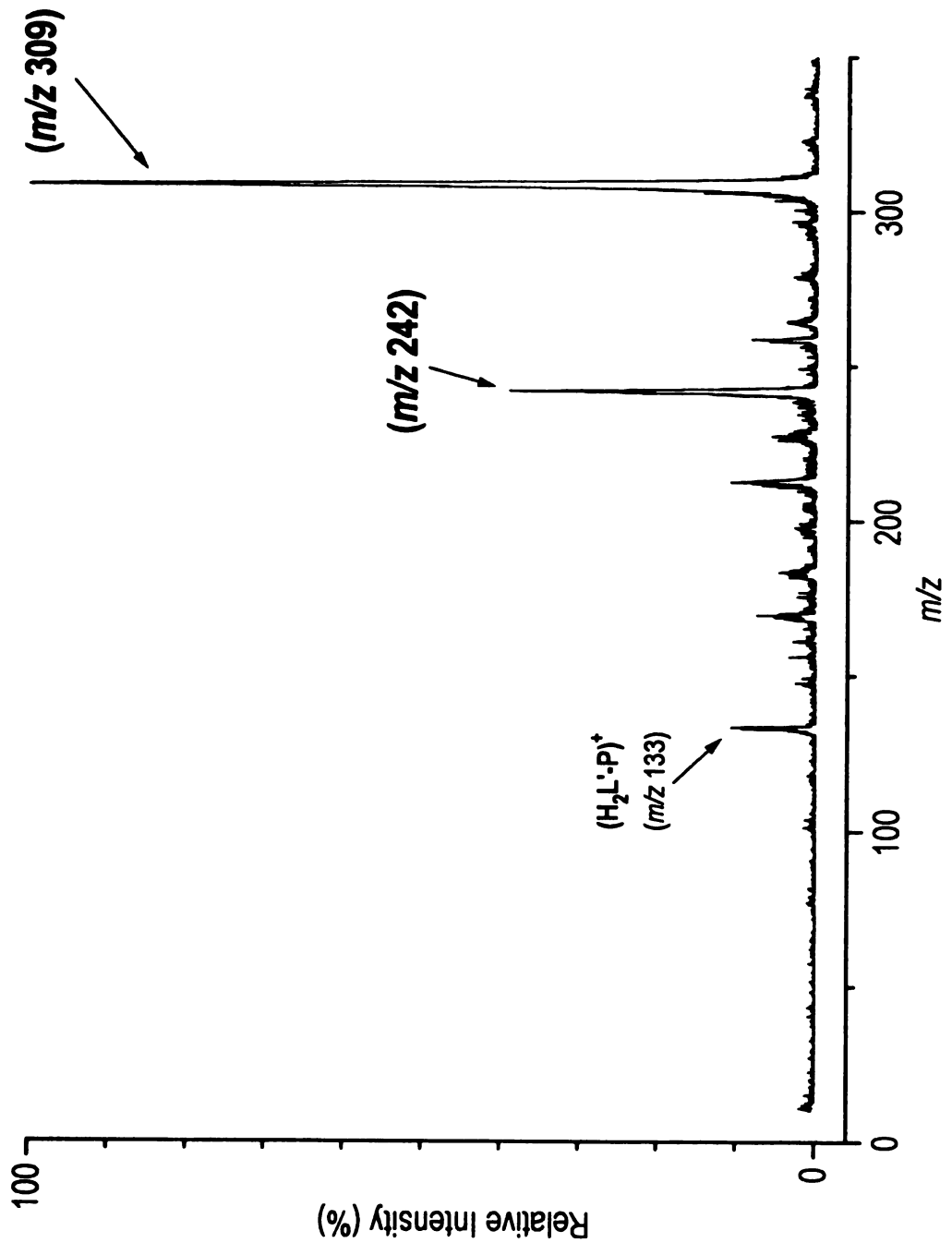

Figure 6.4 *MS/CAD/MS product ion spectrum of m/z 309*

Based only on this experiment the only information obtained about the ion of *m/z* 309 is that a likely structure would be consistent with the coordination of Sc(III) by a dimeric ligand substructure.

The structural similarity between most of the complexes involving Sc(III) and Y(III) is beneficial in the context of our study. The ES-MS spectrum of yttrium complex in methanol (Figure 6.5) provides some answers to questions raised during the analysis of scandium complexation. First, the same protonated uncomplexed ligand and ligand fragments are present in the spectrum, independent of the nature of the metal, confirming the initial assignments. The structures of some ligand fragments are shown in Figure 6.6. The base peak in the spectrum is at *m/z* 331 and, like in the case of scandium, its assignment is difficult without taking advantage of the above mentioned parallelism between scandium and yttrium complexation patterns. Indeed, if we assume that the ions at *m/z* 309 (Figure 6.3) and *m/z* 331 (Figure 6.5) have the same charge and ligand structure, the difference between their m/z values (22 m/z units) suggests that both ions may be doubly charged and each contain one Sc (A=45) ion and Y (A=89) ion, respectively. However, the evidence concerning this aspect is not yet sufficient.

Like the spectrum of the scandium complex, the spectrum of yttrium complex contains the triply charged "sandwich" complex as well (*m/z* 472). Tandem mass spectrometry helps once again solve the problem regarding its

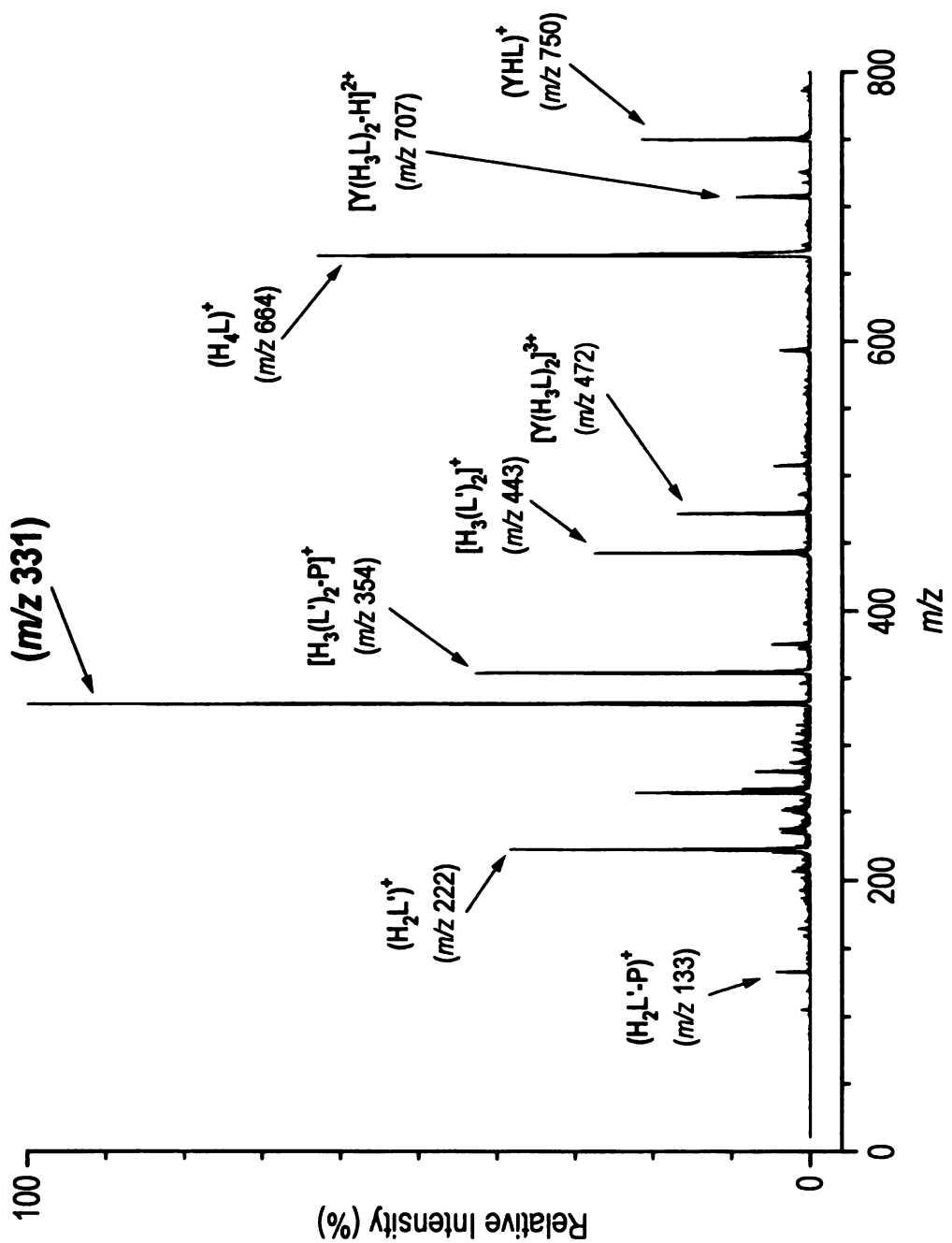

Figure 6.5 *ES-MS spectrum of a Y^{3+} : H_3L (1:1) solution in methanol. Capillary temperature = 200 C*

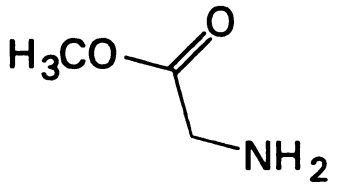

Pendant arm (M=89)

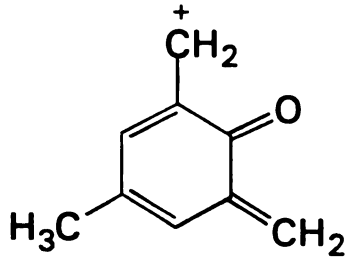

***m/z* 133**

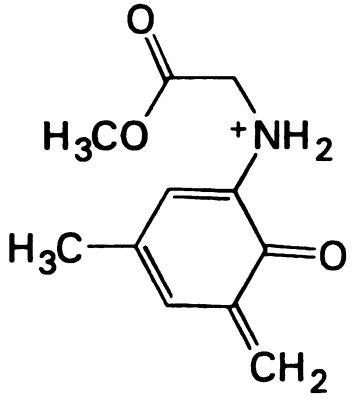

***m/z* 222**

Figure 6.6 *Structures of representative fragmentation products that result in the ES-MS processes involving H_3L and its metal(III) complexes*

structural assignment. The MS/MS product spectrum resulting from CAD of *m/z* 472 confirms the multiple charge carried by the precursor ion, since one of the products, $(YHL)^+$ (*m/z* 750) is the result of a favored structure splitting combined with a charge reduction process (Figure 6.7).

The structural confirmation regarding the ion at *m/z* 707 also emerges from an MS/MS experiment. By using a collision energy of 20 eV, the CAD product spectrum in Figure 6.8.a is obtained. A more advanced fragmentation can be achieved, as expected, by using a larger collision energy (30 eV) (Figure 6.8.b). The products of the dissociation process unambiguously confirm the charge and the structure of the ion of *m/z* 707. This conclusion can now be extended to the ES-MS spectrum of the scandium complex (Figure 6.3) as well, confirming the assignment of the peak at *m/z* 685 to $[Sc(H_3L)_2\text{-}H]^{2+}$.

The third metal considered in this comparative study, lanthanum (III), behaves, however, differently. The complexation between the metal ion and H_3L occurs to a very limited extent, even in methanol, the (1:1) complex ion $(LaHL)^+$ (*m/z* 800) being virtually inexistent in the ES-MS spectrum (Figure 6.9). The usual protonated ligand-derived ions are present as predominant peaks, as a consequence of the availability of a large fraction of uncomplexed ligand in the solution matrix.

An ion that may be relevant with respect to the possible complexation of lanthanum is present at *m/z* 400. While its mass-to-charge ratio is

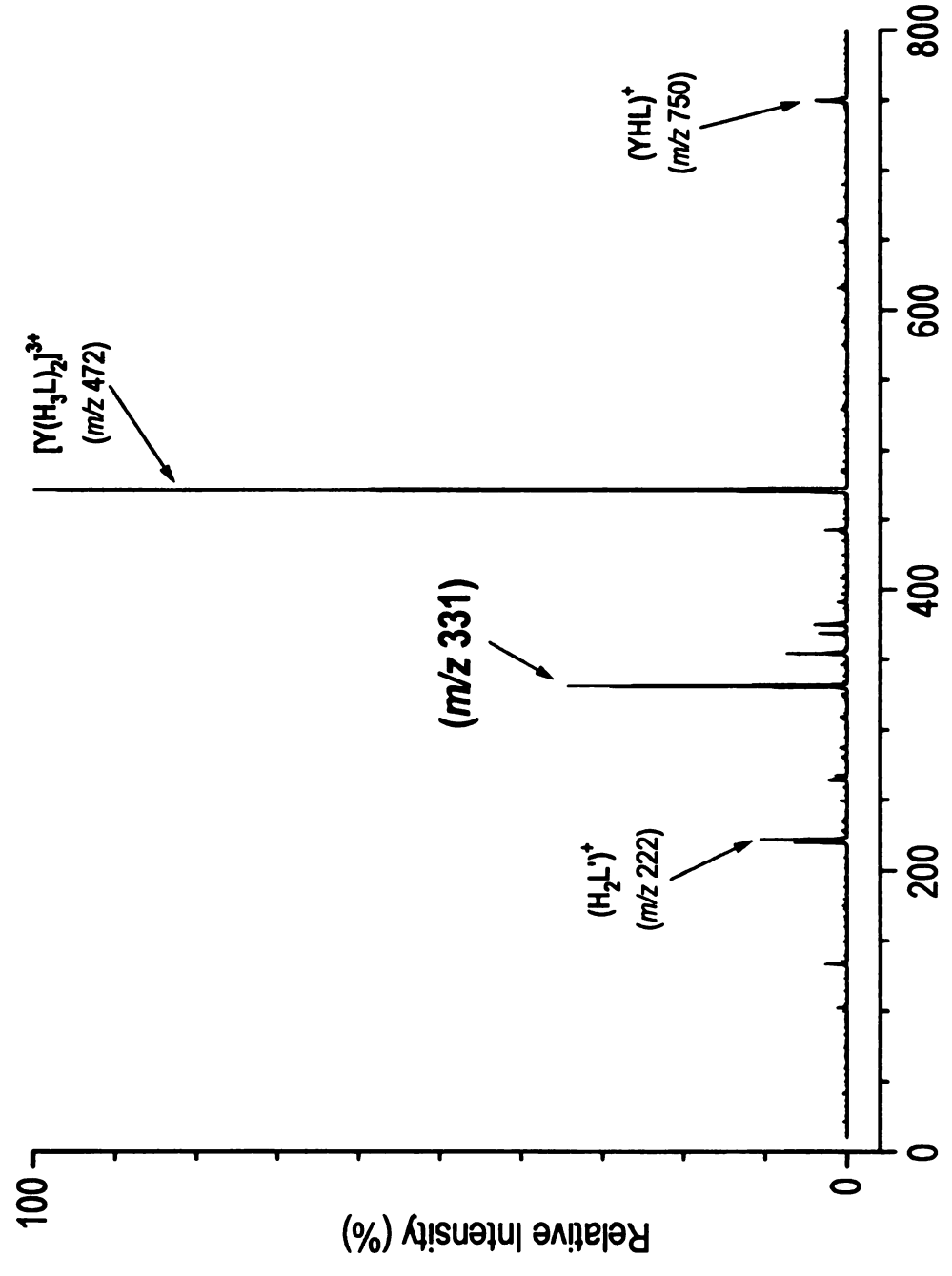

Figure 6.7 *MS/CAD/MS product ion spectrum of m/z 472*

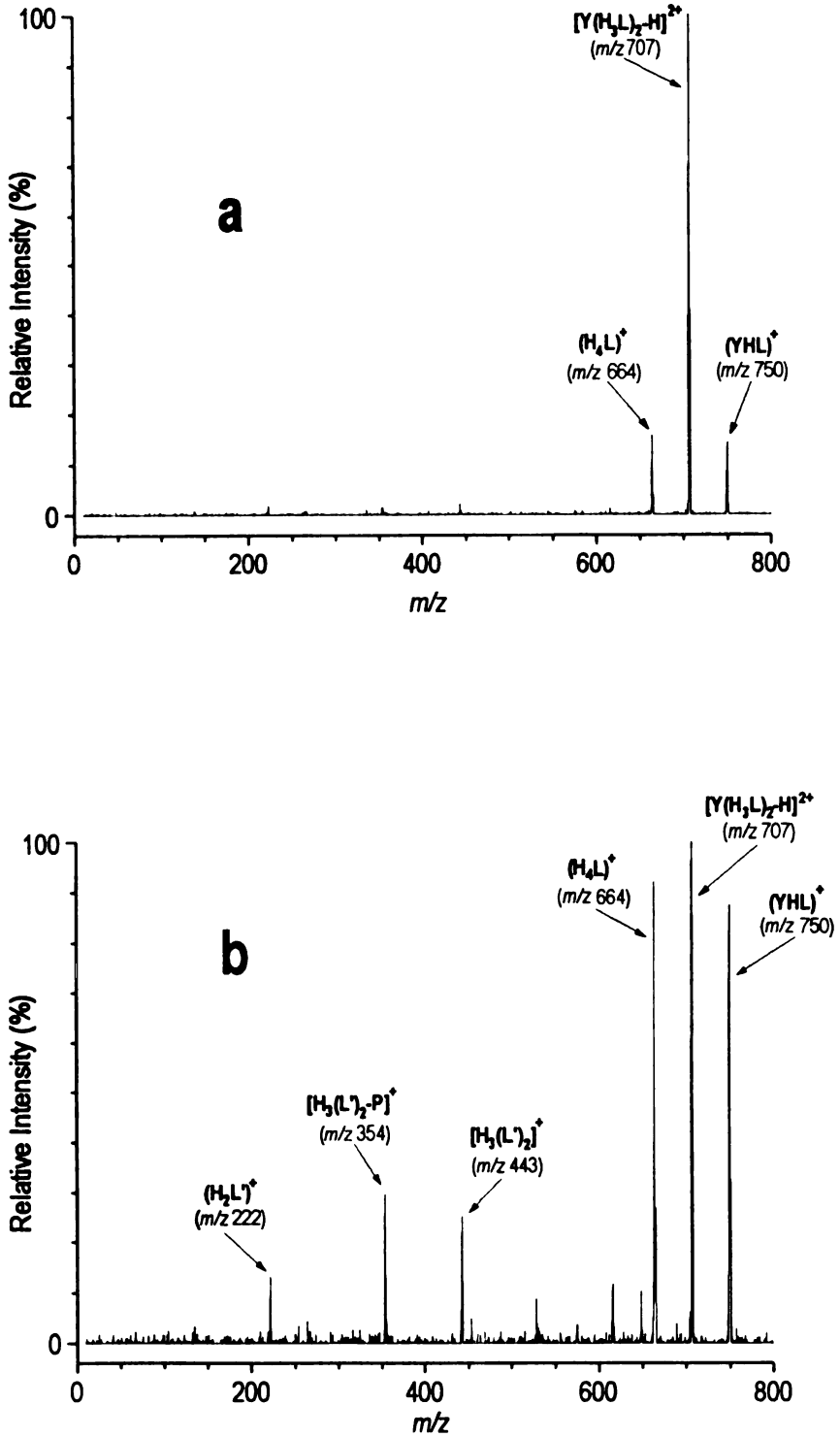

Figure 6.8 *Product ion spectra of CAD of m/z 707. Collision gas pressure = 0.6 mTorr. Collision energy: (a) 20 eV, and (b) 30 eV*

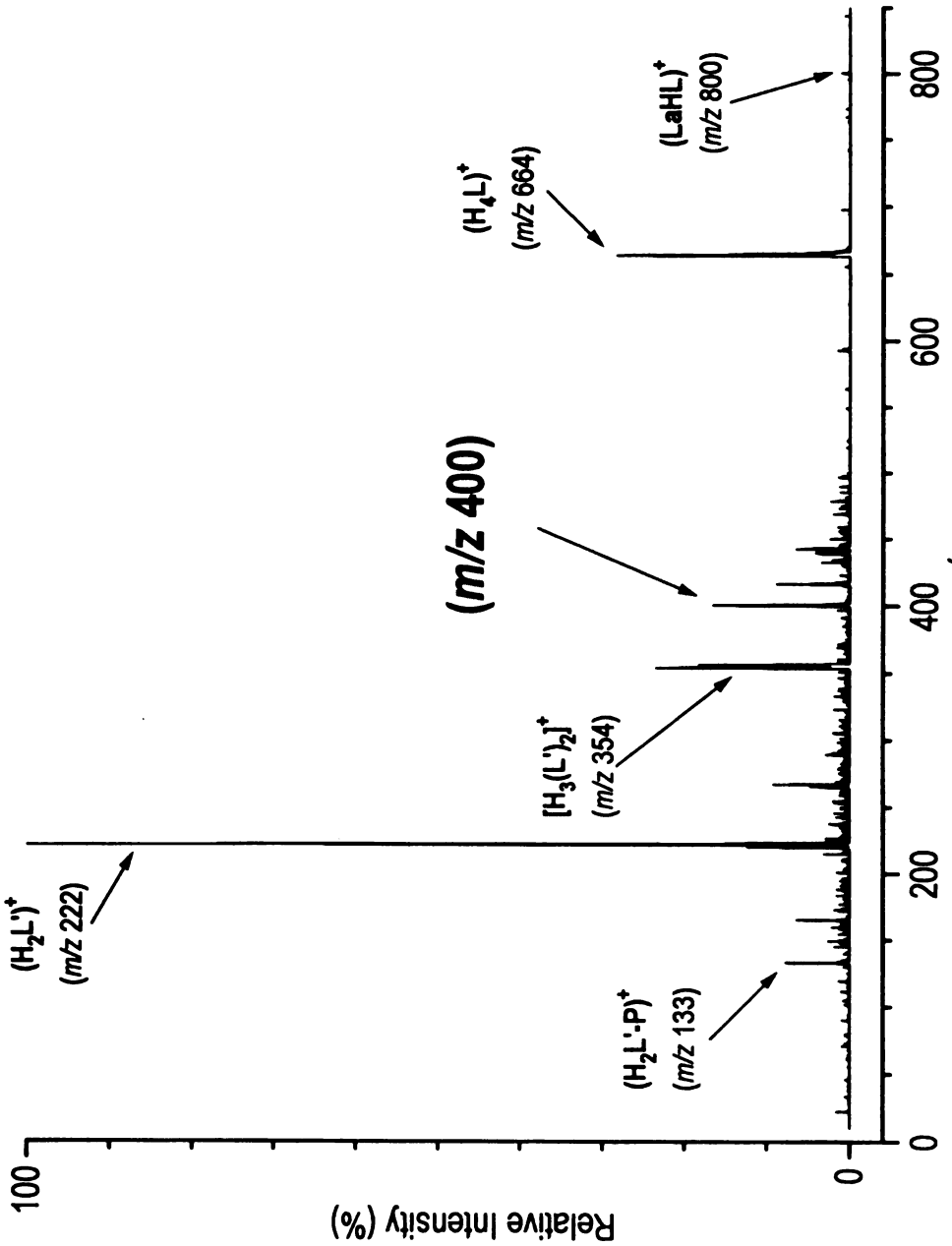

Figure 6.9 *ES-MS spectrum of a* La^{3+} *:* H_3 *L (1:1) solution in methanol. Capillary temperature = 200 C*

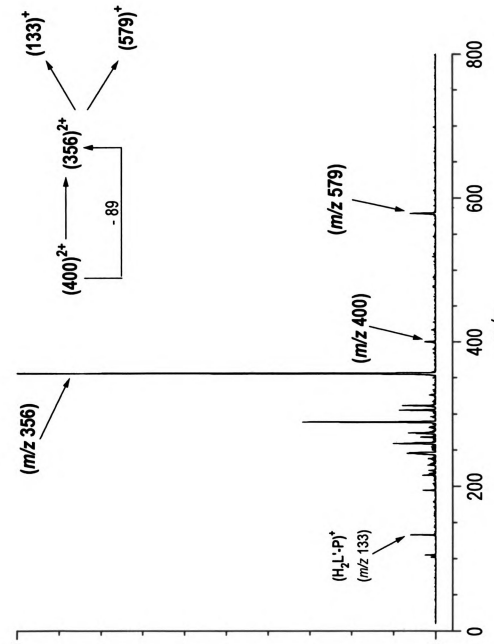

Figure 6.10 *Product ion spectrum of m/z 400. Collision gas pressure = 0.6 mTorr, Collision energy = 35 eV*

consistent with a structure in which the $(LaHL)^+$ (m/z 800) would undergo a charge increase reaction, such a structure is unlikely. CAD of the ion at m/z 400 (Figure 6.10) does not help much, even though the dissociation pattern denotes a multiple-step fragmentation mechanism, not elucidated at this point.

MICHIGAN STATE UNIV. LIBRARIES
31293015552403